Thin Film Electrochemical Sensor for Water Quality Monitoring

A thesis presented in partial fulfilment of the

requirements for the degree of

Doctor of Philosophy

in

Engineering

Massey University, Auckland,

New Zealand

Kartikay Lal

December 2023

I dedicate this doctoral thesis to my dearest sister Radhika Lal.

Merci beaucoup, petite sœur. Vous étiez mon inspiration et vous croyiez que je pouvais faire un doctorat.

Declaration of Authorship

This thesis has been furnished according to the Massey University "PhD thesis with publications" guidelines. The thesis is based on the technical manuscripts either published or currently under review or in preparation for submission to the reputable academic journals.

- Kartikay Lal

Acknowledgements

I would like to begin by expressing my gratitude to my beautiful sister, who always believed in my ability to pursue the highest form of education while working. I extend my heartfelt thanks to the rest of my family for their unwavering help, support, and encouragement throughout my PhD tenure; without them, I would not have been able to navigate through this journey.

I want to convey my sincerest thanks and appreciation to my supervisor and colleague, Associate Professor Khalid Arif, for his guidance and support that kept me on the right research path. Thank you so much for your patience and understanding. I also wish to acknowledge the support of my co-supervisor, Dr. Frazer Noble, for his guidance and stress-relieving conversations, which were much needed during the long five-year journey.

Additionally, I want to recognize the support of all current and former colleagues and students with whom I had the incredible joy and pleasure of working. My gratitude extends to Dr. Swapna Jaywant and Dr. Asif Rehmani for their valuable advice and support. I am immensely grateful to the NZ Product Accelerator for providing primary funding support for this research.

Abstract

Freshwater is the most precious natural resource, essential for supporting life. Aquatic ecosystems flourish in freshwater sources, and many regions around the world depend on aquatic food sources, such as fish. Nitrogen and phosphorous are the two nutrients, in particular, that are essential for growth of aquatic plants and algae. However, with rising population and anthropogenic activities, excessive amounts of such nutrients enter our waterways through various natural processes, thereby degrading the quality of freshwater sources. Elevated levels of nitrate-nitrogen content, in particular, lead to consequences for both aquatic life as well as human health, which has been a cause for concern for many decades.

As recommended by the World Health Organization, the maximum permissible nitrate level in water is 11.3 mg/L. These levels are often exceeded in coastal areas or freshwater bodies that are close to agricultural land. Therefore, it is essential to monitor nitrate levels in freshwater sources in real-time, which can be achieved by employing detection methods commonly used to detect ionic content in water. Hence, a comprehensive review was carried out on various field-deployable electrochemical and optical detection methods that could be employed for in-situ detection of nitrate ions in water. The primary focus was on electrochemical methods that could be integrated with low-cost planar electrodes to achieve targeted detection of nitrate ions in water. Designing resilient sensors for real-time monitoring of water quality is a challenging task due to the harsh environment to which they are subjected.

There is a significant need for sensors with attributes such as repeatability, sensitivity, low-cost, and selectivity. These attributes were first explored by evaluating the performance of silver and copper materials on three distinct geometric patterns of electrodes. The experiments produced promising results with interdigitated pattern of copper electrodes that were successful in detecting 0.1-0.5 mg/L of nitrate ions in deionised water. The interdigitated geometric pattern of electrodes were further analyzed in four distinct materials namely, silver, gold, copper, and tin with real-world freshwater samples that were collected from three different freshwater bodies. The water samples were used to synthesize varying concentrations of nitrate ions. The results showed tin electrodes performed better over other materials for nitrate concentrations from 0.1-1 mg/L in complex matrix of real-world sample. The nitrate sensor eventually needs to be deployed in freshwater bodies, hence a real-time water quality monitoring system was also built that incorporated sensors to monitor five basic water quality parameters with the aim to monitor and study the quality of water around the local area.

Publications

1. Lal, K., Jaywant, S.A. and Arif, K.M., 2023. Electrochemical and Optical Sensors for Real-Time Detection of Nitrate in Water. Sensors, 23(16), p.7099. http://dx.doi.org/10.3390/s23167099

2. Lal, K. and Arif, K. M., 2023. Investigation of Planar Electrodes for Electrochemical Impedance Spectroscopy-based Detection of Nitrate in Water. Sensing and Imaging. Revision under review.

3. Lal, K. and Arif, K. M., 2023. Thin-Film Electrochemical Sensor For Nitrate Detection in Freshwater Sources. MDPI Sensors. Revision under review.

4. Lal, K., Menon, S., Noble, F. and Arif, K.M., 2024. Low-cost IoT based system for lake water quality monitoring. Plos one, 19(3), p.e0299089. https://doi.org/10.1371/journal.pone.0299089.

5. Rehmani, M.A.A., Lal, K, Shaukat, A, Arif, K.M. Laser ablation assisted micropatterned screen printed transduction electrodes for sensing applications. Nature Scientific Reports. http://dx.doi.org/10.1038/s41598-022-10878-6. Presented as full text in Appendix A.

6. Lal, K., Thomas, T. and Arif, K., 2022, December. Performance Evaluation of Interdigitated Electrodes for Electrochemical Detection of Nitrates in Water. In International Conference on Sensing Technology (pp. 407-413). Cham: Springer Nature Switzerland. http://dx.doi.org/10.1007/978-3-031-29871-4_41

Contents

List of Figures

List of Tables

Abbreviations

EIS	Electrochemical Impedance Spectroscopy
AC	Alternating Current
PMMA	Poly(methyl methacrylate)
PDMS	Polydimethylsiloxane
MUT	Material Under Test
ASIC	Application Specific Integrated Circuit
PET	Polyethylene Terephthalate
CNC	Computer Numerical Control
CO2	Carbon dioxide
DI	Dissolved Oxygen
Ag	Silver
Au	Gold
Cu	Copper
SEM	Scanning Electron Microscope
IoT	Internet of Things
pH	power of Hydrogen
DO	Dissolved Oxygen
TDS	Total Dissolved Solids
NTU	Negative Temperature Coefficient
WHO	World Health Organization
ORP	Oxidation-Reduction Potential
EC	Electrical Conductivity
GSM	Global System for Mobile Communication
LCD	Liquid Crystal Display
WQI	Water Quality Index

CCME	Canadian Council of Ministers of Education
ADC	Analog and Digital Converter
TSS	Total Suspended Solids
GPH	Gallons per Hour
RTC	Real Time Clock
IDE	Interdigitated Electrode
LoRa	Long Range
Wi-Fi	Wireless Fidelity
AI	Artificial Intelligence
ML	Machine Learning
IC	Integrated Circuit
EUD	European Union Directives
UV	Ultraviolet
RE	Reference Electrode
WE	Working Electrode
CNT	Carbon Nanotubes
CV	Cyclic Voltammetry
DPV	Differential Pulse Voltammetry
SWV	Square Wave Voltammetry
LSV	Linear Sweep Voltammetry
LOD	Limit of Detection
ISE	Ion-Selective Electrode
LOC	Lab-on-Chip
FET	Field Effect Transistor
WSN	Wireless Sensor Network
SEM	Scanning Electron Microscope

Chapter 1

Introduction

1.1 Overview

Freshwater is essential to support life, serving as our most invaluable natural resource. It plays a vital role in promoting well-being, driving the economy, facilitating recreation, and support agriculture. In New Zealand, Māori share an innate connection with the freshwater environment, which is central to Māori customs, knowledge, and food gathering practices [1]. However, due to several factors, our freshwater environment is under pressure from rising anthropogenic activities. Sources such as agricultural fertilizers, urbanization, and sewage contamination, are common causes of polluting our freshwater bodies. This leads to changes in physical and chemical parameters of water. Physical parameters include turbidity, odor, temperature, and dissolved solids, while chemical pollutants include salinity, conductivity, pH, and dissolved oxygen. There are also nutrients and microbial contaminants such as suspended solids, Escherichia coli, nitrate, phosphate, and ammonia. Among these, nitrate-nitrogen is the most prominent cause of pollution. Nitrogen pollution can also emanate from other sources, such as ammonia, nitrite, and various nitrogen-based compounds. Nitrate is a naturally occurring compound and is ubiquitous in the environment.

Furthermore, air also contributes towards rising nitrogen levels in water, which may be significantly lower compared to other ways but still has an impact [2]. The air is composed of 78% nitrogen (N_2). When nitrogen combines with carbon, hydrogen, or oxygen, through natural processes, it forms organic nitrogen compounds such as

ammonia (NH_4), or nitrate (NO_3-). Natural processes such as lightning, converts oxygen and nitrogen to nitric oxide (NO) and then to nitric acid (HNO_3) [3]. Natural processes such as lightning, converts oxygen and nitrogen to nitric oxide (NO) and then to nitric acid (HNO_3) [3]. Nitric acid in gaseous form, settles on the ground through rain, snow, or hail. The top soil is often rich in nitrogen content that originate from manures, decay of plants, fertilizers, and other organic materials [4]. When it rains, it causes nutrients from top soil to drain into our waterways, although the amount of nitrate and ammonium created from this process maybe negligible.

Nitrate dissolves easily in water, which makes it mobile. The contaminated water enters our freshwater supply such as lakes and rivers, through a process called nitrate leaching [5, 6]. Nitrate has some positive health affects that are used to treat and manage heart related issues such as dilating venous vessels and coronary arteries. Nitrate provides instant relief for patients suffering from cardiovascular diseases such as acute anginal pain, acute coronary syndrome, arterial hypertension, and heart failure. Despite the medicinal value of nitrate, negative impacts outweigh its positive effects. Nitrate could reduce hemoglobin levels in the blood, leading to weakness, increased heart rate, and, in some cases, triggering thyroid disease. Continuous intake of high levels of nitrate could also cause certain types of cancer [7, 8].

Nitrate contamination is a widespread issue that poses a significant threat to our freshwater resources. A study conducted in New Zealand by Rogers et al. involved the collection of 1042 freshwater samples from 14 regions around New Zealand by various institutions, including regional councils, universities, and industrial water researchers, spanning from 2010 to 2020. The samples underwent testing for nitrogen and oxygen isotopes [9]. The findings revealed that over 60% of the samples tested had nitrate concentrations above 0.9 mg/L. Groundwater, in particular, exhibited a higher concentration at 2.89 mg/L compared to surface water at 0.65 mg/L.

Nitrate ions dissolve seamlessly in water, lacking a discernible color, odor, or taste, which makes their detection in water challenging. Nitrate originate from various sources, including atmospheric processes and terrestrial activities. Water bodies in proximity to industrial facilities or agricultural land tend to exhibit high nitrate levels. Elevated nitrate concentrations in water bodies can lead to algae blooms, which sink from the

surface and decompose. As algae decomposes, it depletes oxygen from the water. Excessive removal of oxygen renders the water a "dead zone", indicating a body of water with very low oxygen levels, making it incapable of supporting the majority of aquatic life forms [10].

1.2 Motivation

High concentrations of nitrate in freshwater bodies have been a cause for concern for many decades, posing severe health risks. Aquatic ecosystems thrive in freshwater, and many regions around the globe depend on aquatic food sources. Several optical and electrochemical methods are used for the detection of nitrate ions in water, among which electrochemical impedance spectroscopy (EIS) has been commonly utilized, offering sensitive, fast, and accurate detection. Current research on nitrate detection in water using EIS has not filled the gap for a low-cost sensor that is sensitive, reusable, exhibits a small form factor, and is easy to fabricate, capable of detecting nitrate ions in a wide array of impurities present in real-world freshwater samples.

With the growth in population and the rise in the use of chemicals for industrial and agricultural purposes, the quality of our freshwater sources is deteriorating, resulting in various health issues caused by a high level of nitrate intake through water. Hence, there is also a need to monitor the quality of freshwater bodies to continuously gauge water quality parameters as well as nitrate ion levels. The literature has revealed no suitable sensor capable of field deployment due to the use of laboratory equipment, a complex sensor fabrication process, the high cost of the sensor, low sensitivity in real-world water samples, and reusability issues. There is, therefore, a need to develop a sensor that can overcome these drawbacks to monitor nitrate levels in freshwater bodies in real-time.

This research evaluates the performance of different geometric patterns of electrodes made using various materials for the detection of nitrate ions in water samples collected from three different freshwater sources. The main focus is to develop a sensor that could easily be fabricated while keeping the cost low and exhibiting certain attributes such as reusability, long-lasting sensitivity to the target ion with minimum drift, and having a small form factor that could collectively qualify it as a field-deployable sensor.

1.3 Contributions

The main contributions of this thesis can be summarized as below:

- A comprehensive review on various nitrate detection techniques in real-world water samples.
- Performance evaluation of interdigitated electrodes, fabricated from four distinct materials, used for detection of varying concentrations of nitrate ions in real-world water samples.
- A water quality monitoring system was also built to measure five water quality parameters: turbidity, pH, electrical conductivity, temperature, and total dissolved solids. The aim of this system was to understand the quality of water in freshwater sources in the local area.

1.4 Thesis Layout

This thesis with publications is organised as follows:

Chapter 2 presents a comprehensive review of techniques that are ideal for field-deployable nitrate sensing applications, with an emphasis on electrochemical and optical detection methods. It discusses the underlying principles, recent advances, and various measurement techniques. Furthermore, the review explores the latest developments of real-time nitrate sensors and discusses the challenges of real-time, in-situ implementation.

Chapter 3 includes a study on the performance evaluation of various electrode geometries for sensitive and accurate detection of varying levels of nitrate ion concentration in deionised water. The paper is currently in review with Springer - Sensing and Imaging.

Chapter 4 presents a study on the performance evaluation of four materials of interdigitated electrodes, used for sensing various concentrations of nitrate ions in real-world freshwater samples collected from three distinct bodies of water. This paper has been submitted and is currently under review for publication in MDPI Sensors.

Chapter 5 highlights the design and development of an IoT-based water quality system. Included in the chapter is the testing and analyses of basic water quality parameters from

three bodies of water, namely Lucas Creek, Lake Albany, and Lake Pupuke. Alongside, providing an insight into the quality of freshwater sources, the system also serves as a testing platform for the nitrate sensor presented in chapter 3 and 4. A paper based on this chapter has been published in PLoS ONE.

Chapter 6 summarizes the thesis and discusses the future work.

Chapter 2

Electrochemical and Optical Sensors for Real-time Detection of Nitrate in Water

2.1 Abstract

The health and integrity of our water sources are vital for the existence of all forms of life. However, with the growing population and anthropogenic activities, the quality of water is being impacted globally, particularly due to a widespread problem of nitrate contamination that poses numerous health risks. To address this issue, investigations into various detection methods for the development of in-situ real-time monitoring devices have attracted the attention of many researchers. Among the most prominent detection methods are chromatography, colorimetry, electrochemistry, and spectroscopy. While all these methods have their pros and cons, electrochemical and optical methods have emerged as robust and efficient techniques that offer cost-effective, accurate, sensitive, and reliable measurements. This review provides an overview of techniques that are ideal for field-deployable nitrate sensing applications, with an emphasis on electrochemical and optical detection methods. It discusses the underlying principles, recent advances, and various measurement techniques. Additionally, the review explores the current developments of real-time nitrate sensors and discusses the challenges of real-time implementation.

2.2 Introduction

Water pollution is a global issue that demands continuous monitoring to ensure the safety and integrity of our water sources. The presence of nitrate in water can be a result of various sources such as runoff or seepage from fertilized soil, wastewater, landfills, animals or urban drainage. This phenomenon is known as eutrophication that poses a significant concern for estuaries. Eutrophication refers to the enrichment of the environment with nutrients, leading to an excessive growth of plants and algae in estuaries and coastal waters [11]. Substances such as heavy metals, nutrients, and pathogens are considered to be primary contaminants [12]. Among nutrients, nitrogen is the most commonly available nutrient in the atmosphere. Different gaseous forms of nitrogen are present in the air, such as nitrogen (N_2), nitrous oxide (N_2O), nitric oxide (NO), nitrogen dioxide (NO_2), and ammonia (NH_3). These gases react with rainwater and lead to produce nitrate. This nitrate mixes with groundwater or becomes a part of the soil layer. On the other hand, many anthropogenic activities such as excessive usage of fertilizers in agriculture, disposal of animal excretion, and industrial waste lead to an excess amount of nitrate content in the atmosphere that are the primary cause for nitrate pollution in water [13].

FIGURE 2.1: Nitrate leaching from soil/fields and industrial waste into surface water and groundwater.

The presence of nitrate ions can have a significant impact on the environment [14]. When present in nominal amounts, it can promote aquatic life. However, excess amount of nitrate levels could lead to harmful effects on the aquatic ecosystem such as increased production of algae and phytoplankton that stimulates eutrophication as illustrated in Figure 2.1. As these organisms decompose, they utilize more oxygen, leading to adverse

effects on marine life. Similarly, nitrate poisoning can also occur in animal farming which results in livestock abortions and reduced dairy production that leads to significant losses for farmers [15]. On the other hand, nitrate consumption can be beneficial to humans, as it can improve blood flow and lower blood pressure [16]. Meanwhile, excessive nitrate intake is always hazardous for humans and animals. Often nitrate is allowed to use as a food preservative in the food processing industry and helps in curing meat hence mostly used in fishery and salted meat preparations.

Furthermore, bacteria found in the human system can reduce nitrate ions to nitrite, resulting in the formation of carcinogenic N-nitrosamine compounds. As a consequence of these compounds, many health issues can occur including esophageal and gastric cancer [17], spontaneous abortion, congenital disabilities [18], and Parkinson's disease [15]. Newborns can experience "blue baby syndrome" or methemoglobinemia. Thus Nitrate has a vital role in environmental and human health monitoring, its detection and estimation are important [13, 19]. Hence, authorities such as European Union Directives (EUD) [16, 20] and World Health Organization (WHO) [16, 21] suggest 50 mg/L as the maximum permissible nitrate concentration in drinking water and food. Italian regulations recommend 45 mg/L for adults and 10 mg/L for infants [16, 20]. The United States Environmental Protection Agency (EPA) advises 44.2 mg/L [16, 22]. Additionally, the EPA, EUD, and Australia New Zealand Food Standards indicate 365, 10-500, and 50-500 mg/kg as the suggested levels in food, respectively [16, 23].

Traditionally, a variety of analytical techniques have been utilized for nitrate detection, that includes atomic absorption spectrometry, inductively coupled plasma mass spectrometry, ion chromatography, UV/VIS spectrometry, chemiluminescence, and electrophoresis. These techniques have demonstrated a high degree of nitrate detection accuracy. However, such techniques require periodic collection of water samples that would need to be transported to a laboratory for testing. This process could be costly due to the need for a specialized facility with expensive laboratory equipment, chemical reagents, and skilled technical personnel to operate the equipment. Such methods can generate chemical waste, adding to the overall cost. Moreover, periodic sample collection may not capture short-term contamination events [24, 25]. For this reason, it is always desirable to have a simple and field-deployable device that performs real-time nitrate detection cost-effectively. Hence, an increase in available portable monitoring devices has been observed. While implementing such portable devices, researchers come across

various challenges such as rapidly changing environmental and temperature conditions, limitations in accessing and servicing the equipment, and the lack of grid-power connections [26]. An ideal field-deployed nitrate sensor for water must be sensitive to detect nitrate concentration less than 1 mg/L in surface water. However, there are several challenges involved with the detection of nitrate in real-world samples. The complexity of the sample matrix is the most prevalent one. Real-world samples often contain various impurities such as dissolved solids, organic matter, and other ionic content that interferes with the detection of nitrate, which could affect measurement accuracy. Another challenge for a field-deployable sensor is biofouling. Over a period of time, biological growth on the sensor can interfere with accurate detection of nitrate, which could require regular cleaning and maintenance of the sensor.

In recent years, various methods have been explored to develop real-time nitrate monitoring systems that incorporated analytical techniques such as chromatography, colorimetry, electrochemistry, and spectroscopy. Among these methods, electrochemical analysis has emerged as a promising approach due to its simplicity, high sensitivity, accuracy, wide dynamic range, affordability, user-friendliness, and suitability for field deployable applications. As a result, researchers have begun to view electrochemical sensing as a favourable alternative to the more expensive conventional analytical techniques [24]. Hence, this review aims to provide an overview of the detection techniques that can be employed for real-time detection of nitrate ions in water with an ideal accuracy of less than 1 mg/L, that would allow integration with field deployable applications. The electrochemical approach is thoroughly investigated, including its underlying principles, electrode configuration, and various measurement strategies. The optical methods are discussed in detail as well. Furthermore, the review provides a thorough examination of current real-time nitrate sensors and their recent improvements. Lastly, the advantages and disadvantages of the potential methods are briefly highlighted.

2.3 Electrochemical method

2.3.1 Working principle

In an electrochemical method, oxidation or reduction current detect a particular analyte [27]. The primary element of any electrochemical sensor is an electrochemical transducer.

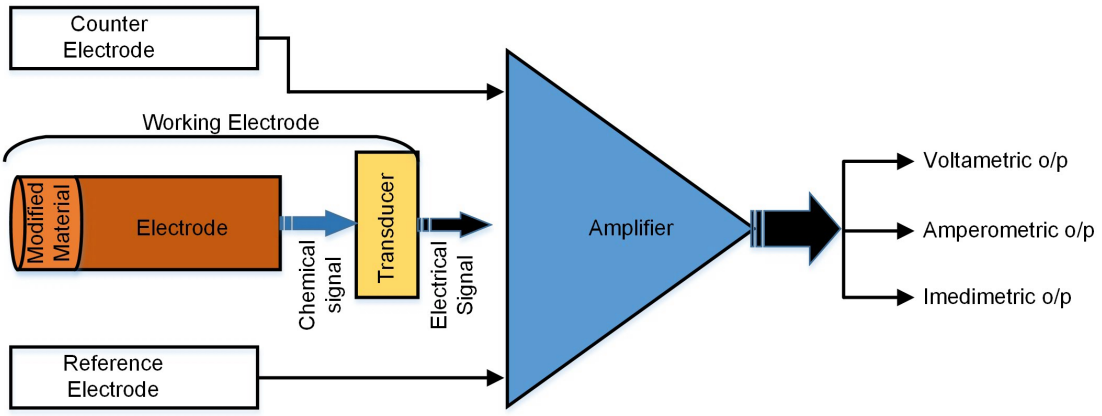

FIGURE 2.2: Working principle of the 3-electrode electrochemical method.

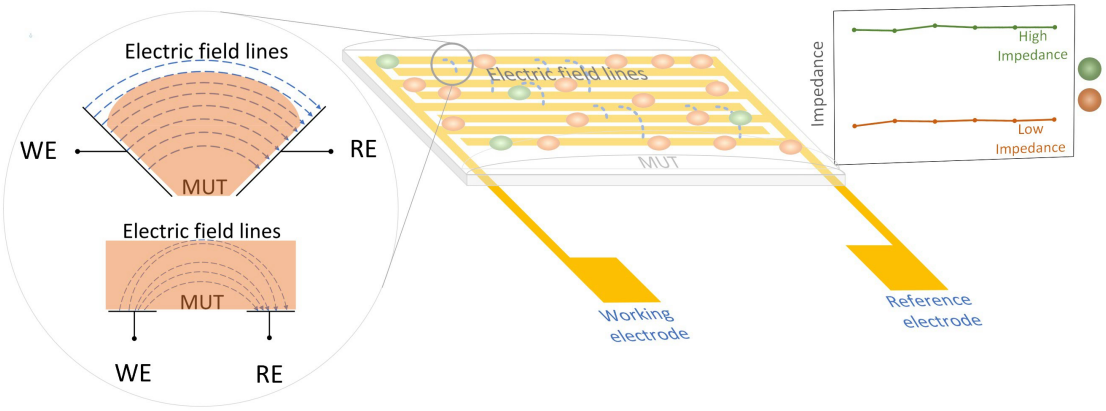

FIGURE 2.3: Working principle of 2D planar electrodes.

Transducer consists of a sensing element that reacts with the target analyte and transforms the chemical reaction into an analytical signal. Typically, the electrochemical sensor is a three-electrode system that includes the reference electrode (RE), the sensing/working electrode (WE), and the counter electrode (CE). The electrolyte reaction occurs at the working electrode. This electrode is generally modified with nanomaterial to accelerate the electrolytic reaction. The reference electrode provides the correct application of the working electrode potential. The counter electrode is used to complete the circuit and helps in continuing the electron flow [16]. Figure 2.2 illustrates the working principle of the method in a 3-electrode system.

On the other hand, simpler "two-dimensional planar electrodes" is the phrase given to a configuration of parallel geometry of electrodes that are constructed on a flexible or rigid substrate. A traditional pair of electrodes comprises of a working electrode (WE) and a reference electrode (RE) [28]. RE is used as the excitation electrode and WE senses the resulting phase shift of current with respect to the input signal on RE. The ability of

single-sided access to the MUT makes IDEs ideal for in-situ analysis. Figure 2.3 illustrates the working principle of 2D planar electrodes. Recently, 2D planar-style sensors have gained popularity in sensing applications. The most commonly employed pattern is a parallel comb-like structure referred to as an interdigitated geometrical pattern. However, there are other geometric patterns that can be used in sensing applications that were evaluated for their performance in our previous work [29]. The working principle of planar electrodes involves the generation of an electric field when a low-amplitude AC signal is applied across the two electrodes. The ions present in the material under test (MUT) react to the applied signal by aligning themselves with the produced electric field, surpassing their random thermal motion, leading to modifications in parameters like electrical impedance [30]. This interaction results in changes to the electric field and the current in the working electrode. Either of the two well-known measurement quantities, namely capacitance and impedance can be utilized to determine the amount of ionic content in the solution [31]. Table 2.1 highlights some advantages and disadvantages of 2 and 3 electrode systems.

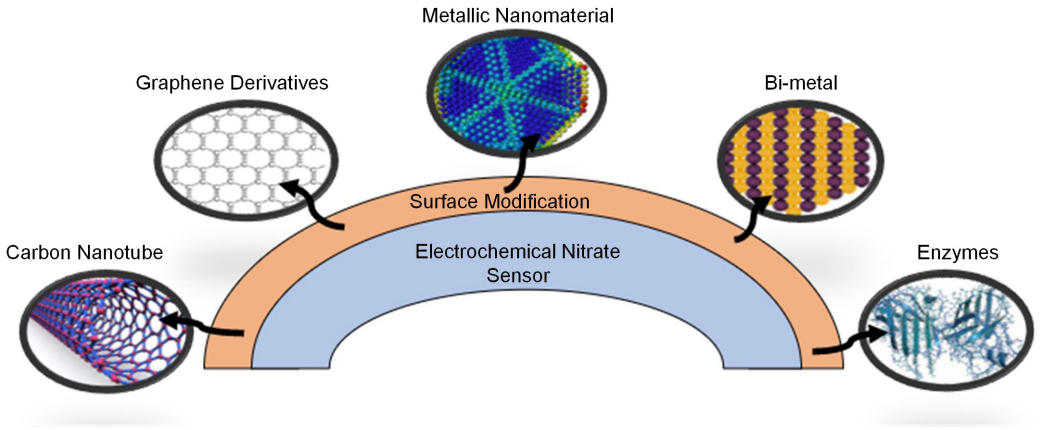

FIGURE 2.4: Material used for surface modification of the working electrode.

2.3.2 Electrode design

Nitrate reduction on the cathode surface is an essential characteristic of electrochemical sensors. Hence, electrode material and electrode design play a significant role in the performance of an electrochemical sensor. In the last two decades, metals like Ru, Rh, Ir, Pt, Pd, Cu, Ni, and Ag have been studied for nitrate detection using electrochemical analysis. Cu was found to be the most promising electro-catalyst in the nitrate reduction

reaction among all of these. [32–36]. Hence, many Cu-based electrodes such as copper-deposited platinum micro-electrode [37], copper-coated bismuth [38], copper-modified pencil graphite [39], an array of copper micro-electrodes [40], copper co-modified carbon fibre electrodes [41], and nanowire-based Cu electrodes [32] have been used in nitrate analysis.

Furthermore, various catalyst nanomaterials are synthesized with the working electrode to achieve a significant result in nitrate detection. Modified electrodes in electrochemical analysis lead to the advantages like a rapid response, decreased over-potential, high sensitivity, and high selectivity compared to conventional electrochemical sensors. The nanomaterials (Figure 2.4) that have been considerably studied for surface modification of working electrodes in nitrate sensors comprise graphene derivatives [42–44], carbon nanotubes (CNTs) [34, 45], carbon fibres [46], metal, bi-metal, and metal oxide nanoparticles, and conductive polymers. Alongside enzymes have been explored for the same [16]. Various adaptations of electrode materials have been employed in conjunction with IDEs. These electrodes are fabricated from metals like gold [47], silver [48], copper [49], and carbon [41] which exhibit excellent electrical conductivity. For example, IDEs have frequently been utilized to measure the pH level of an aqueous solution by detecting H+ ions [47, 50, 51]. Often electrodes are modified for enhanced detection of the desired ion [52]. Modifications with nanoparticles such as gold, silver, and non-metallic elements such as sulphur and carbon have also been applied [36, 53–55]. Similarly, for the detection of nitrate ions in water, the electrodes are often modified with various metals for enhanced sensitivity to nitrate ions [56, 57].

2.3.3 Electrochemical measurement techniques

The sensor's output can be either current, voltage, or impedance. Hence, electrochemical methods for nitrate detection can be categorised into voltammetry, amperometry, potentiometry, and Electrochemical impedance spectroscopy (EIS). Different voltammetric schemes are used for nitrate detection such as cyclic voltammetry (CV), differential pulse voltammetry (DPV), square wave voltammetry (SWV), and linear sweep voltammetry (LSV). The difference among these strategies remains in the way the voltage is applied. In CV, the current generated during nitrate reduction is determined by changing the anodic and cathodic sweep of the working electrode potential. Comparatively, LSV is

TABLE 2.1: Advantages and disadvantages of 2 and 3 electrode design

	Advantages	Disadvantages	Ref
2-electrode	- Suitable for portable or handheld sensor - Provides a cost-effective design - Simple design and implementation - Easy to operate	- Limited dynamic range - Prone to drift	[60, 61]
3-electrode	- Accurate and stable results - Wider dynamic range of detection - Reduced drift and improved reliability	- Expensive and larger in sensor size - Increased complexity of measurement setup - Require regular maintenance and calibration	[62, 63]

the simplest method, where the applied potential is increased linearly with the corresponding current measurement over time [58]. On the other hand, in DPV and SWV, pulse techniques are used by superimposing a potential staircase. In SWV, the difference between forward and reverse pulse currents indicates the nitrate concentration. In DPV, the current is measured just before and after applying each pulse. Then the current difference is obtained for the applied staircase potential [16]. DPV is a widely used technique for real-time nitrate detection among the various available electrochemical methods since it is suitable for field deployment, requires short processing time, and is cost-effective [59].

Extensive research has been conducted in the past decade, utilizing IDEs to identify dissolved impurities in the form of ions in water for the purpose of water quality assessment. Techniques such as DPV, LSV, and CV are frequently employed with 3-electrode sensors. Conversely, As previously mentioned, impedance and capacitance are the two measurement techniques that are often used with a 2-electrode interdigitated form of sensors (IDE) [64] to detect the presence of ions in water or other aqueous solutions that are favored for their compact size, affordability, ease of fabrication, and non-destruction of sample [65]. Capacitance and impedance are related to each other of which impedance is a broader term that encompasses both resistance and reactance. Reactance is further divided into two components namely, capacitive and inductive reactance. Capacitive measurements are performed by treating the material under test as a dielectric that measures the amount of charges stored within the material. Charges in the solution build up around the oppositely charged surface of the electrodes and this accumulation of charge closely resembles the working principle of a capacitor [66]. This concept can be extended to nitrate ions and the variations in the density of the ionic content in MUT would influence the dielectric properties. To analyse the capacitive behaviour of the IDEs, Alahi et al. [67] studied the capacitance sensitivity of the IDEs with a nitrate-sensitive polymer coating on top of the electrodes, achieving a limit of detection

of 4 mg/L up to 14 mg/L with capacitance measurements of 5.3 nF to 5.9 nF respectively. This approach was explored further by Ludena-Choez et al. [30] who studied the capacitance sensitivity of IDEs using graphene as the electrode material for the detection of nitrate concentration in water. Their temperature-controlled experiment showed linearity with respect to temperature at -2.54 kΩ °C with 1.71 ppm of nitrate level in agricultural soil as the limit of detection. The impedance measurement is well-suited for interdigitated sensors due to its ability to capture a broader range of electrical changes and provide more detailed information about the sensing behavior.

Bui, M.P.N et al. [59] reported a paper-based electrochemical sensor for the detection of both nitrate and mercury ions in lake water and polluted agricultural runoff using the DPV technique. Functionalized disposable carbon paper was used for the electrodes. Selenium particles (SePs) and gold nanoparticles (AuNPs) were synthesized to modify the electrode. The AuNPs worked as a catalyst for the nitrate ions reduction and nucleation sites for mercury ions. The modified electrode showed high sensitivity towards nitrate and mercury without any interference. The limit of detection reported for nitrate was 8.6 μM and for mercury 1.0 ppb. Thus, this sensor shows the significant possibility for the simultaneous detection of nitrate and mercury ions in potable and environmental water. In another assay [32], Cu electrodes were prepared with thermal annealing of Cu nanowires. The authors observed a well-shaped reduction peak for even low nitrate concentration via DPV. They reported a LOD of 1.35 μM with a sensitivity of 1.375 μA/μM at a signal-to-noise ratio of 3. Similarly, Mumtarin, Zannatul et al. [68] reported a simple and economical approach of nitrate sensing via reduction reactions at Cu immobilized platinum surface in the neutral medium. The sensor parameters were ascertained by DPV technique. The sensor exhibited excellent sensitivity (2.3782 μA $\mu M^{-1} cm^{-2}$), very low LOD (0.159 μM; S/N = 3) and long-term storage ability with good reproducibility. In the same vein, a nanostructured sensor based on a copper nanowires array is obtained using the simple method of galvanic deposition. This sensor has a quick reaction time and can detect concentrations below 10 μM [69].

In amperometric methods, the current is measured over time at a constant applied potential. The current is proportional to nitrate concentration. It is mentioned in the literature that this method has excellent sensitivity with low nitrate detection limits [16]. For example, Inam, A. K. M. S. et al. [70] developed a nitrate sensor with a sensitivity of 19.578 μA/mM and a LOD of 0.207 nM or 0.012 μg/L using flexible screen-printed

electrodes functionalized with electrodeposited copper. Whereas, Can F. et al. [45] fabricated a biofilm electrode for amperometric nitrate measurement with a low LOD of 0.17 mM with a sensitivity of 300 nA/mM.

Potentiometry is another distinguished nitrate detection electrochemical method exceptionally used for complex sample matrices like soil. It measures the potential difference between the ion-selective electrode (ISE) fabricated with nitrate-specific ionophore and the reference electrode in the absence of current. ISE can be either liquid-contact ISEs (L-ISEs) or solid-contact ISEs (S-ISEs), based on the contact type of the inner side of the membrane. The maintenance of S-ISEs is easy compared to the L-ISE. Hence, S-ISEs are preferred over L-ISEs, for nitrate detection, where they serve as an ion-to-electron transducer [16]. EIS is one more highly sensitive electrochemical method. In EIS, the system characterization can be assessed by measuring the sensor impedance. Generally, a sinusoidal signal with an amplitude of 5–15 mV is connected to the working electrode, and the resulting voltage is measured from the sensing electrode. The overall measurement process is carried out in a specific frequency range to obtain the impedance profile [71]. Alahi Md. Eshrat EE et al. [72] used the interdigital capacitive sensor functionalized by an acrylic resin with an embedded coating material for nitrate detection with the detection limit was 1-10 mg/L, with the sensor costing less than $10. Similarly, Ali Md Azahar et al. [73] reported a microfluidic nitrate sensor using an enzyme-modified electrode with a sensitivity of 0.316 $k\Omega/\mu M/cm^2$. Even though, EIS method-based sensors require less sample pretreatment, the sensitivity of these sensors is lower compared to amperometric or potentiometric sensors [16]. Table 2.2 summarizes the specifications of different electrochemical methods.

Thus, electrochemical analysis of nitrate detection has been explored extensively by researchers due to its short response time, as an inexpensive instrument and can be used for direct onsite measurement [72]. Wan et al. [77, 78] demonstrated a rapid and sensitive procedure to determine lead and copper simultaneously using the commercial screen-printed gold electrode modified with the gold nanoparticles. A variety of catalysts including metals and nano-materials have also been incorporated to improve the overall performance of electrochemical assays. Noteworthy advancement has been observed to achieve nitrate-specific electrochemical properties by applying various synthesis processes [16]. For example, Essousi et al. [79] developed an ion-imprinted polymer-coated working electrode with Cu nanoparticles to improve the sensitivity. On the other hand,

TABLE 2.2: Comparison of various electrochemical methods.

Method	**Electrode**	**LOD**	**Linear range**	**Sensitivity**	**R^2**	**Ref**
DPV	PEG-SH/SePs/ AuNPs modified carbon paper	8.6 μM				[59]
DPV	Cu nanowires	1.35 μM	8 to 5860 μM	1.375 μA/μM	0.999	[32]
DPV	Cu immobilized platinum surface	0.159 μM	0.12 to 4.75 mM	2.3782 μA/μM		[68]
LSV	Cu nanowire array	9.1 μM	10 to 50 50 to 1500 μM	0.0636 0.73 μA/μM		[69]
Amperometry	Screen-printed Silver	0.207 nM	0.05 to 5 mM	19.578 μA/μM	0.987	[70]
Amperometry	Screen-printed graphite	100 nM	0.1 to 10 mM	0.12 μA/μM	0.999	[74]
Amperometry	Screen-printed carbon		0.01 to 0.25 nM	3.13 μA/μM	0.97	[75]
Amperometry	Polypyrrole/Carbon nanotubes film	0.17 mM	0.44 to 1.45 mM	300 nA/mM	0.97	[45]
Potentiometry	Screen-printed carbon	100 mM	0.1 to 100 mM			[76]
EIS	Interdigital capacitive	1 to 10 mg/L				[72]
EIS	Graphene foam based		1 to 1000 μM	0.316 kΩ/μM/cm^2		[73]

Wu et al. [80] used Cu nanoparticles by thermal oxidation to lower the LOD (12.2 μM). Even though, these methods are based on handled devices, still have disadvantages, like being still expensive, and the requirement of a person to move to the sample place. Additionally, it is difficult to synchronise the data obtained from several sample points. Most importantly data is not acquired in real-time and many additional features may not be achieved. Thus many of these methods are not suitable for in-situ monitoring, due to complex measurement procedures. This shows the need for investigating new in-line monitoring nitrate detection techniques to acquire real-time data with minimal processing cost [72, 81].

2.4 Optical method

2.4.1 Working principle

The principle of optical techniques is based on the behaviour of a sample when exposed to electromagnetic radiation (ultraviolet, visible, and infrared). Various materials, including organic and inorganic, living and non-living materials, are suspended and dissolved in the water. When light shines on the water's surface, some part is reflected off the surface while the rest travels through the water, interacting with the suspended and dissolved matter. The components of suspended and dissolved matter that can interact with electromagnetic radiation utilizing absorption, refraction, and scattering are known as optically active constituents (OAC). Common optical characteristics that can be used to measure concentration include the absorption or emission of radiant energy, the refraction of radiant energy, the scattering of radiant energy, and the delayed emission of radiant energy [82]. Typically, the optical instrument comprises a light source, a light detector, and various optical parts such as lenses, mirrors, prisms, and gratings. Among various optical techniques, UV spectroscopy is widely used for nitrate detection due to its simplicity, versatility, and feasibility. The optical sensors utilize the UV absorption spectrum to directly measure nitrate in real-time while in the field. The sensor's approach of using the UV absorbance of nitrate is in line with how benchtop UV spectrophotometry is performed in a laboratory. Within the sensor, a photometer gauges absorbance, which is the amount of light absorbed in the solution at a specific wavelength. The absorbance has a logarithmic relationship with the transmittance.

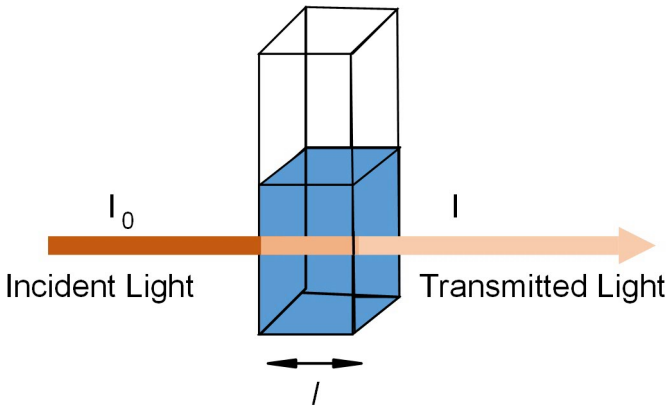

FIGURE 2.5: Transmission of light through a sample solution.

TABLE 2.3: Comparison of various optical methods.

Method	Absorbance range	LOD	Dynamic range	Sensitivity	Ref
Spectrophotometric	540 nm	3 uM	3-334 uM	0.5 uM	[84]
UV-Vis spectrometry	365 nm	2.3 mg/L	2.3-3.4 mg/L		[85]
Colorimetric		0.025 uM	0.025 - 350 uM	0.025 uM	[86]
Fibre optic	575 mn		0 - 2.5 mg/L		[87]

The transmittance, T, of the solution, is defined as the ratio of the transmitted intensity, I, over the incident intensity, I_0 as shown in Fig. 2.5 and represented by

$$T = \frac{I}{I_0}, \tag{2.1}$$

The absorbance, A, of the solution is related to the transmittance and incident and transmitted intensities through the following relations:

$$A = log_{10}\frac{I_0}{I}, \tag{2.2}$$

$$A = -log_{10}A, \tag{2.3}$$

2.4.2 Wavelength selection

This technique for analyzing nitrate concentration relies on measuring its absorbance at 210 nm. However, there are several interferences caused by other substances such as chlorine, nitrite, iron (III), and organic matter that also absorb in this same region, making it difficult to accurately determine nitrate concentration. To address this issue, the American Public Health Association (1992) developed a protocol that involves measuring the difference in sample absorbances at 220 and 275 nm using distilled water as a blank. This method helps to account for the interference caused by dissolved organic matter, which can absorb UV radiation at 220 nm, while nitrate does not absorb at 275 nm. Previous methods used for direct UV spectroscopy of nitrate involved measuring absorbance at 210 nm and another wavelength in the region where nitrate does not absorb UV radiation [83].

2.4.3 Measurement methods

There are three categories of spectrophotometric methods for determining nitrate: Griess Assay, nitrosation-based spectrophotometry, and catalytic spectrophotometry [88]. Johann Peter Griess discovered the Griess reaction in 1879 as a means to detect nitrate levels in saliva through a process called diazotisation. Since then, the Griess reaction has been utilized for a significant period of time to identify bacterial infections in the urogenital tract. Bacteria reduction reduces nitrate, the primary nitrogen oxide anion present in human urine, to nitrite which can be detected through the Griess reaction. The Griess test involves the conversion of an aromatic amine to a diazonium salt using acidified nitrite. This is then followed by a coupling reaction to produce a brightly colored azo compound. The concentration of this compound is determined spectroscopically within the range of 500-600nm, which helps measure the amount of nitrite present [88]. Miranda K.M. et al. [84] used vanadium (III) to reduce nitrate and detect nitrate and nitrite concentrations simultaneously, employing the acidic Griess reaction. Catalan-Carrio et al. [85] developed a compact and portable device that can detect nitrite and nitrate in water samples using multivariate analysis of color readings from the device's sensing sites. The device incorporates both the sample analysis and calibration sites. It is based on an ionogel material with an integrated Griess reaction. This handheld device is the first of its kind. It enables the determination of nitrite and nitrate levels in actual water samples. Beaton A.D. et al. [86] created a portable platform for measuring nitrate levels in the field, which used the Griess assay and microfluidic technology. This was the first of a new generation of small analyzers and had low power consumption. To ensure accuracy, the system utilized on-chip absorption cells made from colored PMMA that blocked out any background light. As a result, the system was highly sensitive and had a broad dynamic range (0.025 to 350 μM), making it suitable for analyzing nitrate levels in different types of natural water [87].

Furthermore, significant advancements have been made in the development of a fibre optical sensor for analyzing water quality. This sensor comprises of three crucial components: a light source, an optical fibre, and a photodetector responsible for detecting the optical signal. When selecting an optical sensor, there are two main categories to choose from: intrinsic and extrinsic sensors. Intrinsic sensors rely on a continuous and consistent light source to enable a phase-modulation technique. This modulation takes

place within the optical fibre, and the sensor design specifically employs a single-mode fibre. On the other hand, extrinsic optic sensors utilize fibre as a means of transmitting the optical signal. They are particularly advantageous for remote sensing applications due to their compact size and low power requirements. Additionally, extrinsic sensors find utility in the detection of nitrate and nitrite levels in the water [13]. Camas-Anzueto J.L.et al. [89] reported an extrinsic sensor having Lophine as a sensitive layer on the fibre. The sensor can detect concentrations of 1 to 70 mg/L and has a response time of 20 milliseconds. The sensor operates at a wavelength range of 300-1100 nm for detection. In a similar manner, Chong, M. Y. and colleagues utilized fibre optics and optical sensing technology to investigate nitrate levels in the water. Wavelengths of 350 nm to 2500 nm have been reported to detect the nitrate, and the detection range was 0–2.50 mg/L. To illuminate the samples, they utilized a halogen lamp in conjunction with an ASD FieldSpec 3 Hi-Res Portable Spectro-radiometer. A disposable optical sensor was created for detecting nitrate. The sensor utilizes a recognition system based on an artificial C_3 symmetry amide-based ionophore and has the ability to detect nitrate within a broad range of concentrations (26 μMM to 63 mM). However, this sensor has been noted to have longer response times of up to 5 minutes and reduced accuracy as its drawbacks [60].

Sensors that use spectrophotometers and don't need reagents to show potential for monitoring nitrate in the environment. Nevertheless, additional research is necessary to tackle sensor drift that can occur over extended periods. It is worth highlighting that the deuterium light sources found in UV/Vis spectrophotometric systems are highly stable and can last up to 5000 hours (around 7 months). However, there are significant issues with chemical fouling, which causes chemical precipitation, and biofouling, which leads to the accumulation of organic substances on the sensor optics. As a result, regular cleaning and rinsing of the sensors are required when measuring nitrate [90].

2.5 Real-time nitrate sensors and recent developments

In the past decade, researchers explored different methods to develop a real-time nitrate monitoring system. Su et al. [91] reported a novel approach to real-time monitor nitrate concentration through the competitive relationship between microbial denitrification and electrogenesis processes. This development offered to extend the application

of bio-electrochemical technology in water technology. Bluett S. et al. [92] implemented an in-situ ion chromatography analyser to measure nitrate and nitrite concentration in remote surface water applications. They also developed a self-cleaning 3D-printed Sediment Trap to filter the sample before the measurement preventing silt and sediment from causing blockages. In addition, they also developed a solar-powered battery and an internal heater to facilitate off-grid deployments of the analyser in remote locations. Beaton A. et al. [86] developed a lab-on-chip (LOC) colorimetric system with a membrane sample filter for measuring nitrate and nitrite levels at a remote glacier where high sediment loads were regular. They used microfluidic technology to obtain a miniaturised version of the field analyser. Reported LOD of the system was 0.025 μM and 0.02 μM for nitrate and nitrite, respectively. On the other hand, field-effect transistor (FET)-based sensors have drawn considerable attention in chemical and biomaterial sensing due to their high sensitivity, real-time response, outstanding performance, straightforward operation, and label-free detection. Chen X. et al. [93] reported an rGO-based FET platform modified with benzyl triethylammonium chloride (TEBAC) for sensitive and selective electronic detection of nitrate ions in water. This sensor can detect nitrate concentration level from 0.0028 to 28 mg/L and is suitable for real-time and in situ.

Current alternative methods include in-line analysis with electronic instruments. In recent years, the use of machine learning for estimating water quality through remote sensing has gained popularity due to advancements in algorithm development, sensor systems, computing power, and data accessibility. Machine learning refers to a collection of statistical techniques that allow a computer to automatically learn from data and develop models for detection, estimation, or classification that minimize the difference between the training and prediction data sets without explicit programming. This approach, also known as statistical learning, involves feeding data into a computer that can be "trained" using pre-defined features or objects to enable semi-automated or automated detection, classification, or pattern recognition [82]. Additionally, Wireless Sensor Networks (WSNs) and Internet of Things (IoT) technologies have been rigorously investigated for in-line water quality monitoring in the literature [94–98]. WSNs expand the abilities of in situ monitoring systems. Although classic in situ approaches allow computation on-site, they require that the gathered information be transported manually to control centres or remote stations for further examination and action. WSNs allow the automatic transfer of data. They provide a feedback process in some instances

TABLE 2.4: Comparison of wireless transmission protocols

Wireless transmission	**Merits**	**Shortcomings**	**Ref.**
Bluetooth	1.Simple and convenient communication 2.Data transfer rate can meet the short distance transmission 3.Completely free	1.Less distance covered 2.Support less no. of nodes 3.Transmission stability is not high 4.Unreliable communication	[101]
Wi-Fi	1.High bandwidth 2.Fast communication due to higher transmission speed 3.Get a variety of large-scale wireless device manufacturers affirmed	1.Short range 2.High power consumption 3.Cost is involved 4.Security issues	[28]
ZigBee	1.Low power consumption 2.Easy to install 3.Support large number of nodes 4.High reliability network 5.Strong security	1.Low data speed 2.Low transmission, as well as low network stability	[98]
LoRa	1.Low power consumption 2.Long range coverage 3.Supports a large number of nodes	1.Limited Bandwidth 2.Limited message size 3.Complex network setup	[57]
Sigfox	1.Low power consumption 2.Long range coverage 3.Low cost 4.Easily scalable	1.Limited Bandwidth 2.Limited network availability 3.Small data packet	[102]

as well to enhance the quality of data collection. Generally, a WSN includes the sensor unit called sensing nodes, a processor for signal processing, the interfacing circuitry, a transmitter/receiver system for connectivity, and a power supply [99]. WSN has obvious advantages such as wireless communication, multiple in-line sample points, temporal and spatial evolution, low cost, and fast deployment [100]. The strengths and weaknesses of various wireless transmission protocols used in WSN are summarized in Table 2.4.

Various authors reported WSN-based water quality monitoring systems in the past few years. For example, Gartia et al. [103] designed miniature nitrate sensors to monitor nitrate concentration through the WSN. This method has the constraint that it was a sample-based system and unable to provide continuous in-line measurements. Corke P. et al. [97] developed a sensor node to monitor salinity in ground waters as well as the water temperature in surface waters. Tuna et al. [104] proposed portable sensor nodes mounted on buoys with wireless interfaces to monitor electrical conductivity, dissolved oxygen,

pH, temperature, turbidity, and nitrate. Wang et al. [105] presented a wireless network based on TinyOS, LabVIEW, and MySQL for pH, nitrate, and phosphate monitoring. However, due to multiple sensor nodes, energy-harvesting techniques and hibernation play a crucial role while extending the system life span [98]. Nasser N. et al. [106] implemented a WSN-based water quality monitoring system using Squidbee sensor motes and pH sensors to provide pH data in real-time. They designed a system with an information portal and an alternate sleep mechanism to prolong the network lifetime. In [107] and [81], the researchers developed a WSN and a solar panel-based energy harvesting system to detect nitrate, chloride, and ammonium concentration in lakes and rivers.

The IoT helps any physical entities to be sensed, monitored, and transmit data to a specific server via the Internet. Thus, it makes it possible to integrate the physical world into computer-based systems, which enhances precision and decreases human intervention. Extensive computing, smart sensors, embedded devices, communication technologies, Internet protocols, and applications are essential for IoT. Over a period, IoT has developed and is being applied in water quality monitoring. A smart system that uses IoT technology to analyze sensor data can automatically monitor water quality and promptly alert water analysts if there are any abnormalities. The implementation of Machine to Machine Communication makes it easier and more efficient to analyze and communicate the data [108]. IoT-enabled WSNs assist in securing more entity connections for monitoring purposes and help in building smart cities, smart industries, smart agriculture, etc.

In [71], authors integrated WSN with IoT by designing a smart sensing node to monitor the nitrate levels in the field. The sensing node collects water from a lake, stream, or river, measures the instant nitrate concentration, and transfers the data through the gateway to a user-defined cloud server. Agir I. et al. [109] proposed an electro-analytical wireless sensor for online monitoring of nitrate and ammonium in water. They developed ion-selective nitrate and ammonium electrodes and combined them with a portable IoT system. Similarly, in another study [110], authors proposed a real-time water quality monitoring system based on a wireless sensor network enabling IoT capability. This affordable system can perform real-time analysis of various water quality parameters such as pH level, temperature, nitrate, chloride, and dissolved oxygen that issues timely warnings. Yet another IoT-enabled real-time smart nitrate sensing system was developed

[111] where the authors reported the fabrication process of carbon nanotubes (CNT) with PDMS polymer coupled with graphene-based interdigitated sensors.

2.6 Discussion

Conventionally nitrate level measurement is accurately performed offline in the laboratory. The disadvantages of such offline methods have already been discussed in the introduction. Additionally, it's understood that when samples are stored, their quality may be compromised by various factors such as biological activity and matrix effects, despite adherence to proper handling protocols [81]. Inline analysis has significant benefits over traditional offline methods. Firstly, it eliminates or reduces sample contamination resulting from sample handling, as there is minimal sample transformation involved. Secondly, it reduces the overall cost of data acquisition by saving time on sampling, handling, and analysis of the sample [81].

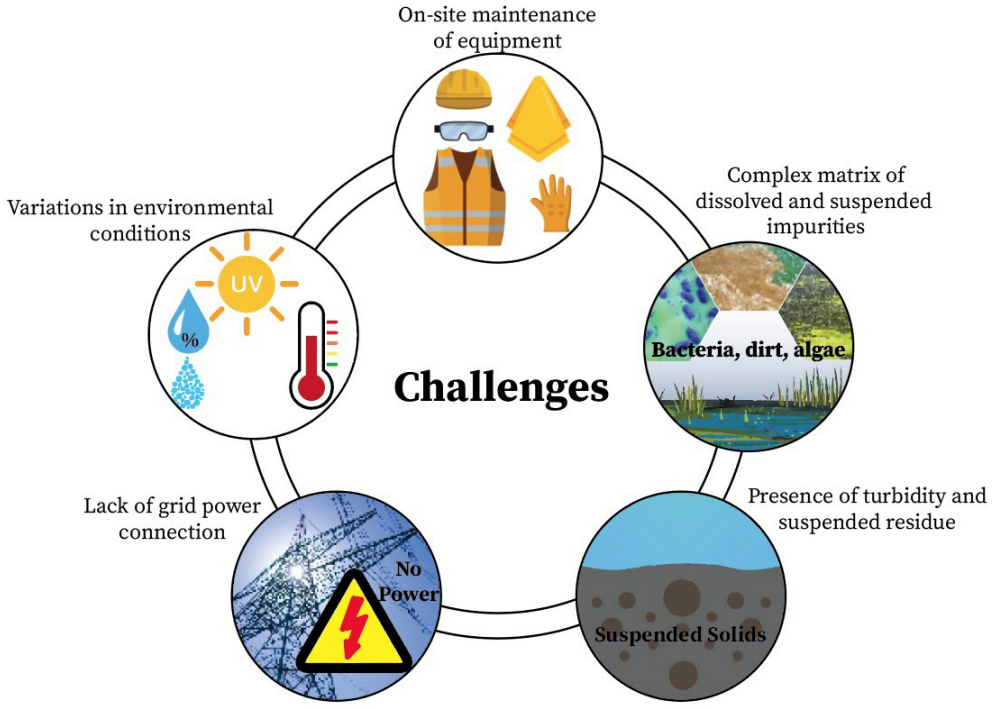

FIGURE 2.6: Challenges during implementing real-time nitrate sensors.

Several analytical techniques can be conceivably employed for the real-time detection of nitrate, such as chromatography, UV spectroscopy, various colorimetric methods, and electrochemistry [92]. However, each of these methods has one or other challenges during implementation (Figure 2.6). Most of the time natural waters are situated in remote

places where there can be a lack of grid power connection. Environmental and temperature conditions are not constant all the time. Additionally, factors such as changing levels of turbidity and suspended residue in natural waters can limit the performance reliability of the analytical equipment [92, 112]. Furthermore, restrictions in accessing, cleaning, and servicing should be considered. Many in-line nitrate sensors require regular and effective cleaning of the probes to ensure accurate readings. The cost of cleaning is a significant factor, sometimes making up to 50% of operational expenses. Common cleaning techniques include ultrasonic, brush, water-jet, or chemical-based automatic cleaners. However, some new and cost-effective methods have been suggested, such as electrolysis, which actively removes buildup, or using copper mesh or CuO_2 doped materials, which passively prevents fouling [96].

The techniques discussed in this review that can be incorporated in autonomous field-deployed applications are a step towards industrial revolution 4.0, often referred to as Industry 4.0 [113]. Continuous monitoring of contaminants in water is beneficial and useful for environmental agencies and city councils. Currently, water quality monitoring largely takes place in laboratories where trained personnel operate expensive machinery in specialized facilities. Sample collection also involves an arduous process, which involves careful transportation to the lab. Industry 4.0 factors in the cost and labour involved and offers low-cost solution to monitor the quality of water by researching techniques that can be incorporated with sensitive and selective sensors, having small form factor that could be integrated for autonomous monitoring of nitrate ions in water.

There is a strong correlation between suspended residue levels and turbidity. In UV absorbance-based optical nitrate analyzers, turbidity induces a scattering effect that influences the absorption spectrum and results in detection errors. Besides, many dissolved components are present in natural water that absorb the UV wavelength and influence the UV sensor response due to interference and matrix effect [92, 114].

Colorimetric analyzers offer potential for real-time nitrate determination due to the lower energy demand and reagent consumption of microfluidic systems [115]. Nevertheless, colorimetry is susceptible to temperature changes and necessitates constant calibration using reference standards to compensate for these alterations [112]. Additionally, sample turbidity variations can influence analysis accuracy [116]. The colorimetric reagents and

TABLE 2.5: Summary of potential method

Potential methods	Strengths	Limitations
Colorimetry	Lower energy consumption Use of microfluidic system reduces reagent quantity	Influenced by temperature variation Needs regulator calibration Requires regular cleaning of sensor Reagents are often hazardous and toxic Turbidity variations affect accuracy
UV spectroscopy	High sensitivity Non-destructive technique Rapid measurements Wide wavelength range Quick response	Sensitive to turbidity Prone to inaccurate data due to sample matrix Variability in absorbance maxima
Electrochemistry	Affordable equipment Wide dynamic range Non-destructive technique Ability to perform on-site measurements	Suffers from drift overtime Sensitivity to temperature changes Prone to inaccurate data due to sample matrix

standards required are often hazardous and toxic, making the development and upkeep of remote systems more difficult.

The popularity of using electrochemical analysis to detect nitrate is increasing due to its advantages, including fast response times, affordable equipment, and the ability to measure on-site. However, current research on this type of analysis has certain limitations, such as the need for sample collection, challenges in synchronizing data from multiple sample points, and the inability to obtain real-time data or additional features. As a result, existing electrochemical methods are not suitable for on-site monitoring due to their complex measurement procedures. Table 2.5 presents a summary of the strengths and weaknesses of different approaches that could be utilized to install nitrate sensors in real time. Nevertheless, there is potential for electrochemical analysis to be used for real-time nitrate detection.

2.7 Conclusion

The utilization of thin-film electrodes for the detection of nitrate ions in water has shown great potential for accurate and efficient analysis. The unique geometric design with closely spaced fingers, provides a large surface area for enhanced interaction with nitrate ions. This feature enables sensitive detection and precise quantification of nitrate levels, making interdigitated planar electrodes a valuable tool for water quality monitoring.

Various detection techniques have been employed with interdigitated planar electrodes to detect nitrate ions in water, including impedance spectroscopy, cyclic voltammetry, and amperometric methods. Each technique offers distinct advantages such as high sensitivity, rapid response, and wide dynamic range. Researchers have been able to customize the detection technique based on their specific requirements and optimize the performance of interdigitated planar electrodes for nitrate ion detection.

As research in this field continues to advance, further improvements in interdigitated planar electrode design, material selection, and detection techniques can be explored. Such improvements have shown enhanced sensitivity, selectivity, portability, and reliability that are ideal for applications that require field deployment. A few studies have also come to light for real-time systems, determining the amount of nitrate ions in the water while providing sensor data instantaneously. This involves interfacing the sensing electrodes with the IoT platform to enable remote monitoring of sensor data.

In this review, we delve into the wide range of detection techniques that include various field-deployable electrochemical and optical methods such as optical fibre and UV-visible spectroscopy that can be used to monitor nitrate levels in real-time, but primarily focusing on electrochemical methods that have been integrated with planar electrodes to achieve targeted detection of nitrate ions in water. The review comprehensively examines the advantages and limitations of various detection techniques, as well as the utilization of both 2-electrode and 3-electrode systems. Furthermore, we provide an overview of the existing research conducted on real-time nitrate monitoring systems. Interdigitated electrodes have gained popularity in the past 2 decades in the detection of nitrate ions in conjunction with impedance and capacitive measurement techniques. Among these techniques, impedance measurements have gained popularity due to their simplified measurement process that can also be achieved using dedicated impedance converter integrated circuits (ICs). We discuss the intricacies and advancements of impedance-based measurement methods and highlight their widespread use in nitrate ion detection with interdigitated electrodes. By examining these diverse detection techniques and their integration with planar electrodes, this review sheds light on the progress made thus far in the field of nitrate ion detection in water. The findings contribute to a better understanding of the strengths and limitations of various approaches, paving the way for further advancements in real-time nitrate monitoring systems and the improvement of water quality management strategies.

Looking ahead, the field of nitrate ion detection in water using interdigitated planar electrodes holds promising prospects for future advancements. One potential direction for future research is the development of miniaturized and portable detection systems that can provide real-time monitoring of nitrate levels in various water sources. This would enable rapid and in-situ assessment of water quality, facilitating proactive measures to address nitrate pollution and ensure the safety of drinking water. Furthermore, there is scope for exploring novel materials and surface modifications for interdigitated electrodes to enhance their sensitivity and selectivity towards nitrate ions. The integration of nano-particles or conductive polymers could offer enhanced electrochemical properties and facilitate more precise nitrate ion detection. It is also possible to combine planar electrodes in schemes such as microwave resonators [117–119]. Furthermore, integration of 3D-printed microfluidics [120] could allow the system to work more efficiently. Additionally, the incorporation of smart sensing technologies, such as wireless communications and data analysis algorithms, could enable the development of intelligent nitrate monitoring systems that could perhaps be linked to weather forecasts to predict a rise in nitrate levels and inform authorities.

Sensors that measure various physical parameters are often subjected to harsh environments, which makes building robust sensors challenging. There is a high demand for properties such as repeatability, sensitivity, low cost, and selectivity in sensors, which presents opportunities for advancements in sensor technology. Several commercial sensors and systems are available, specifically designed for sensing various parameters related to water, such as water quality, nutrient levels, and heavy metals [121–123]. Some of these systems can even provide real-time monitoring by utilizing sensors for continuous data collection. However, it's important to note that each system comes with its own set of advantages and disadvantages, which should be carefully considered during the selection process.

Chapter 3

Investigation of Planar Electrodes for Electrochemical Impedance Spectroscopy-based Detection of Nitrate in Water

3.1 Abstract

Electrochemical impedance spectroscopy (EIS) is frequently utilized in a wide range of sensing applications due to its versatility. The accessibility provided by low-cost impedance devices has further enhanced their usefulness in various fields. To improve sensitivity and reduce costs in sensing applications, miniature planar electrodes are commonly used for performing impedance spectroscopy. While the interdigitated geometric pattern is the most popular, other geometries, such as square and serpentine, can also be employed and compared based on their performance. In this study, nitrate ions dissolved in deionized water were used to investigate the behavior of different electrode geometries at varying concentration levels. The study aimed to determine the effect of different geometries and materials on sensing nitrate ions and establish performance characteristics of various electrode patterns fabricated using silver and copper on PMMA and fiberglass laminate substrates, respectively. The results showed that both interdigitated and

square geometries provided reliable impedance curves when sweeping frequencies from 100 Hz to 100 kHz, sensing a range of nitrate ion concentrations from 0.5 to 0.1 mg/L.

3.2 Introduction

Fresh water sustains natural ecosystems and is the most precious natural resource essential to life. One of the most common contaminants is nitrate (NO_3^-), which is composed of nitrogen and oxygen atoms. It is an essential plant nutrient that has no discernible odor, color, or taste. Nitrate can originate from various anthropogenic sources, such as agricultural land runoff, industrial discharge, and wastewater treatment plants [124]. Nitrate is known to have adverse effects on human health, such as reduced hemoglobin levels, which could lead to weakness, increased heart rate, and, in some cases, trigger thyroid disease. Continuous intake of high levels of nitrate could also cause certain types of cancer.

The safe level of nitrate in drinking water is said to be less than 10 mg/L. A study conducted in 2021 showed that the safe level of nitrate in drinking water was exceeded by 11 times in some rural areas [125]. This is why monitoring the levels of nitrate at least in our drinking water supply is imperative.

The determination of nitrate ions in water has been the focus of study by many researchers for the last two decades due to a surge in anthropogenic activities [126]. As shown in Fig. 3.1, a diverse range of analytical methods have been developed to detect the level of aqueous nitrate ions in water. This can be achieved through various detection methodologies such as capillary electrophoresis, chromatography, spectroscopy, and electrochemical [127]. Most of these are laboratory-based methods that require expensive equipment, specialized facilities, and trained personnel. The traditional approach for the determination of nitrate ions in water involves sample collection which needs to be carefully transported to the lab for testing. This approach would require a certain level of mediation which would be both inefficient and costly for regular procurement of samples. These drawbacks can be reduced or mitigated by the use of sensors that can be deployed in the field to provide regular sensor data. This can be achieved by employing a detection method that can be carried out autonomously, yet provide

sensitive, selective and cost-effective, and on-site implementation. These characteristics can be implemented with the electrochemical analytical method which has been the most frequently employed detection technique due to its aforementioned advantages over laboratory-based methods [127]. Numerous materials with extraordinary characteristics, such as metals, conductive polymers, and metal oxides have been integrated into electrochemical sensors to improve analytical performance [128].

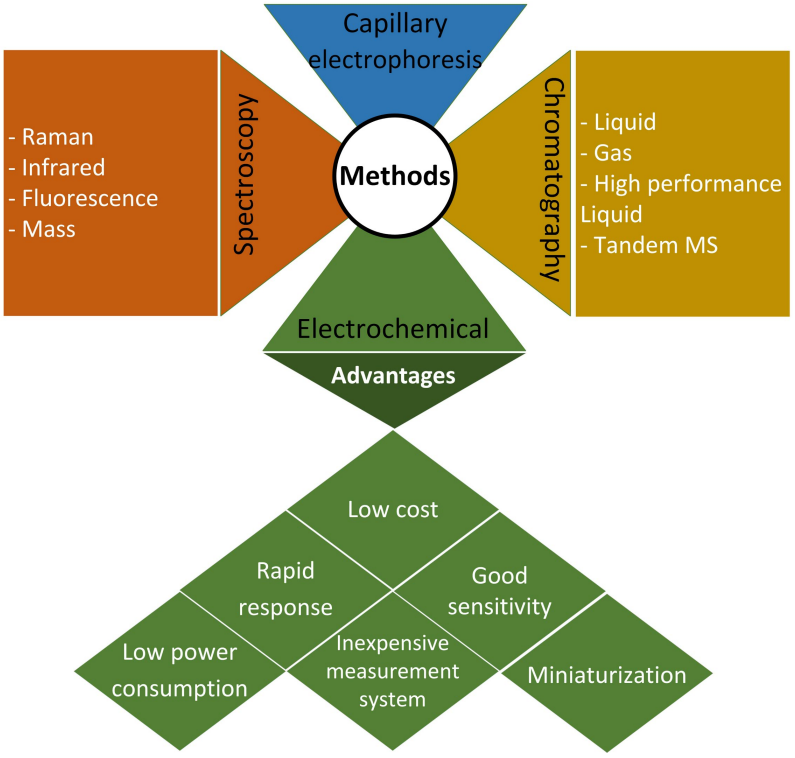

FIGURE 3.1: Detection methodologies and advantages of electrochemistry.

The electrochemical detection technique is most commonly carried out using thin film planar interdigitated electrodes (IDE) that have proven to be a powerful configuration in sensing applications. The method of operation for the planar interdigitated electrodes resembles that of two parallel-plate capacitor, with one-sided access to the material under test (MUT) provided by electrodes that open on one side. The electric field lines generated by the sensor penetrate the MUT, causing a change in the impedance of the sensor as illustrated in Fig. 3.2. Thus, the system properties can be determined by measuring the impedance of the sensor, which becomes a function of these properties. The electric field strength is majorly influenced by the pitch spacing between two oppositely charged electrodes. A wider pitch spacing results in improved penetration depth, though the electric field strength is weakened due to the electrodes being farther at the same potential [129].

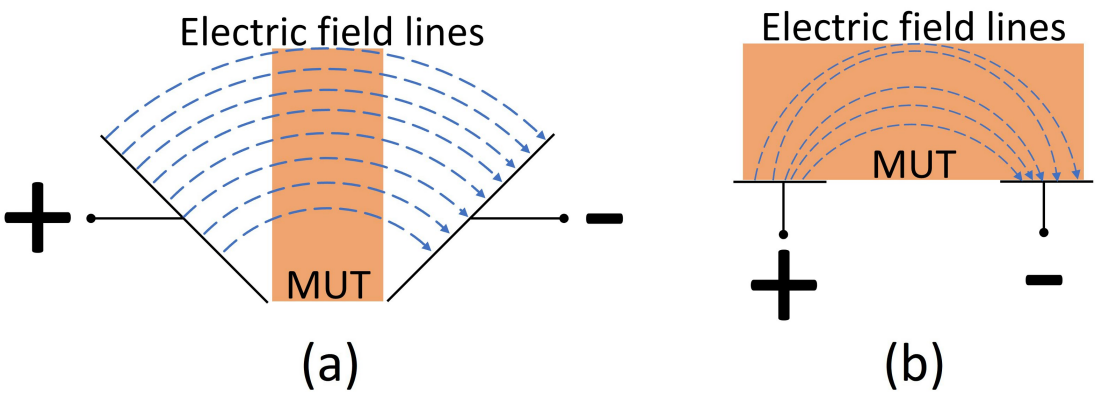

FIGURE 3.2: Penetration of electric field through the material under test (MUT).

IDE consists of patterns of finger-like structures that are placed close together on a non-conductive substrate, separated by a small gap, typically in the order of a few micrometers. The fingers are usually made of conductive materials such as gold, silver, platinum, etc. which can be fabricated in many ways. Photolithography [130], shadow mask evaporation [131, 132], inkjet printing [133–135], electroplating [136, 137], micro-contact printing [138], screen-printing, laser ablation [139, 140], and electro-hydro dynamic printing [141] are a few techniques of fabricating the electrodes on flexible and rigid substrates.

The electrochemical method offers quite a few detection techniques with the most common ones being amperometry - measurement of current at a fixed potential, potentiometric - measurement of electrode potential, voltammetry - measurement of current as a function of applied voltage, cyclic voltammetry - measurement of current as a function of applied potential while cycling through different potentials, and impedance spectroscopy that measures the impedance between electrodes as a function of frequency [142]. Electrochemical Impedance spectroscopy (EIS) is chosen as the preferred detection technique for this research because it is non-destructive and does not alter or destroy the sample being measured. As illustrated in Fig. 3.1, EIS also offers low-cost implementation, capable of in-situ measurements while providing sensitive measurements. Being frequency-dependant, it can provide information about the sample over a wide range of frequencies [143, 144]. The impedance that gets computed is in a complex form where both voltage and current carry magnitude and phase. Therefore, by capturing the magnitude and phase of both voltage and current, complex impedance can be calculated. Development of application-specific integrated circuit (ASIC) such as precision

impedance converter system that measures impedance data directly from the sensor has supported miniaturised, power efficient, and simplistic design, ideal for field deployment.

3.2.1 Research focus

The research focuses on evaluating the performance of IDE of two different materials namely silver and copper on two respective substrates PMMA and fiberglass that were laid out on three different geometric patterns of electrodes. To assess their performance, an ion was required. Due to the weather condition in New Zealand and abundant rainfall, the run-off from fields and anthropogenic sources add to levels of nitrate in the water supply. Thus, nitrate ions were chosen as the analyte which was dissolved in deionised water with various concentration levels.

The main aim of this research was to study the physics of different patterns of electrodes and the chemistry that takes place between the electrode material and the analyte as well as the polymer such as polydimethylsiloxane (PDMS). This would help us establish a sensing base for the sensors that can be characterized to detect the ion of interest, which in this case is nitrate ions. Furthermore, the process of manufacturing was also a research factor using cost-effective techniques and materials. Silver and copper were the chosen materials mainly because both are good electrical conductors, cost-effective, and easy to procure. The novelty of this research lies in the facile fabrication process for economical sensors using equipment that is commonly found in mechanical workshops. The performance evaluation encompasses two electrode materials: silver and copper, where silver electrodes consist of nanoparticles, while copper electrodes are solid metal.

3.2.2 Theoretical analysis of electrochemical impedance spectroscopy (EIS)

Determining Electrochemical Impedance involves applying an AC signal, and measuring the phase shift of the current in response to the applied potential. By using a low excitation signal, the electrode's response is kept pseudo-linear [145]. In a linear system, the current will follow a sinusoidal pattern with the same frequency but shifted in phase compared to the excitation potential as demonstrated in Fig. 3.3.

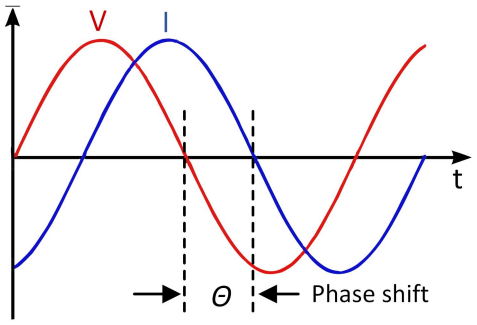

FIGURE 3.3: Phase shift in current with respect to applied voltage.

Impedance measures the circuit's ability to oppose the current flow when a voltage is applied. In AC circuits, impedance is represented as a complex value including real part (resistance) and imaginary (reactance).

Ohm's law expresses resistance as a ratio of voltage and current;

$$R = \frac{V}{I} \tag{3.1}$$

The AC excitation signal can be expressed as a function of time;

$$V_{\mathrm{t}} = V_0 \ sin \ \omega t \tag{3.2}$$

where V_{t} is the voltage the time t, V_0 is the amplitude of the signal, and the angular frequency is ω which is expressed as $\omega = 2\pi f$, measured in radians/second and frequency f in hertz [145].

In a linear system, the response signal, I_{t}, has a phase shift, θ, with an amplitude of I_0 which can be expressed as;

$$I_{\mathrm{t}} = I_0 \ sin(\omega t - \theta) \tag{3.3}$$

Ohm's law from Eq. (3.1) can be used to calculate the impedance of the system expressed as;

$$Z = \frac{V_{\mathrm{t}}}{I_{\mathrm{t}}} = \frac{V_0 \ sin \ \omega t}{I_0 \ sin(\omega t - \theta)} \tag{3.4}$$

$$Z = Z_0 \frac{sin(\omega t)}{sin(\omega t - \theta)} \tag{3.5}$$

The impedance, Z, can now be expressed in term of a magnitude of Z_0 and the phase shift, θ.

Eq. (3.5), can also be expressed as Euler's relationship given by;

$$e^{j\theta} = cos\theta + j\ sin\theta \tag{3.6}$$

The impedance, Z, can be expressed in terms of potential, V, and current, I, given by;

$$V_t = V_0 e^{j\omega t} \tag{3.7}$$

$$I_t = I_0 e^{j(\omega t - \theta)} \tag{3.8}$$

Therefore, the impedance, Z can be expressed as;

$$Z(\omega) = \frac{V_t}{I_t} = \frac{V_0 e^{j\omega t}}{I_0 e^{j(\omega t - \theta)}} = Z_0 e^{j\theta} \tag{3.9}$$

$$= Z_0(cos\theta + j\ sin\theta) \tag{3.10}$$

As seen in Eq. (3.10), the impedance can now be expressed as a combination of real part $(Z_0\ cos\theta)$ and imaginary part $(Z_0\ sin\theta)$

3.2.3 Substrate evaluation

The substrate, electrode materials and fabrication techniques are important factors when fabricating electrochemical sensors. A substrate forms the primary mechanical support for the sensor. There are many different types of substrates used for various applications. Rigid substrates [146, 147] include silicon, glass, ceramics and certain metals and plastic

like polymethyl methacrylate (PMMA), while flexible substrates [148, 149] include certain polymers like PDMS and polyaniline and plastics like Polyethylene terephthalate (PET) and polyimide.

While various types of substrates listed above have been widely used in the past in sensing applications, for a sensor intended to be submerged in water, the substrate would need to possess certain attributes. Corrosion resistant is one such attribute that can affect the performance of the electrodes over a period of time when exposed to water. Surface roughness is another, that can affect the alignment and spacing of the IDEs which in turn influences the performance of the sensor. Lastly, manufacturing large batches or mass production of the sensor, the cost would be a significant aspect since most electrochemical sensors are disposable. Thus, using recyclable material with a prolonged lifespan that is readily available while keeping the cost low, substrate materials like silicon, glass, metals, or ceramics may not be the best option compared to its plastic counterpart [150] such as PMMA. It is also known as perspex or acrylic which is produced from synthetic resin making it economical, recyclable, durable, and rigid [151].

3.2.4 Geometric pattern

The geometric pattern that is most frequently seen in sensing applications is the interdigitated pattern that has electrodes aligned in a comb-like structure. The electrodes are usually uniformly spaced out which is in the range of a few hundred micrometers. While interdigitated pattern proves to be effective, it is beneficial to examine other geometric patterns.

In our previous study [140][152], evaluation of the performance of seven different geometric patterns of electrodes employing computer simulation on COMSOL Multiphysics, was performed. The simulations were carried out to measure the electric field generated at 1V, alongside the measurement of capacitance with air being the dielectric. All the patterns were designed to have 200 μm of the distance between two consecutive electrodes. The results showed strong electric fields were generated for interdigitated, spiral, swiss spiral and serpentine geometric patterns. Triangular and Arrow were not considered for having a somewhat higher surface area compared to others. For the laser cutting head, straight lines are relatively easy to cut because the beam can be directed along a straight continuous path. Conversely, round or curved lines demand the laser

head to continuously alter its direction, leading to a less accurate cut. According to the observations via microscopic imagery, the engraving resolution was reduced in curved regions due to x-y offset interpolation. This resulted in the laser head slowing down, causing adjacent areas to be ablated unevenly and leading to irregular engraving width. Thus, evaluation of electrodes in this research was limited to interdigitated, square, and serpentine geometric patterns. Fig. 3.4 displays the three selected computer-aided geometric designs.

3.3 Methodology

Earlier discussion highlights key factors in sensor design for optimal electrochemical measurements, including substrate, electrode material, pattern, and fabrication technique. Silver and copper electrodes were fabricated using distinct methods. Fabrication of silver electrodes on acrylic substrate was more intricate and elaborate, while copper electrodes underwent a simpler CNC machining process. The production of both silver and copper electrodes is detailed in the following sections.

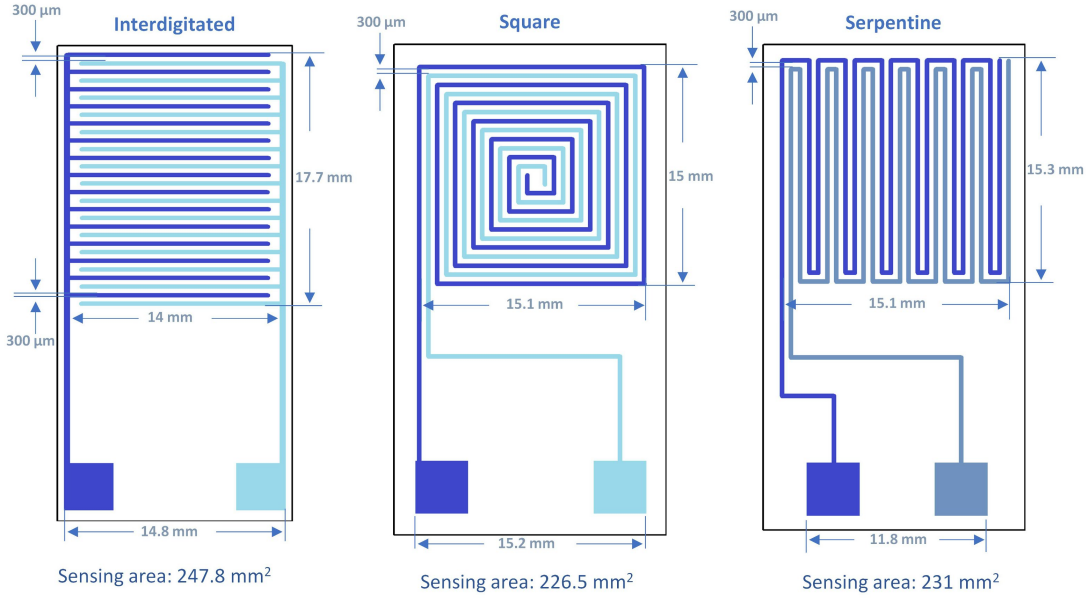

FIGURE 3.4: The three selected geometric patterns of electrodes with dimensions and the surface area of the sensing area.

3.3.1 Fabrication of silver electrodes

The laser engraving technique involves a meticulous removal of material to create a replica of the digital design. The engraving is performed in a raster pattern by rapidly shifting the laser head and firing at specified points. When a CO_2 laser cutter engraves a surface such as acrylic, the energy from the beam is absorbed by the acrylic surface, heating it swiftly. As the surface temperature of acrylic rises, the laser beam vaporises the material, removing small amounts of it with each pass of the laser. This results in reduction of the thickness of the acrylic sheet at the engraving site. The material is removed by the vaporisation that pushes down on the softened material, creating a small channel, leaving behind a carbon residue that remains on the surface of the material. This residue looks like fine powder, a faded version of the original colour of the material. The beam continues on engraving other parts of the surface, while the engraved parts cool, and solidify, retaining the shape of the engraving. After completion of the engraving process, the engraved area results in a slight uneven surface. The embossed edges of acrylic are left slightly irregular or rough due to rapid heating and cooling of material by the laser and in some cases deformation/warping of the part may also occur when using a thin sheet of material such as 3mm thick. Fig. 3.5 shows a 3mm thick acrylic that warped slightly from the center during engraving. Thus, 5mm thick acrylic sheet was chosen for this application to avoid the warping issue. To attain the desired outcome, the laser cutting process utilized power set at 100% and speed set to 60%.

FIGURE 3.5: Warping of 3mm thick acrylic caused by the laser ablation process.

As illustrated in Fig. 3.6, upon completion of the engraving stage, the resulting stamp was wet-polished using a 1200-grit sandpaper on a flat and smooth slab of granite to ensure homogeneity of embossed elements while polishing. The sandpaper comprises of silicon carbide abrasive particles that are fine enough to not cause any damage to

the delicate embossed regions, instead even out any jagged or uneven edges to result in a uniform height of embossed ridges across the stamp. The stamp is then washed under running tap water to rinse remnants of polishing and carbon residue from the laser engraving process.

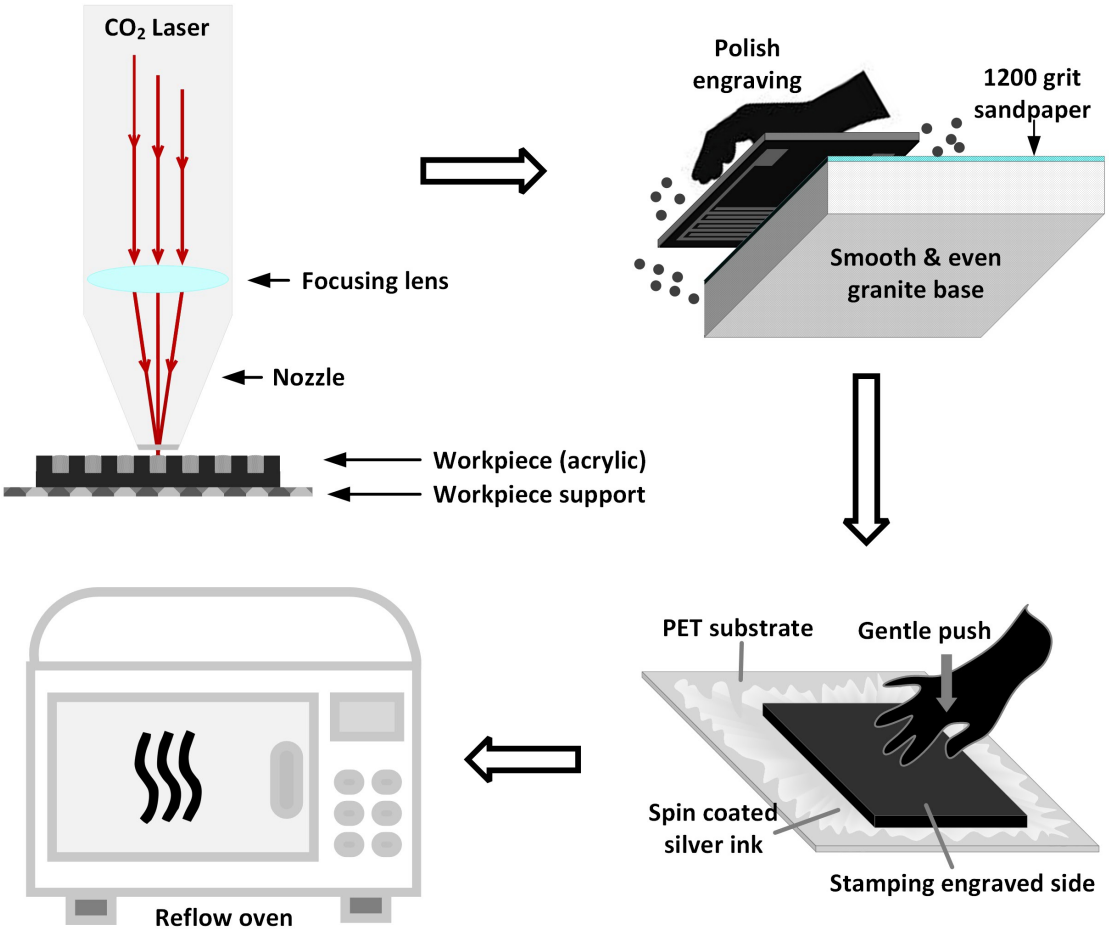

FIGURE 3.6: Illustration of transferring silver ink from spin coated PET substrate to laser ablated pattern using stamping process to generate silver electrodes.

Following the process of washing the laser cut parts, the next step involves coating the freshly engraved embossed ridges with conductive silver ink. Novacentrix HPS-021LV is the silver ink that consists of nanoparticles of silver of size 1.5 μm. The ink is aqueous-based and possesses high viscosity with very low resistance of 5.1μ to 0.28μ ohm-cm resulting in high conductivity. Using a precision weighing scale, a dab of approximately 0.45g of silver ink was dropped on a flexible PET surface which was then coated with the ink using a spin coater at 5000 RPM for 240 seconds. The stamp was then placed on the freshly silver coated substrate with the embossed side facing downward on to the silver ink, applying a gentle push and then lifting the stamp, transfers the coated

silver on the PET substrate to the embossed ridges. This was then subjected to heat in a convection oven to evaporate the solvent at 100°C for 60 minutes which is below the glass transition temperature of PMMA of 105°C.

The final step involves coating the silver coated electrodes with polymer that would protect the electrodes from oxidation, hence increase the life span of the electrodes. The polymer used in this research is PDMS which is an amalgamation of Sylgard 184 silicone elastomer base and the curing agent. The base and the curing agent were mixed in a 10:1 ratio, measured using a precision weighing scale. The mixture produced a liquid with a high level of viscosity, and a drop of 0.4g of this mixture was deposited onto the silver electrodes. The electrodes were then spin-coated at 5000 RPM for 240 seconds for the polymer to create a consistent protective layer, followed by a reheating process at 100°C for 90 minutes. PDMS would create a thin barrier between two consecutive electrodes, altering the dielectric of the coated silver electrodes. The process of preparing the acrylic base, coating the embossed regions with silver ink and producing silver electrodes is depicted in Fig. 3.6.

3.3.2 Fabrication of copper electrodes

There are two main methods of fabricating copper electrodes. The first is chemical etching, which involves immersing the copper clad board in an etching solution, such as ferric chloride, and using a photoresist film that is sensitive to light to define the pattern. The exposed film is exposed to light through a mask and then the etching process removes the unwanted copper. The photoresist film is then removed using a solvent such as acetone. The second method is milling, which uses a high-speed precision tool to cut away the non-required parts of the copper clad board.

While chemical etching is an economical approach to produce electrodes, it involves dealing with hazardous and corrosive etching solutions. Additionally, the process may be slower compared to milling. Massey University offers a milling machine that specializes in milling copper clad boards which also offers a faster and safer alternative. Hence, we chose to get the copper electrodes fabricated using the milling process.

The milling process begins by securing the material to the machining table. The cutting tool is then positioned and secured in the spindle which rotates the cutting tool at high

speed. The material in this case is a fiberglass laminate commonly known as FR4. FR represents flame-retardant and number '4' stands for woven glass-reinforced epoxy resin is known for its high mechanical strength and resistance to water. It is used as an insulator in printed circuit boards which provides electrical isolation between adjacent copper planes while also reinforcing the board's mechanical structure. FR4 substrates feature exceptional thermal, mechanical, and electrical properties, making them a top choice for various electronic uses. The versatility, adaptability to various manufacturing methods, and reliable outcomes of flame-retardant laminates and prepregs further adds to their appeal [153]. The laminate typically comes with a thin film of copper cladding with approximately 80μm in thickness. The milling machine that helps cut FR4 substrate is the automatic LPKF S64 that supports very low resolution cuts down to 100μm.

The first step is choosing an FR4 substrate with a single-sided copper cladding, which is then mounted on the milling machine's vacuum suction table as illustrated in Fig. 3.7. The choice of the correct isolation tool is crucial and a universal cutting tool with a tip diameter of 0.30 mm was used. The tool's fine tip enables it to make precise cuts, but a trade-off in tool durability. The same geometric designs were used in both the milling and the laser cutting processes.

The final step resembles that of silver electrodes, which involved coating electrodes with PDMS. A combination of Sylgard 184 silicone elastomer base and curing agent, in 10:1 ratio, is used, with a 0.4g applied on top of the electrodes. It was then spun in a spin-coater at 5000 RPM for 240 seconds and cured at 100°C for 90 minutes.

3.3.3 Ion selection for electrode performance evaluation

Selecting the appropriate analyte is crucial for evaluating interdigitated electrode performance. Considerations include sensitivity, electrochemical reaction behavior, compatibility with electrode material to prevent unwanted reactions or interference [154], and availability. There are various chemicals or standard ions to choose from for electrode performance evaluation which includes metal ions such as sodium (Na^+), calcium (Ca^{2+}), magnesium (Mg^{2+}), copper (Cu^{2+}), etc. Certain types of anions that include chloride (Cl^-) [155], sulfate (SO_4^{2-}) [156], nitrate (NO_3^-), phosphate (PO_4^{3-}) [157], etc. Organic ions such as glucose, lactose [158] can also be used and some types of proteins

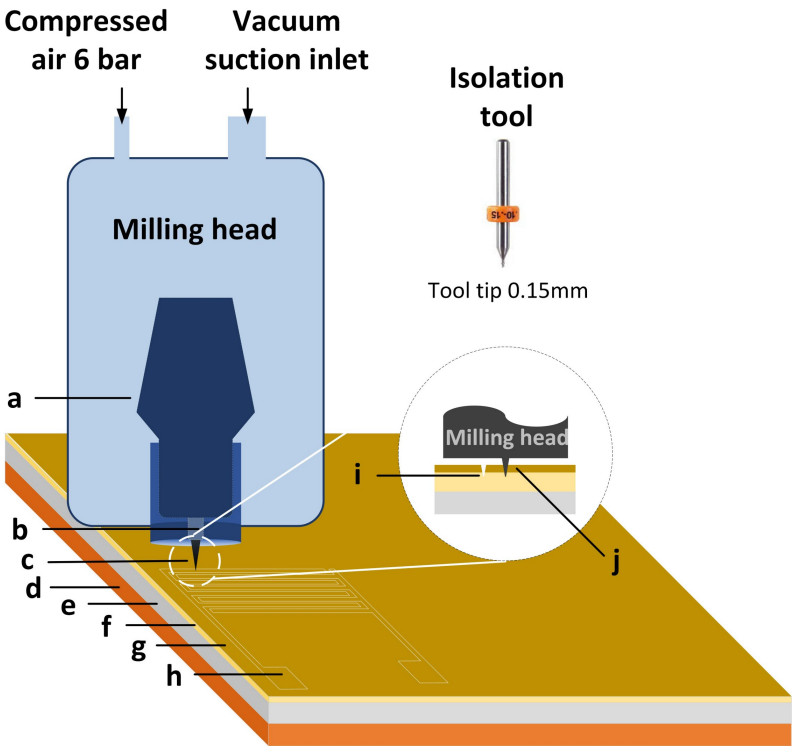

FIGURE 3.7: Parts of the LPKF S64 milling machine. (a) high speed spindle, (b) collet, (c,j) isolation tool, (d) vacuum suction table, (e) sinter plate, (f) single-sided FR4 substrate 1.6mm, (g) copper foil 1.8μm, (h) milled electrodes, (i) depth of cut 0.3mm.

such as enzymes and antibodies [159]. Biosensing for glucose or antibodies have been disregarded as that is outside the scope of study.

Nitrate ion in the form of potassium nitrate or sodium nitrate have a significant redox potential which impacts the electrical conductivity of solutions. These ions can be utilized with popular electrode materials like gold, silver, platinum, etc. without causing any disruption to electrochemical reactions. This study finds nitrate to be a suitable option for electrode performance evaluation due to their relevance in the current context of contaminated waters [160–162] with high levels of nitrate found in our water supply.

3.4 Results and discussion

3.4.1 Conversion calculation for concentration of nitrate

As mentioned in the introduction, the acceptable level of nitrate in our drinking water supply is reportedly 10 mg/L. To ensure a fair comparison of nitrate detection in water,

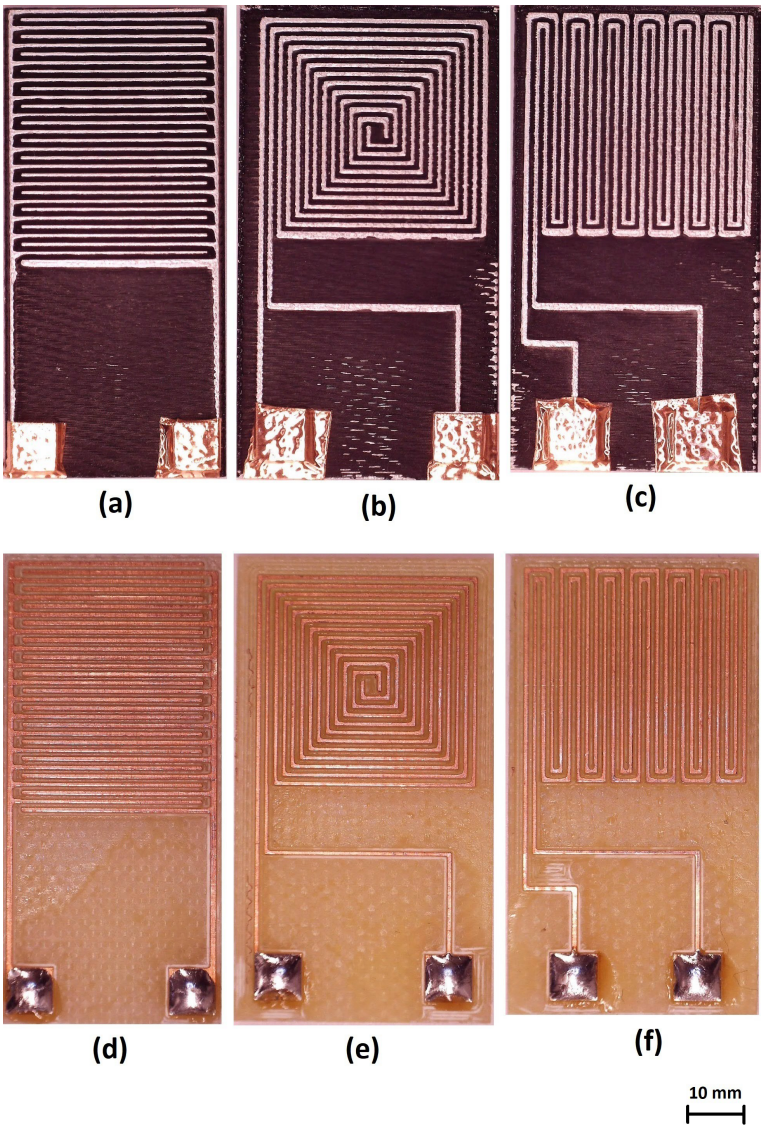

FIGURE 3.8: The final result of fabricated electrodes. Images (a),(b),(c) show silver electrodes and (d),(e),(f) displays copper electrodes in interdigitated, square and serpentine geometric patterns, respectively.

it is important to use consistent units of measurement. The standard nitrate solution in use has the concentration of 0.01 mol.

To convert mol to mg/L, the first step is to determine the atomic weight (AW) of KNO_3, which is the sum of the atomic weights of all the elements in the compound.

$$AW_{KNO_3} = AW_K + AW_N + 3.(AW_O) \tag{3.11}$$

$$= 39.10 + 14.01 + 3(16)$$

$$= 101.11$$

Therefore, 0.01 mol can be converted to mg/L by multiplying atomic weight (calculated above) with concentration in moles multiplied by 1000 to convert to mg which results in a value of 1011.1 mg/L.

3.4.2 Material characteristics

100 mL nitrate ion standard solution with a concentration of 0.01 M (1011.1 mg/L) was procured from Sigma-Aldrich which was used to prepare samples with varying concentration levels.

The Novacentrix HPS-021LV silver ink is composed of 1.5 μm sized silver nanoparticles with 75% loading has high viscosity. The aqueous-based ink has minimal resistance, ranging from 5.1μ to 0.28μ ohm-cm, making it highly conductive and suitable for screen printing and stamping.

The copper clad board from MG chemicals, is an FR4 board with a thin film of copper on top (single side cladding) that are ideal for use with milling machine. The 500 series of boards come with 1 oz or 35 μm of copper cladding on a 1.6 mm thick laminate. The copper film bears a volume resistivity of 5x10^8 mΩ-cm. with a surface resistance of 5x10^7 mΩ.

3.4.3 Probing and examination of electrodes

There are many factors that influence the performance of electrodes such as electrode size, electrode geometries, material, temperature, etc [163, 164]. Resistance is also considered a contributing factor that could influence the performance of the electrodes. The resistance was determined for all the silver and copper electrodes by measuring the resistance of two longest parts of each electrode. As illustrated in Fig. 3.12, two probe resistivity measurement was performed between the electrode pad and the most distant section of the same electrode using Fluke 110 which is a digital multimeter. As seen from the geometry of the electrodes in Fig. 3.4, the patterns consist of two separate traces terminated at a square pad which is then attach to wires for experimentation.

Table 3.1 reports the measurements obtained using a two probe resistivity measurement method.

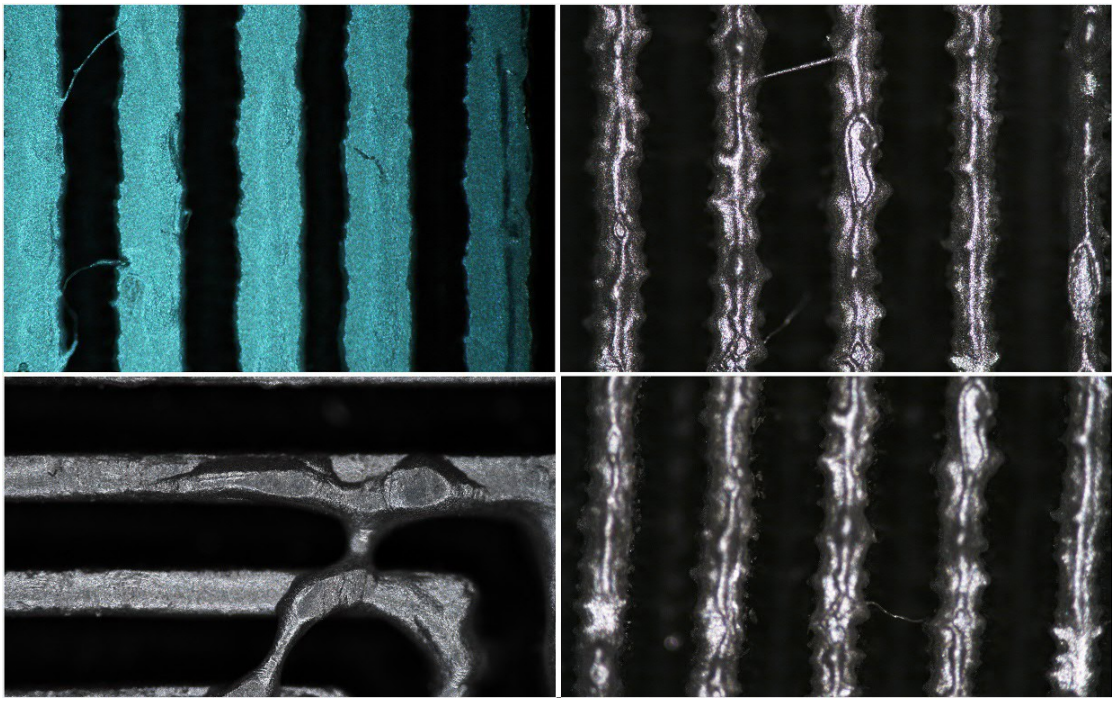

FIGURE 3.9: Minuscule bridges between electrodes, ranging from 1 μm to 10 μm in thickness.

Our work began by designing geometric patterns with electrode widths and pitch spacing of 200 μm. Although, the laser cutter has a low step resolution of 100 μm, engraving fine lines using a 0.1 mm laser point was not well received by the surface of PMMA which resulted in broken or melted embossed regions. Something similar was observed with the LPKF milling machine. Despite its very fine step resolution similar to the laser cutter, the cuts resulted in narrower electrodes. Therefore, we chose width and pitch of 300 μm. The final product of the two materials of electrodes were examined under the microscope. The measurements recorded in Fig. 3.10, display electrode widths and pitch spacing of all the three geometric patterns that were evaluated. The copper electrodes have consistent width and pitch spacing. Approximately 10% variation can be observed in the pitch spacing among the three geometric patterns of copper electrodes. However, a greater variation of 28% can be observed for the actual width of electrodes. This is due to the tool tip diameter of 0.32mm that cuts away edges of the electrodes, resulting in a narrower width. Tool life and condition of the tool tip are contributing factors for this variation. Regarding Fig. 3.11, the discrepancy between the electrodes is quite high, with width and pitch both having almost 40% variation. There could be a

few reasons why variations occur. As the engraving process involves melting of PMMA, which would result in narrower ridges. Another issue could be the pressure applied on to the electrodes during stamping process. Inadequate pressure could result in incomplete coverage of the electrode with the silver ink and vice versa.

During application of silver ink on the acrylic embossed regions, occasionally bridges between two consecutive electrodes would form, which resulted in joining or shorting the two oppositely charged electrodes. This happens due to the high viscous nature of aqueous silver ink. When the acrylic material is lifted off the surface of freshly coated PET substrate with silver, fine strings of the ink would form that would cause bridges as shown in Fig. 3.9. These bridges were removed by gently brushing over the electrodes with a soft bristle brush, dedicated to remove small specs on a printed circuit board without scratching the surface.

3.4.4 Sample preparation

In order to create nitrate solutions with varying concentrations, the 0.01 M (1010 mg/L) nitrate ion standard solution was diluted with deionized water. For a capable sensor, the detection of trace amounts of nitrate in water is crucial, and to ensure this, samples were prepared with nitrate concentrations ranging from 5 μM (0.5 mg/L) down to 1 μM (0.1 mg/L), which is substantially lower than the maximum nitrate content in drinking water (10 mg/L). Detection of low concentration levels would be helpful in investigating the performance as well as sensitivity of the electrodes. Therefore, we chose to work with a set volume of 30 μL of NO_3^- solution to be diluted in varying volumes of deionised water, in order to achieve the nitrate concentrations mentioned above.

To compute the volume of DI water required to dilute a set concentration of NO_3^- such as 30 μL, we follow the Eq. (3.12):

$$Vol_{\mathrm{DI}} = Vol_{\mathrm{set\ (NO_3^-)}} \frac{conc_{\mathrm{set(NO_3^-)}}}{conc_{\mathrm{desired(NO_3^-)}}} \tag{3.12}$$

where,

Vol_{DI} is the volume of DI water required to dilute the desired concentration of NO_3^- given by $conc_{desired(NO_3^-)}$ with the fixed variables being $Vol_{set\ (NO_3^-)}$ of 30 μL and *conc*

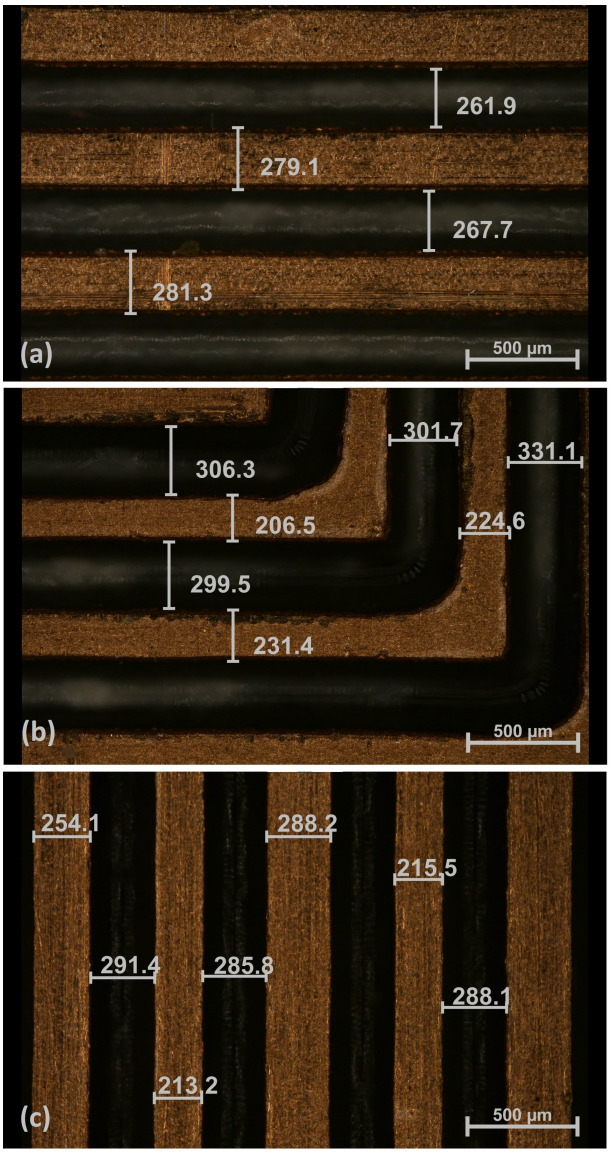

FIGURE 3.10: Copper electrode width measurements in μm; (a) Interdigitated, (b) Square, (c) Serpentine.

$_{set(NO_3^-)}$ of 0.01M. The sample volumes with varying concentration levels are shown in Table 3.2.

The performance of interdigitated and square geometric patterns for both silver and copper was analyzed using graphs shown in Fig. 3.13 and Fig. 3.14. These patterns demonstrated distinct impedance levels for varying concentrations of 0.1 mg/L to 0.5 mg/L, as highlighted on the graphs. Although the serpentine geometric pattern for copper also exhibited good detection levels, we chose to focus on computing the relationship between impedance and concentration for interdigitated and square geometries only. Fig. 3.16 displays the graphs for impedance vs concentration, showing an inverse

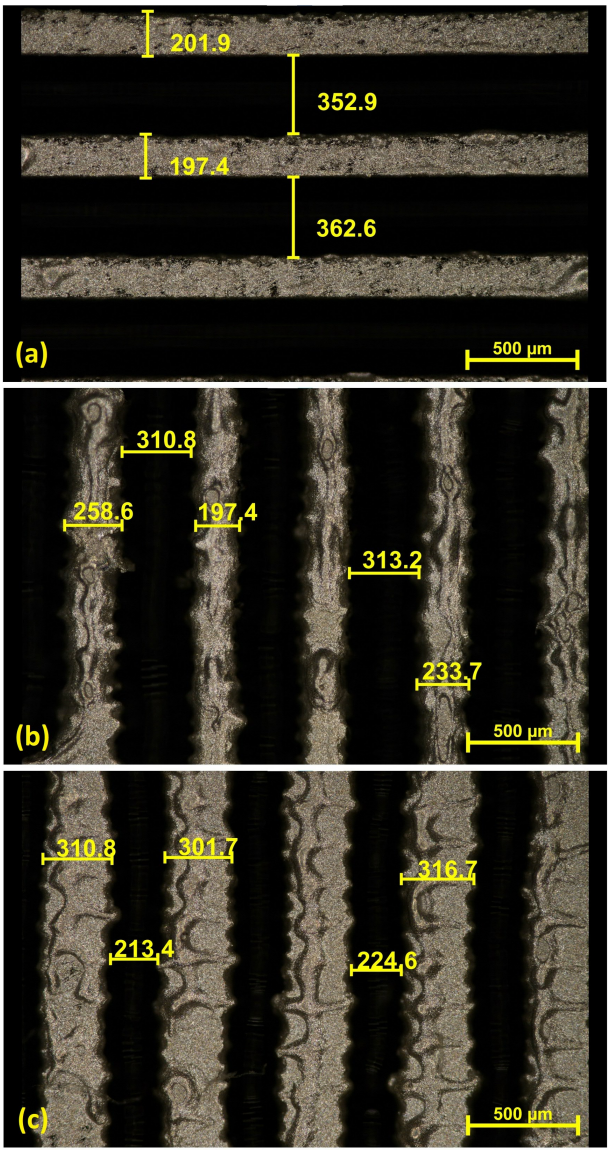

FIGURE 3.11: Silver electrode width measurements in μm; (a) Interdigitated, (b) Square, (c) Serpentine.

linear relationship in which impedance increases as the concentration of nitrate in water decreases. The R^2 value for most of the electrodes is above 0.9, indicating a good linear relationship between the data points. Moreover, this trend of inverse linear relationship has been confirmed by many studies conducted previously on detection of nitrate, that have used impedance analyzers along with LCR meters [143, 165, 166] that validates the results obtained.

By referring to the graphs presented in Fig. 3.13, it is apparent that there is a dip in impedance at exactly 400 Hz. To investigate this dip further, capacitance measurements were conducted over a frequency sweep from 100 Hz to 1 kHz as the area of interest

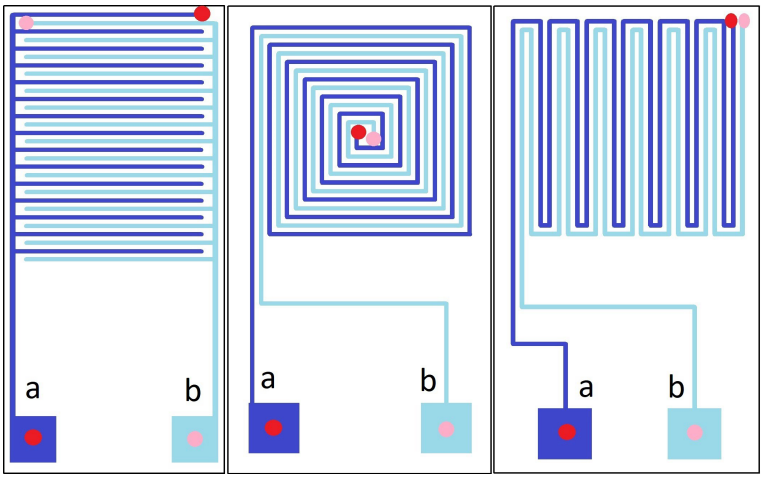

FIGURE 3.12: Figure illustrates two probe resistivity measurement. Driving and sensing electrodes are denoted by labels (a) and (b) respectively.

TABLE 3.1: Resistance of electrodes for various geometric patterns

Pattern	**Sensor No.**	**Driving electrode (Ω)**	**Sensing electrode (Ω)**
Silver electrodes			
Interdigitated	1	44.2	51.2
	2	41.9	44.4
	3	56.3	38.7
Square	1	22.8	18.7
	2	32.5	32.3
	3	19.1	17.7
Serpentine	1	41.6	35.7
	2	40.2	61.1
	3	35.7	42.1
Copper electrodes			
Interdigitated	1	2.0	2.6
	2	1.8	2.2
	3	1.6	1.6
Square	1	1.5	1.4
	2	1.3	1.3
	3	1.9	2.0
Serpentine	1	1.3	1.4
	2	1.3	1.0
	3	1.4	1.3

TABLE 3.2: Sample volume and concentration

	Vol set$_{(NO_3^-)}$	**conc $_{desired(NO_3^-)}$**	**Vol$_{DI}$**	**% conc**
Sample 1	30μL	5μM (0.5 mg/L)	60mL	0.05%
Sample 2	30μL	4μM (0.4 mg/L)	75mL	0.04%
Sample 3	30μL	3μM (0.3 mg/L)	100mL	0.03%
Sample 4	30μL	2μM (0.2 mg/L)	150mL	0.02%
Sample 5	30μL	1μM (0.1 mg/L)	300mL	0.01%

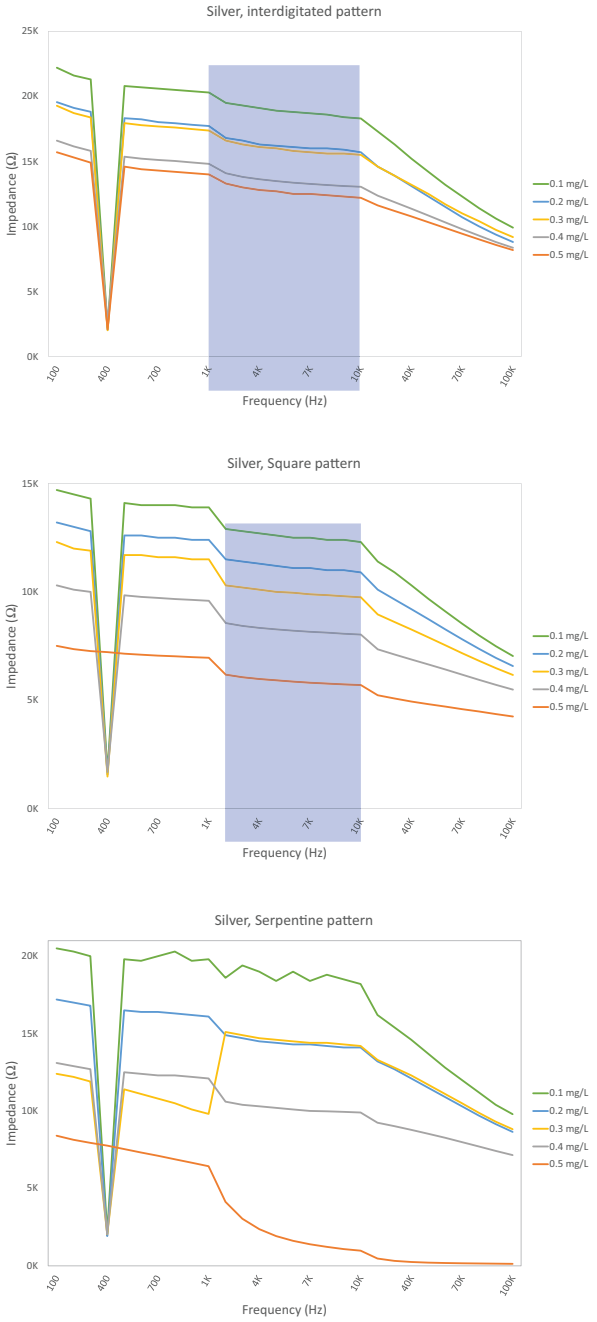

FIGURE 3.13: Frequency sweep for impedance measurement of Silver (Ag) electrodes in varying concentration levels of nitrate in deionised water.

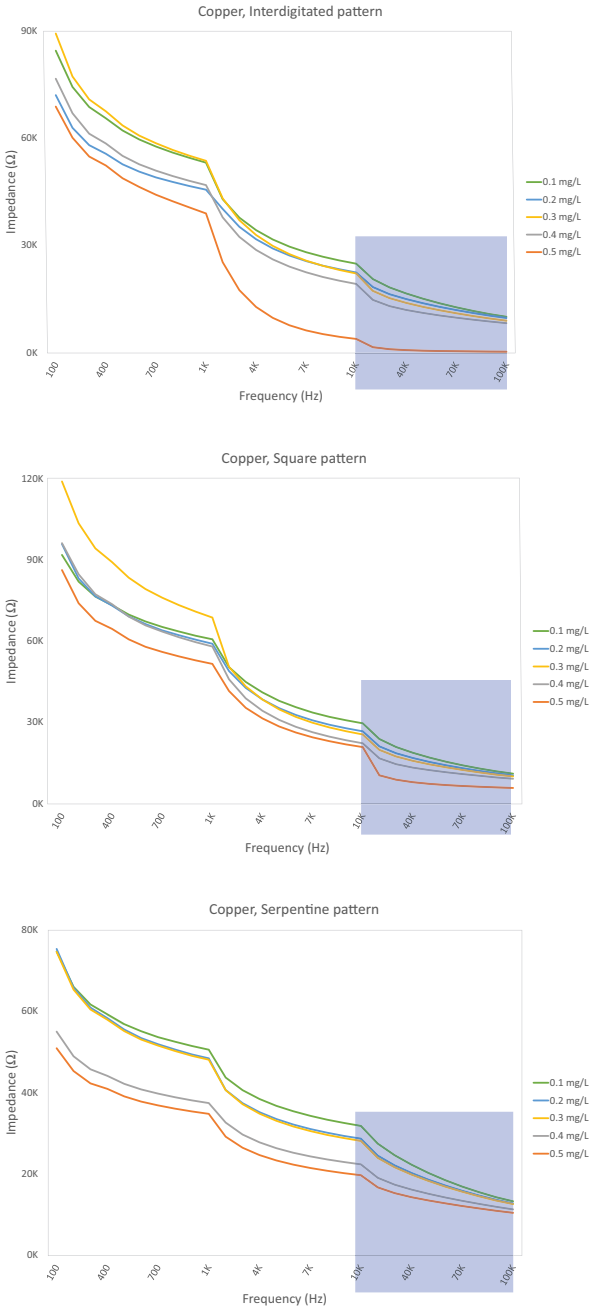

FIGURE 3.14: Frequency sweep for impedance measurement of Copper (Cu) electrodes in varying concentration levels of nitrate in deionised water.

falls within this range. As demonstrated in Fig. 3.15, the capacitance also exhibits a sudden dip at 400 Hz, similar to the impedance. This phenomenon could be attributed to electrode polarization, which occurs when a low-frequency AC electric field is applied to the sensor. The electric field prompts the accumulation of ions in the electrolyte or analyte at the electrode-analyte interface, creating a capacitor-like effect. Therefore, at low frequencies like 400 Hz, this interface charges and discharges during each cycle

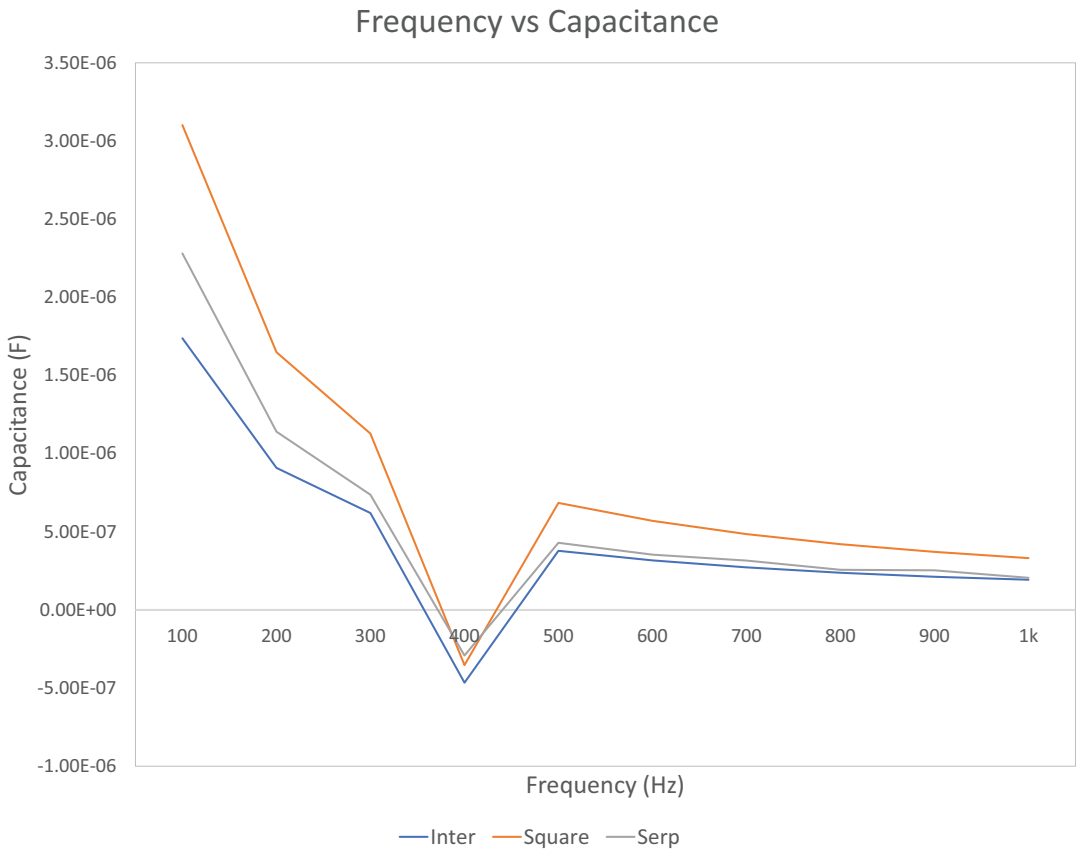

FIGURE 3.15: Capacitance measurement for all the three geometric patterns of silver electrodes for frequencies of 100 Hz to 1 kHz.

of the applied electric field, resulting in a lower measured capacitance and impedance. However, beyond 400 Hz, this interface is unable to charge or discharge as rapidly during each cycle, causing an increase in measured capacitance and impedance. [167, 168].

Alongside the experiments conducted to assess the detection performance of the electrodes, it is essential to evaluate their performance in repeated use scenarios. Therefore, we subjected the interdigitated geometric pattern for both copper and silver to repeatability tests with only 0.5 mg/L of nitrate concentration in DI water. During these tests, the sensors were immersed in the sample for 30 seconds, and impedance readings were recorded at 10 kHz. Following immersion, the sensors were removed from the solution, rinsed with DI water and then blow dried using inert nitrogen gas, and then re-immersed. This process was repeated ten times to determine the usability of the electrodes over multiple applications. The process of rinsing the electrodes with DI water was to ensure no remnants of nitrate ions were presents on the PDMS layer which could influence subsequent measurements. The graph in Fig. 3.17 displays the results of the repeatability

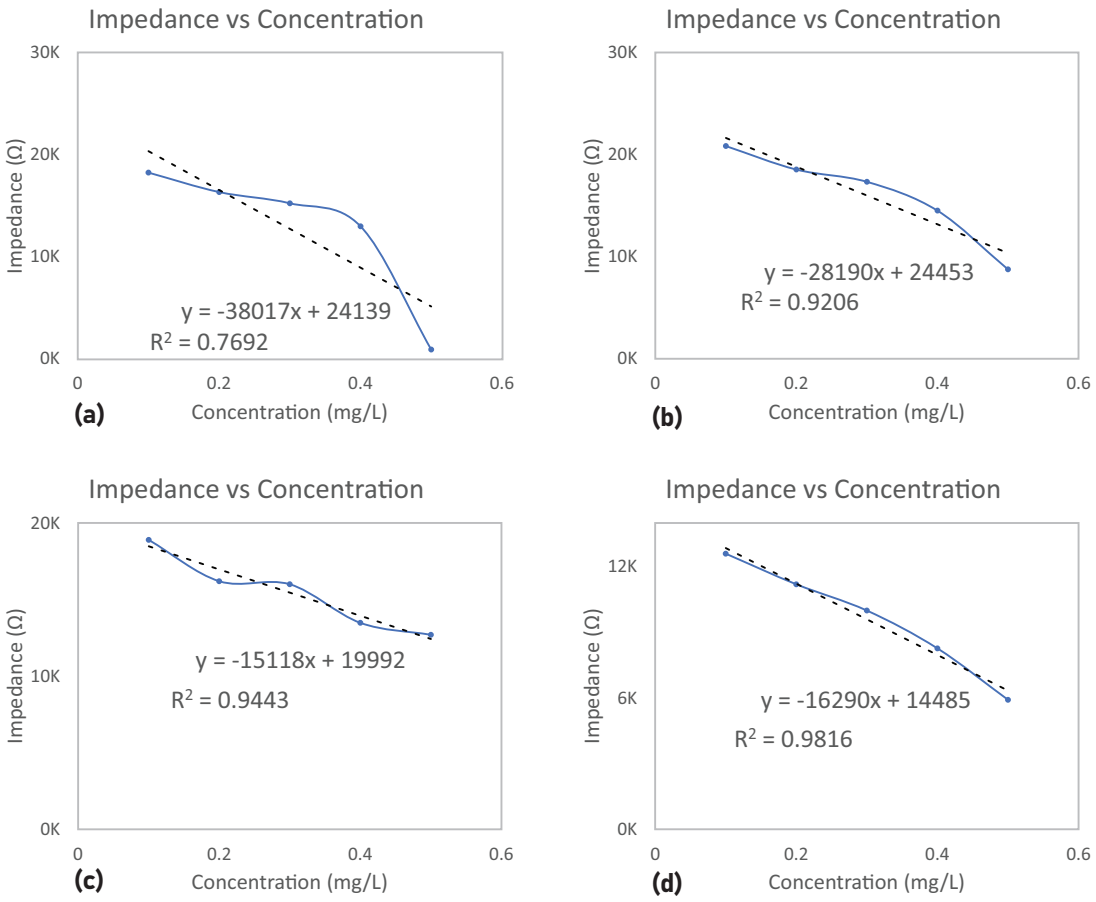

FIGURE 3.16: Impedance vs Concentration graphs for (a) Cu, Interdigitated at 30kHz, (b) Cu, Square at 30kHz, (c) Ag, Interdigitated at 5kHz, (d) Ag, Square 5kHz.

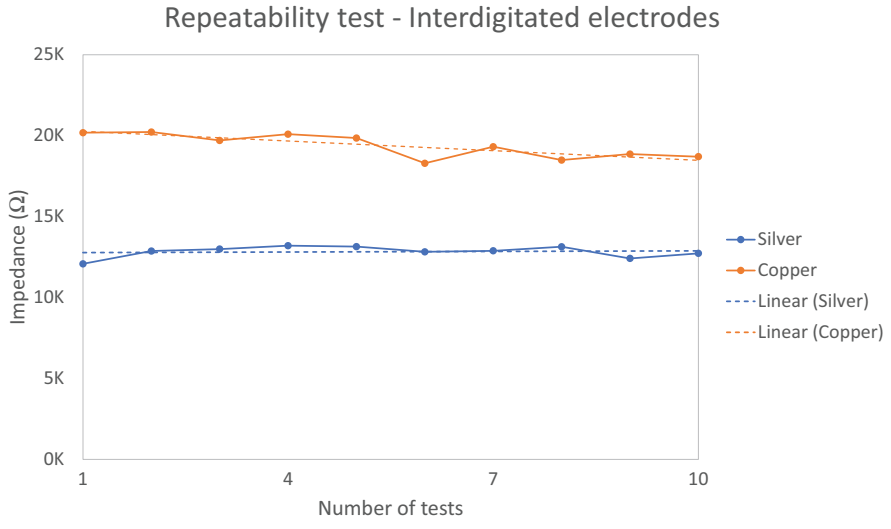

FIGURE 3.17: Repeatability tests for copper and silver electrodes.

tests.

3.5 Conclusion

In this study, we analyzed the performance of different geometric patterns of electrodes that include interdigitated, square and serpentine. These geometries were manufactured using two metals, namely silver and copper on two different substrates and manufactured using two fabrication methods. The primary objective of this study was to investigate how electric field density generated by different geometric patterns affects the sensitivity and speed of detection, and to establish a baseline for the electrodes and compute their performance characteristics. Additionally, it was crucial to develop a cost-effective approach for manufacturing different electrode materials. To evaluate the performance of electrodes submerged in water, we required an application that was ionic and easily dissolved in water. Given the current water quality issues in New Zealand, where nitrate levels in water are on the rise, we selected nitrate ions diluted in DI water with varying concentrations as the analyte. As seen from the results, the interdigitated and square geometric patterns performed well for silver electrodes, while all the electrode patterns performed well for copper for various concentrations of nitrate ions in DI water. The graphs show that impedance is inversely proportional to the concentration of nitrate ions present in water with a good linearity that are capable of detecting low nitrate concentrations from 0.5 mg/L to 0.1 mg/L that are well within the safe level of 10 mg/L of nitrate in drinking water. An interesting anomaly known as electrode polarization was observed at 400 Hz for all geometric patterns of silver electrodes, resulting in an abrupt fall in impedance and consequently, rise again to normal levels for subsequent frequency sweeps. The electrode resistances for silver electrodes were found to be significantly higher than those for copper electrodes that resulted in lower detection impedance in the range of 1kΩ - 24kΩ compared to 0kΩ - 130kΩ for copper electrodes, which is a much wider dynamic range. This wider range would be particular advantageous in detecting slight variations in nitrate concentration levels.

As seen from the collage of images in Fig. 3.18, thorough inspection of the electrode surface was carried out using Scanning Electron Microscope (SEM) that shows the physical appearance of copper and silver electrodes on fiberglass and PMMA substrates respectively. On copper electrodes, the surface appears smooth that indicates a consistent thin film of copper on the substrate. However, silver electrodes consist of individual

silver flakes. The aqueous-based silver flakes result in higher resistance compared to solid thin-film copper, as demonstrated in Table 3.1.

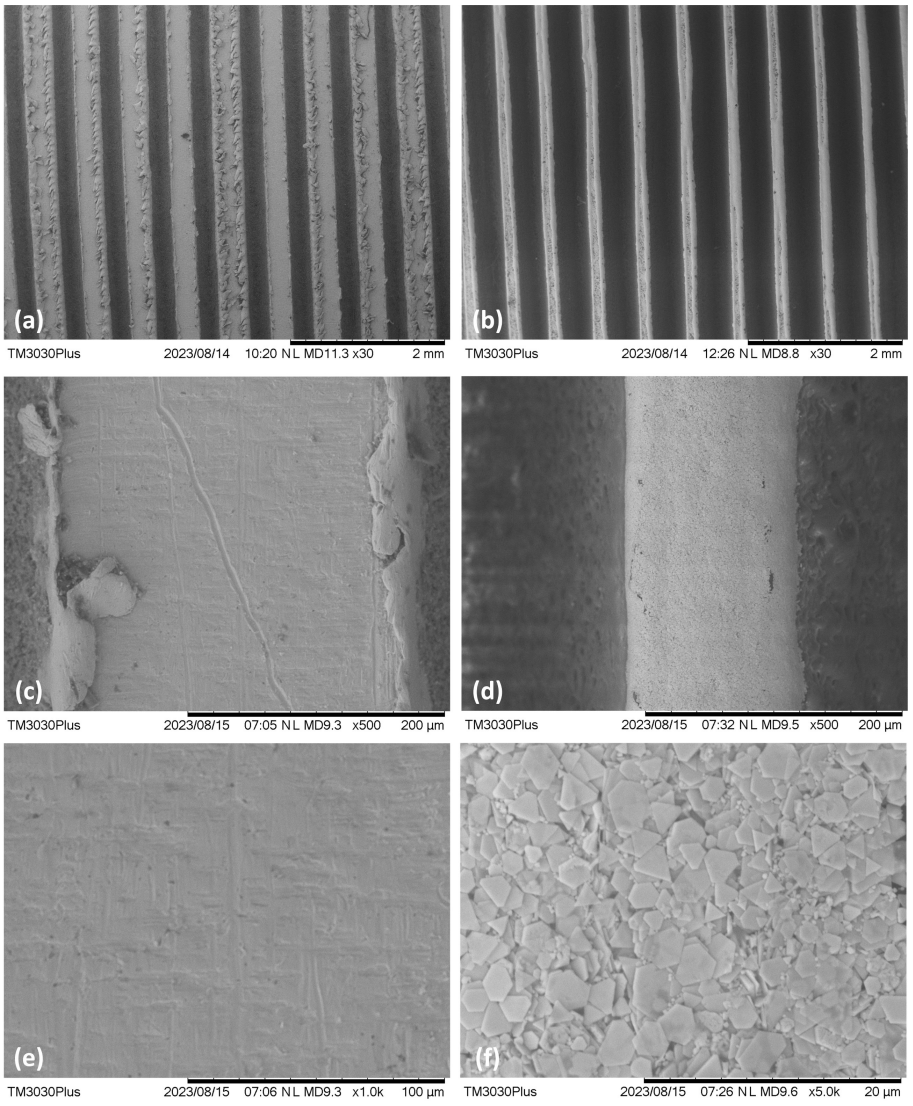

FIGURE 3.18: SEM images of the surface of copper and silver electrodes. (a),(c),(e) show copper electrodes on fiberglass substrate and (b),(d),(f) show silver electrodes on PMMA substrate.

Based on the cost estimates for the fabrication techniques, materials, and PDMS polymer coating, our proposed method provides a cost-effective means of producing a sensor that is submersible and can be used for in-situ detection of nitrate in water, with a projected cost of no more than $1 NZD ($0.60 USD) per sensor for both silver and copper. The testing was conducted using synthetic nitrate solutions in a controlled laboratory environment. The next step is to evaluate the sensor's performance in real-world samples, which may contain a wide range of ions, bacteria, and chemical compounds. This research establishes a foundation for future work in the development of effective and

affordable sensors for monitoring nitrate levels in water, which is essential for ensuring safe drinking water. Further research is required to assess the feasibility and accuracy of using these sensors in real-world applications.

Chapter 4

Thin-Film Electrochemical Sensor For Nitrate Detection in Freshwater Sources

4.1 Abstract

Freshwater sources are regarded as sources of potable water. With growth in anthropogenic activities, freshwater sources are contaminated with various pollutants, one of which is nitrate ions. Nitrate and other contaminants, enter the water bodies through various mediums, through a process called leaching. This affects our aquatic ecosystem and could have extreme affects on human health. According to the World Health Organization, nitrate levels in freshwater supplies must not exceed 11.3 mg/L. High level of nitrate content is a growing concern worldwide. Hence, it is imperative to monitor nitrate levels in freshwater bodies. This study evaluates the performance of four materials of interdigitated electrodes. Silver, copper, gold, and tin, with a thin coating of polymer, have been evaluated on their performance of measuring nitrate ions in real-world samples, that were collected from three different freshwater sources: Waikato River, Lucas Creek, and Lake Pupuke. Detecting nitrate ions in real-world samples poses a significant challenge, primarily because these samples contain a wide array of impurities that collectively form a complex matrix of contaminants. With the help of an LCR meter, we utilized electrochemical impedance spectroscopy as the analytical method of detection

to measure the magnitude of impedance. We established impedance characteristics for nitrate levels of 0.1 mg/L to 1 mg/L for a range of frequencies from 100 Hz to 100 kHz for all four materials of electrodes. Results show that copper and tin electrodes performed better, compared to gold and silver materials of electrodes. A linear correlation between impedance and nitrate ion concentration was observed, where both were inversely proportional to each other.

4.2 Introduction

Nitrogen is the most common natural element in the atmosphere which includes Nitrogen (N_2), Nitrogen-Dioxide (NO_2), Nitrogen Oxide (NO), Nitrous Oxide (N_2O) and Ammonia (NH_3) [169]. These are all present in the atmosphere that make up about 78% of air which are essential components to support life. These nutrients react with rainwater that results in the formation of nitrate (NO_3^-) and ammonium (NH_4^+) ions. The rain causes nutrients from excessively wet soil to drain into our waterways, although the amount of nitrate and ammonium created from this process maybe negligible. The topsoil is often rich in nitrogen content that originate from manures, decay of plants, fertilizers, and other organic materials [4]. Nitrate seamlessly dissolve in water which makes them mobile that can easily be moved by water. The contaminated water enters our freshwater supply such as lakes and rivers through a process called nitrate leaching [5, 6]. Nitrate has some positive health affects that are used to treat and manage heart related issues such as dilating venous vessels and coronary arteries. Nitrate provides instant relief for patients that suffer from cardiovascular diseases such as acute anginal pain, acute coronary syndrome, arterial hypertension, and heart failure. Despite the medicinal value, negative impacts outweigh its positive effects. Nitrate can reduce hemoglobin levels in blood, which could lead to weakness, increased heart rate, and, in some cases, trigger thyroid disease. Continuous intake of high levels of nitrate can also cause certain types of cancer [7, 8].

Aquatic life thrives in freshwater sources and many parts of the world rely on aquatic food source such as fish. However, Nitrate pollution in water promotes algal blooms that could produce toxins that harm aquatic organisms. As algae and plants decompose, they start consuming more oxygen resulting in low levels of oxygen that affect aquatic life such as fish [170, 171]. Nitrate can also enter the food chain through fish that may have

accumulated nitrate in its tissues that humans consume which could also have health implications. Hence, nitrate leaching into freshwater sources can lead to consequences for both aquatic life as well as human health. Therefore, it is important to regularly measure our freshwater sources to ensure nitrate levels are within limits. Freshwater, in most cases is drinkable, comprises of many ions, chemical compounds and biological matter that together forms a complex matrix of impurities [172].

To measure ionic content in water, electrochemical analytical method is widely used due to its simplicity, low power consumption, good accuracy and sensitivity, ability to provide rapid response, and offers miniaturization at low-cost [173]. This research builds on our previous study [174] of detection and measurement of varying concentrations of nitrate ions in deionised water where we designed various geometric patterns of planar electrodes namely, interdigitated, square, and serpentine. These geometric patterns were fabricated using silver (Ag) and copper (Cu) on PMMA and fiberglass substrate respectively, that form a thin-film of conductive material on top of the substrate. These thin-film electrodes were evaluated on detection sensitivity and performance using laboratory synthesized nitrate samples by performing electrochemical impedance spectroscopy using an LCR meter to measure changes in magnitude of impedance as the nitrate ion content in the sample varied. We chose to measure the magnitude of impedance because it provides a holistic view of the system's response which is a combination of both the real and imaginary components of impedance. These measurements were used to establish characteristic curves which gave us insight into the performance of low-cost electrochemical sensors for detection of nitrate ions.

This study delves into the evaluation of aforementioned cost-effective electrochemical sensors to measure various concentration of nitrate ion levels in real-world samples. Hence, water samples were collected from three different sources particularly a creek, a lake and a river. Samples with varying concentration of nitrate ions were synthesized using the collected water samples in a laboratory. Interdigitated electrodes were the chosen geometric pattern due to their performance over the other two geometric patterns. We also evaluated professionally etched tinned (Sn) and gold (Au) electrodes. All four materials (Ag, Cu, Sn, and Au) of electrodes were evaluated on their performance of detecting varying levels of nitrate ion content in water samples that already contains a wide array of impurities. Each of the electrodes were coated with a fine layer of PolyDiMethylSiloxane (PDMS) polymer which served as a protective layer between the

electrode surface and the sample. A combination of Sylgard 184 silicone elastomer base and curing agent, in 10:1 ratio, was used to prepare the PDMS solution. A drop weighing 0.4g was applied on top of the electrodes, which was then spun in a spin-coater at 5000 RPM for 240 seconds. The freshly coated electrodes were then cured at 100°C for 90 minutes in a hotbake oven. This layer contributed to extending the lifespan of the electrodes by preventing direct contact with the sample. Some researchers have also explored the use of ion-selective layer to establish a membrane between the electrodes and the target ion [175]. However, the primary focus of this research was to study the longevity and drift of the sensors by incorporating Electrochemical Impedance Spectroscopy (EIS) and obtaining results with just a polymer coating. This method is highly cost-effective, eliminating the need for extensive membrane preparation and coating. These sensors have the advantage of being washable that also makes them suitable for long-term use.

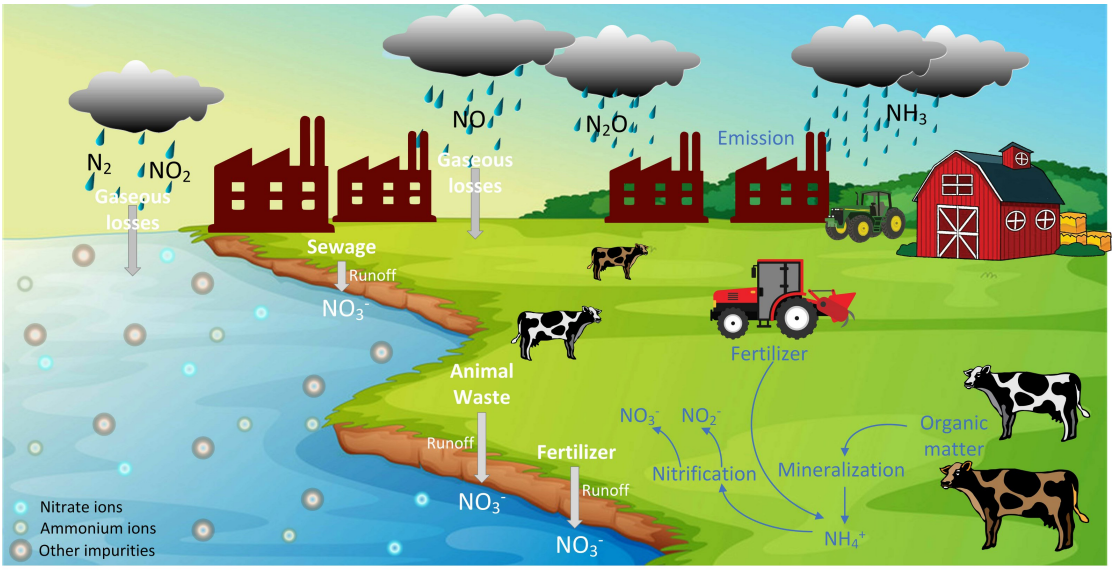

FIGURE 4.1: Leaching of nitrate ions in water

Real-world samples comprise of complex matrix of ions, chemical compounds and biological matter [176], most of which is a result of eutrophication and nitrate leaching that are complex interrelated environmental processes with significant consequences for aquatic ecosystems and human health [177]. Eutrophication is a natural process that occurs when a body of of water becomes enriched with nutrients, primarily nitrogen and phosphorous. These nutrients are essential for the growth of aquatic plants and algae. However, when they are present in excessive amounts, they can have a major impact on the ecosystem. Agricultural runoff is one of the primary sources of nutrient pollution

[178, 179]. Fertilizers used in farming are rich in nitrogen and phosphorous that easily dissolve in water. These dissolved nutrients can be carried by rainfall and irrigation into nearby water bodies. Various other anthropogenic activities such as wastewater discharge that comprise of sewage and industrial effluents can also introduce excess nutrients [180]. These activities also include releasing harmful chemicals into the air that react with rain, causing nutrient levels to rise. The eutrophication process is graphically presented in Figure 4.1.

4.2.1 Research Focus

Detecting nitrate ions, or any other ionic content in deionized (DI) water is a straightforward process because DI water contains only hydrogen (H^+) and hydroxide (OH^-) ions [181]. Therefore, detecting the ion of interest in DI water is relatively simple. However, the challenge arises when dealing with water samples containing diverse impurities such as various ions, chemical compounds, and biological matter which are the contents of water bodies. In such cases, detecting the specific ion of interest, becomes a complex and challenging task that affects the detection efficiency.

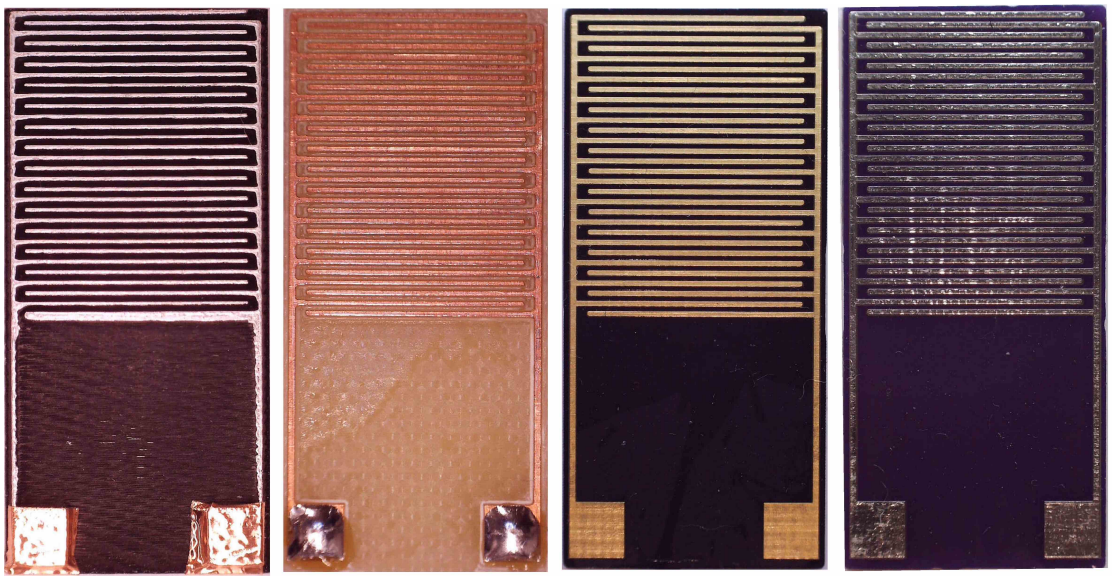

FIGURE 4.2: Images of four interdigitated electrodes fabricated using four materials, from left-right: silver, copper, gold, and tinned.

Current research was carried out using real-world samples that were collected from three different sources of water, namely: Lucas Creek, Lake Pupuke, and Waikato River. In our previous work, we established InterDigitated Electrodes (IDE) to be the better

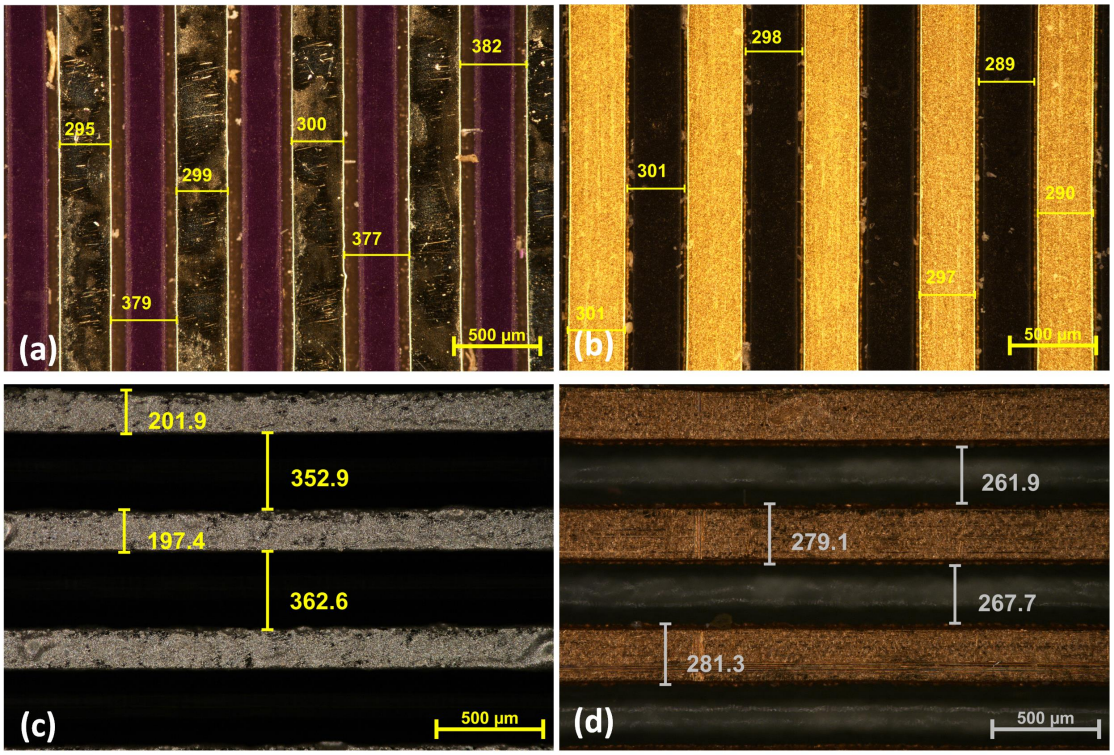

FIGURE 4.3: (a) Tinned, (b) Gold, (c) Silver, (d) copper electrode width and pitch measurements were taken using a microscope with 5x magnification, with the scale of 500 μm.

performing geometric pattern compared to square and serpentine, that were used for sensing various concentration levels of nitrate in deionised water. Hence, we chose IDE as the preferred pattern to carry out experimentation with the real-world water samples. The focus was on evaluating the performance of four different materials of electrodes that are: silver, copper, tin, and gold. The sensors that were used are shown in Figure 4.2 along with the dimensions of the sensors measured using a microscope are shown in Figure 4.3. Real-world water samples can contain a variety of ions, chemical compounds and other substances that form a complex matrix of impurities. This matrix can differ between samples gathered from different locations which may affect nitrate detection efficiency. Basic water quality parameters such as turbidity, pH, dissolved oxygen, total dissolved solids, and temperature can affect detection efficiency. Repeatability and drift tests were also conducted, to study the efficiency of sensing various concentrations of nitrate ions in water samples for a specified duration of time.

The novelty of this research lies in the detection of nitrate ions in a complex matrix of impurities in real-world samples, using low-cost sensors that can easily be fabricated

and a detection method that is efficient and can be miniaturized for field-deployed applications.

4.2.2 Sample collection

Real-world water samples can contain a matrix of impurities that can differ between samples gathered from different locations, which may affect detection efficiency. Basic water quality parameters such as turbidity, pH, dissolved oxygen, total dissolved solids, and temperature also affect detection efficiency.

To efficiently detect the concentration of nitrate ions in water, we chose to collect water samples from three different bodies of water, to cover a wide range of impurities. The levels of impurities differed among these various water bodies, including enclosed bodies like lakes and flowing bodies such as rivers. Water samples were gathered from three distinct sites, namely Lucas Creek, Lake Pupuke, and Waikato River. The sites were first inspected to identify potential hazards, prior to collection of sample. Since, the study focuses on assessing the overall nitrate levels in a body of water, surface water samples were collected rather than depth samples, that comprise of a broad range of water quality parameters and certain pollutants [182]. While water samples were collected, safety precautions were maintained by wearing gloves and storing the samples in new plastic bottles that were obtained from a retail outlet to avoid any contamination. The bottles were properly sealed and labelled with information such as location, date, and time. After collection of sample, bottles were wiped clean and dried, with waste disposed appropriately. One liter of each water sample was then sent to a local laboratory for analytical testing. A list of parameters that were tested along with the results from Hill laboratories are shown in Table 4.1.

4.3 Results

4.3.1 Sample Matrix

One liter of sample was sent to Hill laboratories which is accredited by International Accreditation New Zealand (IANZ). The analytical testing of the samples was carried out by the laboratory and the resulting data is presented in Table 4.1. The results

TABLE 4.1: Results from Hill laboratories showing the level of various water quality parameters as well as impurities present in the three water samples.

	Unit	Lake Pupuke	Lucas Creek	Waikato River
Turbidity	NTU	0.33	6.5	8.0
pH	pH units	8.1	7.5	7.5
Electrical Conductivity (EC)	mS/m	26.9	18.4	14.6
Total Dissolved Solids (TDS)	mg/L	121	122	127
Total Potassium	mg/L	2.0	2.4	3.4
Total Sodium	mg/L	27	16.1	16.2
Chloride	mg/L	34	18	13.5
Total Ammoniacal-N	mg/L	0.013	0.052	0.056
Nitrite-N	mg/L	< 0.002	0.003	0.013
Nitrate-N	mg/L	< 0.002	0.28	0.48
Nitrate-N + Nitrite-N	mg/L	< 0.002	0.28	0.50
Total Phosphorus	mg/L	0.010	0.032	0.045
Sulphate	mg/L	3.8	13.7	9.5

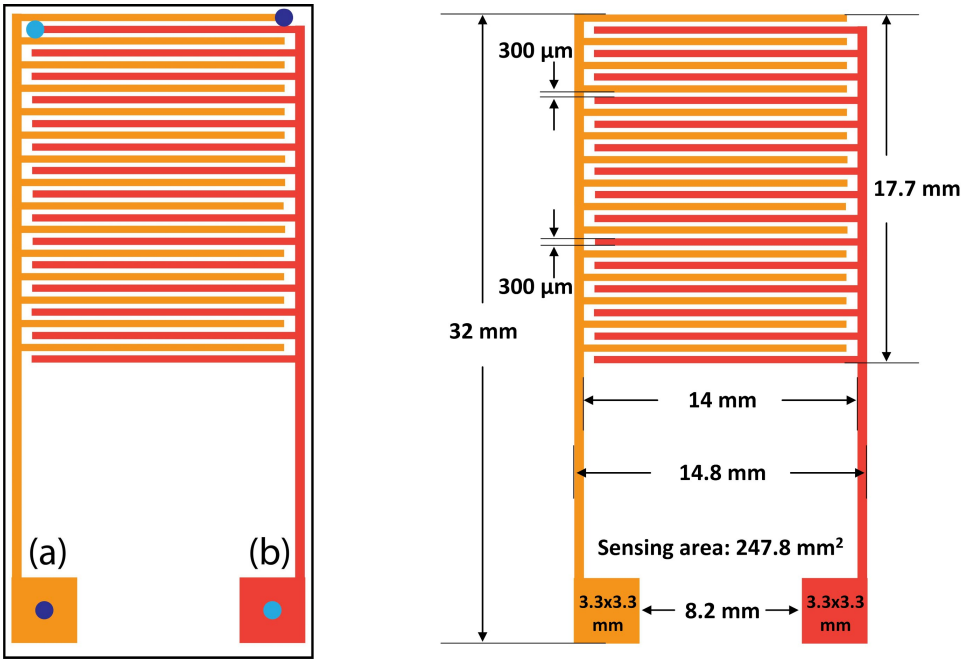

FIGURE 4.4: Figure (left) illustrates two probe impedance measurement. Driving and sensing electrodes are denoted by labels (a) and (b) respectively; Figure (right) shows the dimensions of the electrodes.

TABLE 4.2: Two-probe Resistance measurements of interdigitated electrodes for various materials. Three sensors of each material of electrodes were selected arbitrarily. Cost of each sensor is also stated.

	Sensor No.	Driving electrode (Ω)	Sensing electrode (Ω)	Cost (USD)
Tinned copper	1	0.28	0.24	0.30
	2	0.23	0.19	
	3	0.24	0.19	
Gold	1	0.24	0.18	1.00
	2	0.16	0.16	
	3	0.22	0.21	
Copper	1	0.32	0.27	0.40
	2	0.36	0.33	
	3	0.32	0.31	
Silver	1	44.2	51.2	0.60
	2	41.9	44.4	
	3	56.3	38.7	

comprised of the concentration level of different types of ionic and molecular content present in water, along with an assessment of various water quality parameters such as turbidity, pH, etc.

4.3.2 Experimental Setup

Safe concentration level of nitrate in freshwater sources must not exceed 11.3 mg/L [183] as suggested by the World Health Organization (WHO) and European Union (EU). The standard nitrate solution in use has the concentration of 0.01 Mol. To keep the units consistent, we convert Mol to mg/L. Firstly, the atomic weight (W) of KNO_3 needs to be determined, which is the sum of the atomic weights of all the elements in the compound.

$$W_{KNO_3} = W_K + W_N + 3.(W_O) \tag{4.1}$$

$$= 39.10 + 14.01 + 3(16)$$

$$= 101.11$$

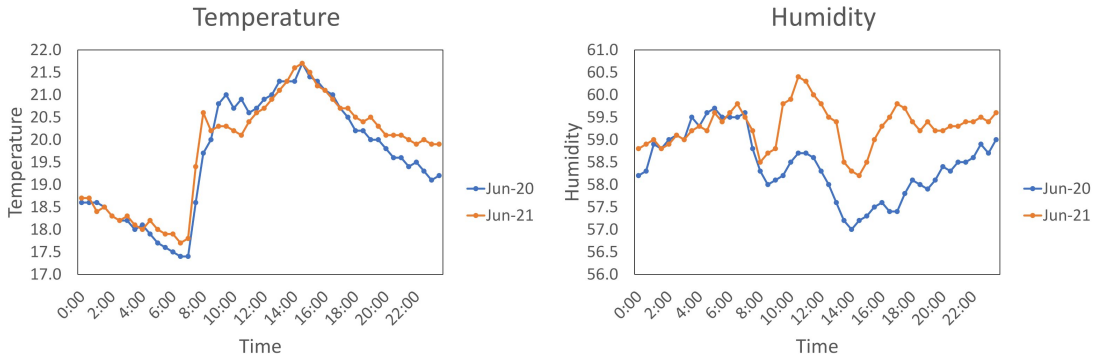

FIGURE 4.5: Temperature and Humidity readings taken every 30 minutes for 48 hours while some experiments were carried out.

Upon calculating the atomic weight of KNO_3, 0.01 Mol can be converted to mg/L by multiplying the calculated weight with the concentration in moles, then multiplied by 1000 to convert to mg which results in a value of 1011.1 mg/L, which is equivalent to 0.01 Mol of KNO_3. The experiments took place within a controlled laboratory environment with clean conditions and air conditioning where both the samples and sensors were stored. Instead of utilizing cold storage, the samples were kept at room temperature. Over a span of 48 hours, we collected temperature and humidity data within the laboratory. We employed the DHT22 sensor, which is a cost-effective digital sensor for measuring temperature and humidity. The graphical representation of the results is presented in Figure 4.5.

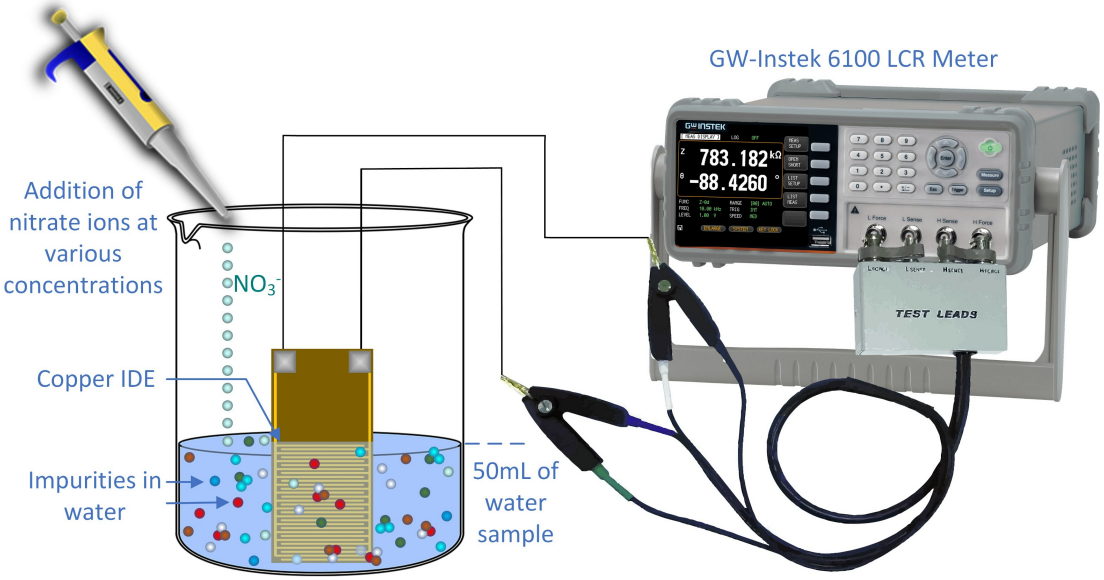

FIGURE 4.6: Figure depicts the experimental setup in a laboratory, using a beaker with 50 mL water sample and observing variations in impedance measurement as nitrate ions are added for concentrations from 0.1 to 1 mg/L.

The samples were synthesized by adding varying concentration levels of nitrate ions from 0.1 to 1 mg/L with increment of 0.1 mg/L into the water sample from each of the three locations. As illustrated in Figure 4.6, each experiment was initiated with 50 mL of a water sample in a 400 mL beaker. Using a 1-10 μL pipette, 5 μL of KNO_3 solution was added to the water sample in the beaker. This diluted the concentrated nitrate solution in the sample, resulting in the nitrate concentration of 0.1 mg/L in the beaker. The solution was then stirred for 5 seconds. An LCR meter was used to take impedance measurement at $1V_{p\text{-}p}$ for a range of frequencies, sweeping from 100 Hz to 100 kHz with increments based on the logarithmic scale. Subsequently, an additional 5 μL of KNO_3 solution was introduced into the water sample, elevating the nitrate ion concentration to 0.2 mg/L, followed by impedance measurements for a range of frequencies were taken again. The process was reiterated until the nitrate ion concentration reached 1 mg/L.

4.3.3 Findings

Fresh electrodes were used for each experiment, with new electrodes utilized every time a fresh sample from any of the locations was tested. The electrodes were not reused except for when we conducted drift tests. The results depicted in Figure 4.7, show that the impedance measurements obtained using silver (Ag) electrodes for various concentrations of nitrate ions are not in the appropriate sequence for any of the test frequencies. For instance, at 1 kHz, there is no clear distinction in the correct sequence of concentration to impedance for any of the locations. A repeat test was carried out with fresh set of silver electrodes in a fresh sample solution, but the outcome was similar.

As seen in Figures 4.8, 4.9, and 4.10, higher frequency sweeps, yield lower gradients. Higher gradient provides a greater dynamic range that would allow detection of small changes in concentration. The electrodes seem to be more responsive in the lower frequency range from 100 Hz to 1 kHz.

4.3.3.1 Aggregated results for each location

Results shown in Figure 4.11, depict an average of the resulting impedance measurement for various nitrate concentrations from five sensors. Five IDEs of each material were arbitrarily selected that included copper, gold, and tin. The most favourable impedance

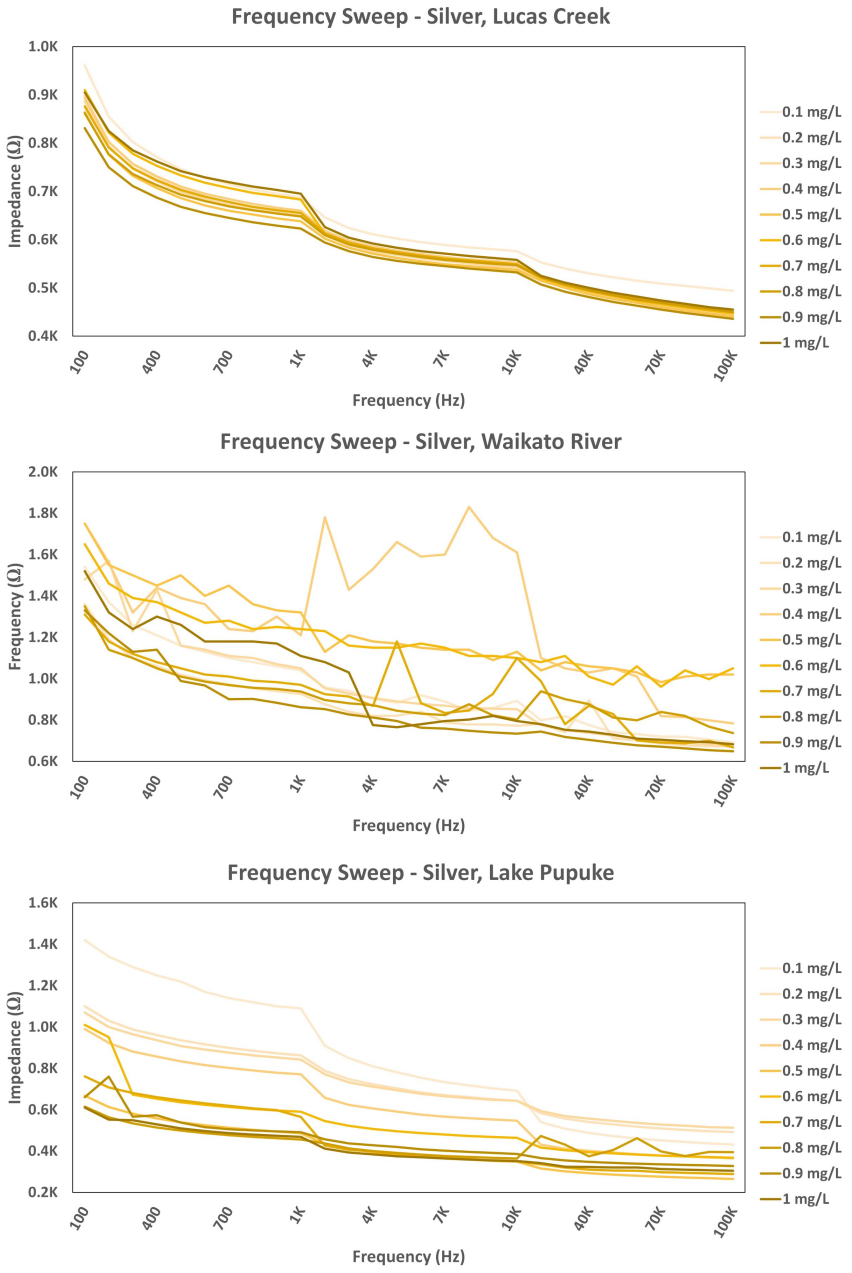

FIGURE 4.7: Figures show results obtained using silver electrodes with frequency sweeps from 100 Hz to 100 kHz. The graphs do not show a clear separation between various nitrate concentrations for any of the three locations.

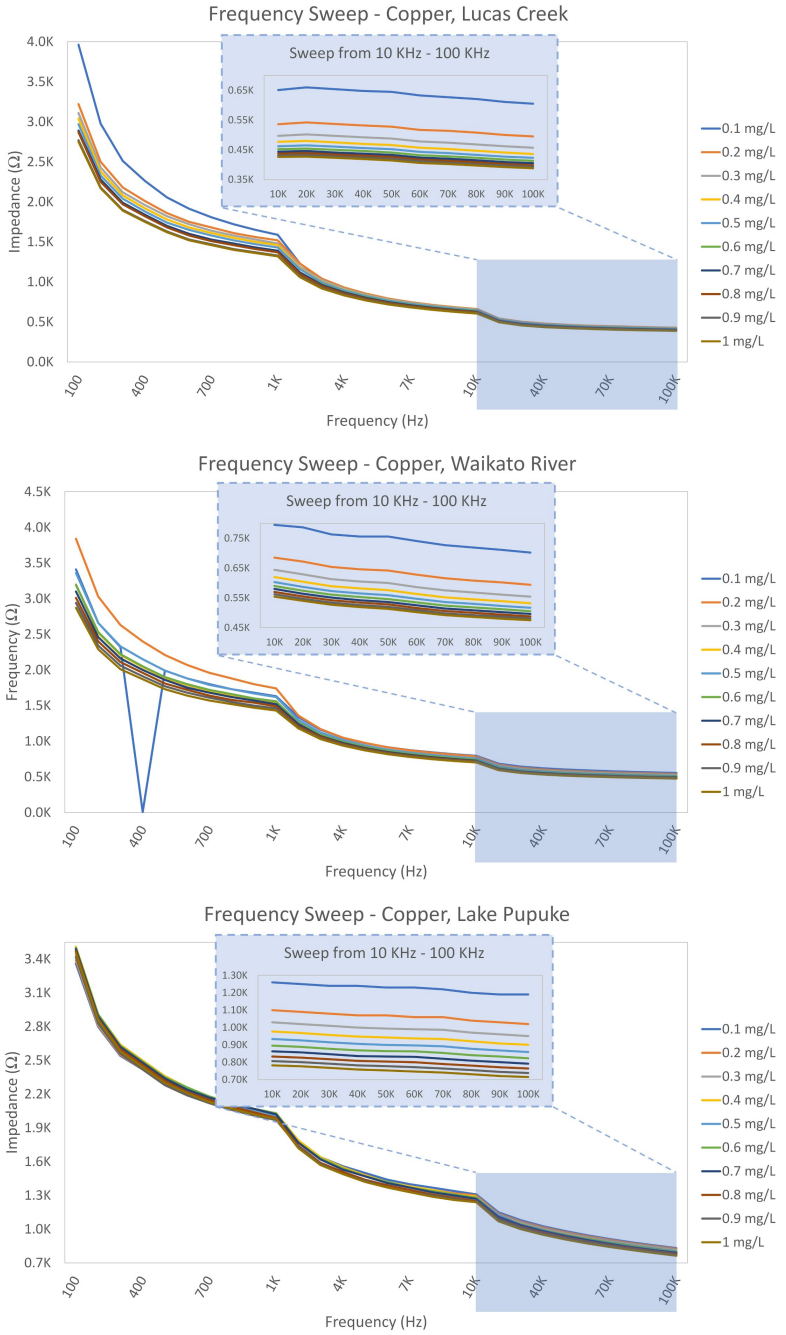

FIGURE 4.8: Frequency sweep for impedance measurement of copper (Cu) electrodes in varying concentration levels of nitrate in the water samples from three locations. The highlighted area shows a separation among different concentration levels for frequencies of 10-100 kHz.

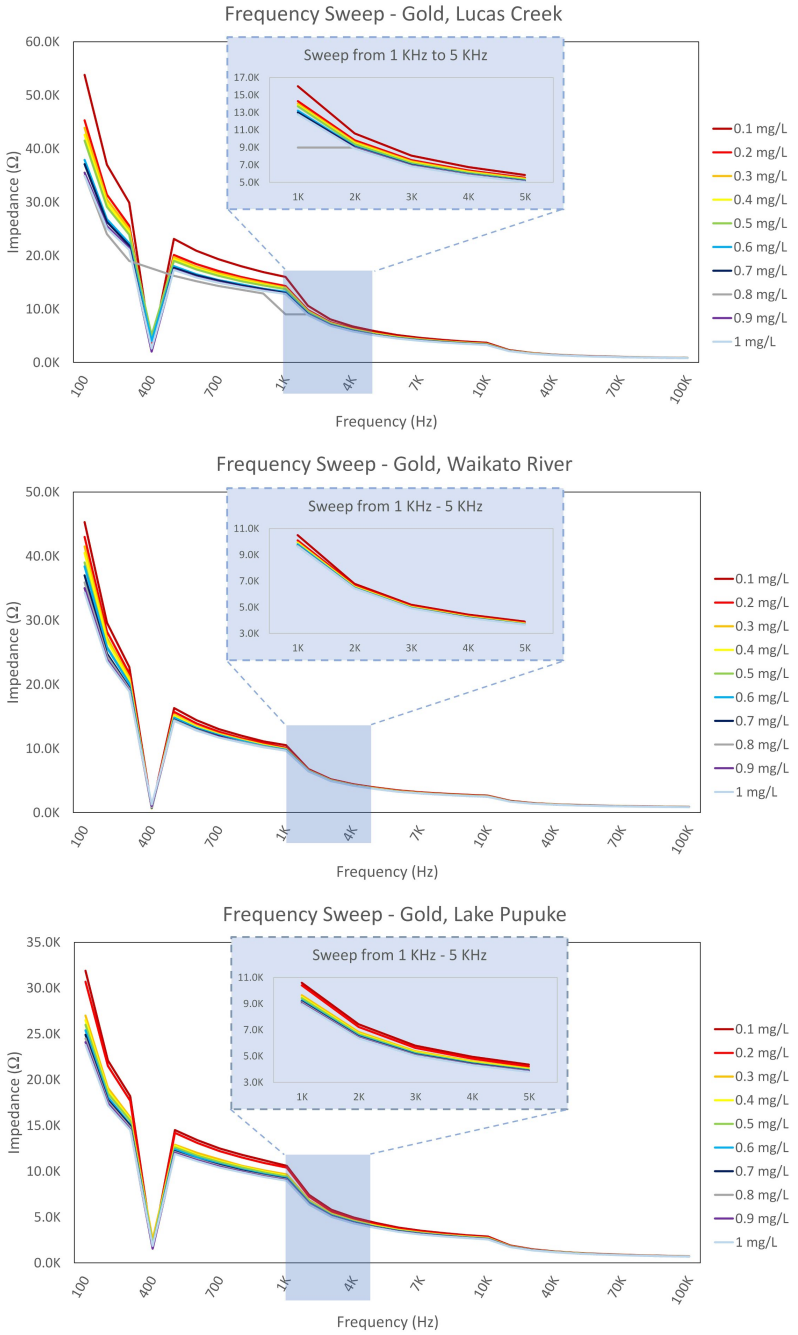

FIGURE 4.9: Frequency sweep for impedance measurement of Gold (Au) electrodes in varying concentration levels of nitrate in the water samples from three locations. The highlighted area shows a separation among different concentration levels for frequencies of 1-5 kHz.

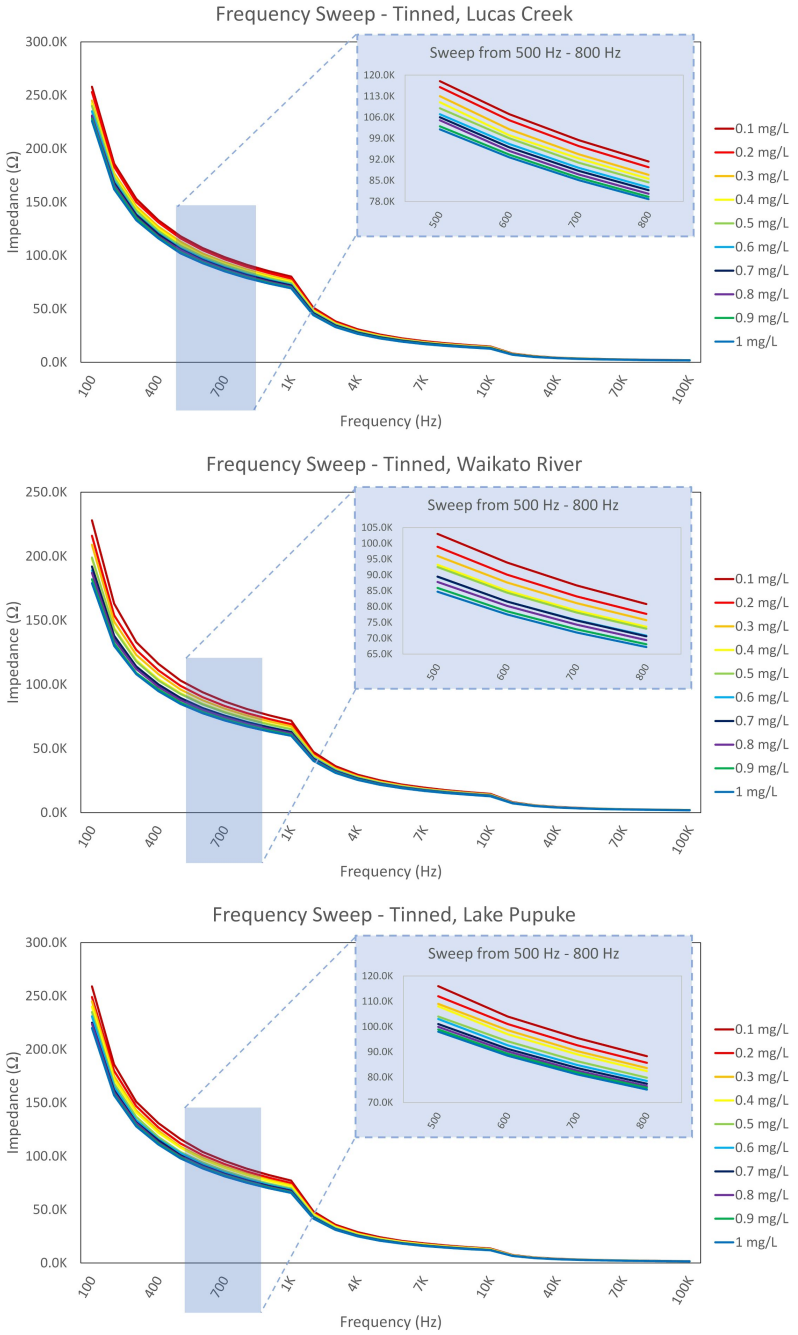

FIGURE 4.10: Frequency sweep for impedance measurement of Tinned (Sn) electrodes in varying concentration levels of nitrate in the water samples from three locations. The highlighted area shows a separation among different concentration levels for frequencies of 500-800 Hz.

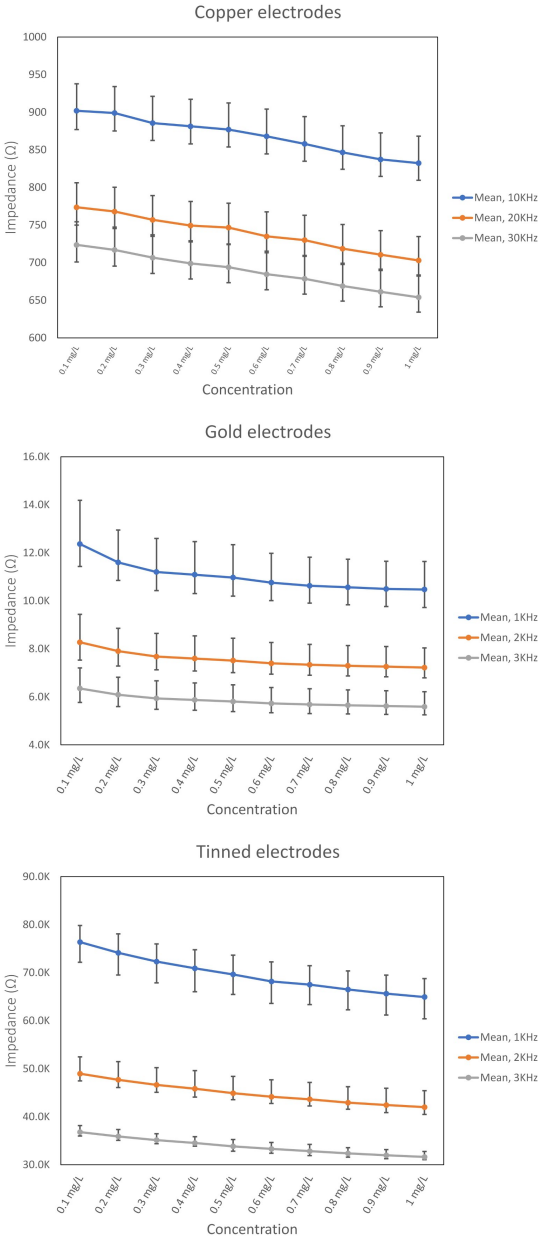

FIGURE 4.11: Results show frequencies of 10-30 kHz performed well for copper electrodes while 1-3 kHz performed well for gold and tinned electrodes. These frequencies showed a clear separation between various concentration levels which is why these frequency ranges were selected. The figure graphically represents the mean of all the three frequencies for the three locations.

measurements would display an inverse linear relationship between impedance and concentration. Such impedance measurements were obtained within the frequency range of 1-3 kHz for gold and tin electrodes, while the optimal range for copper electrodes was found to be within 10-30 kHz.

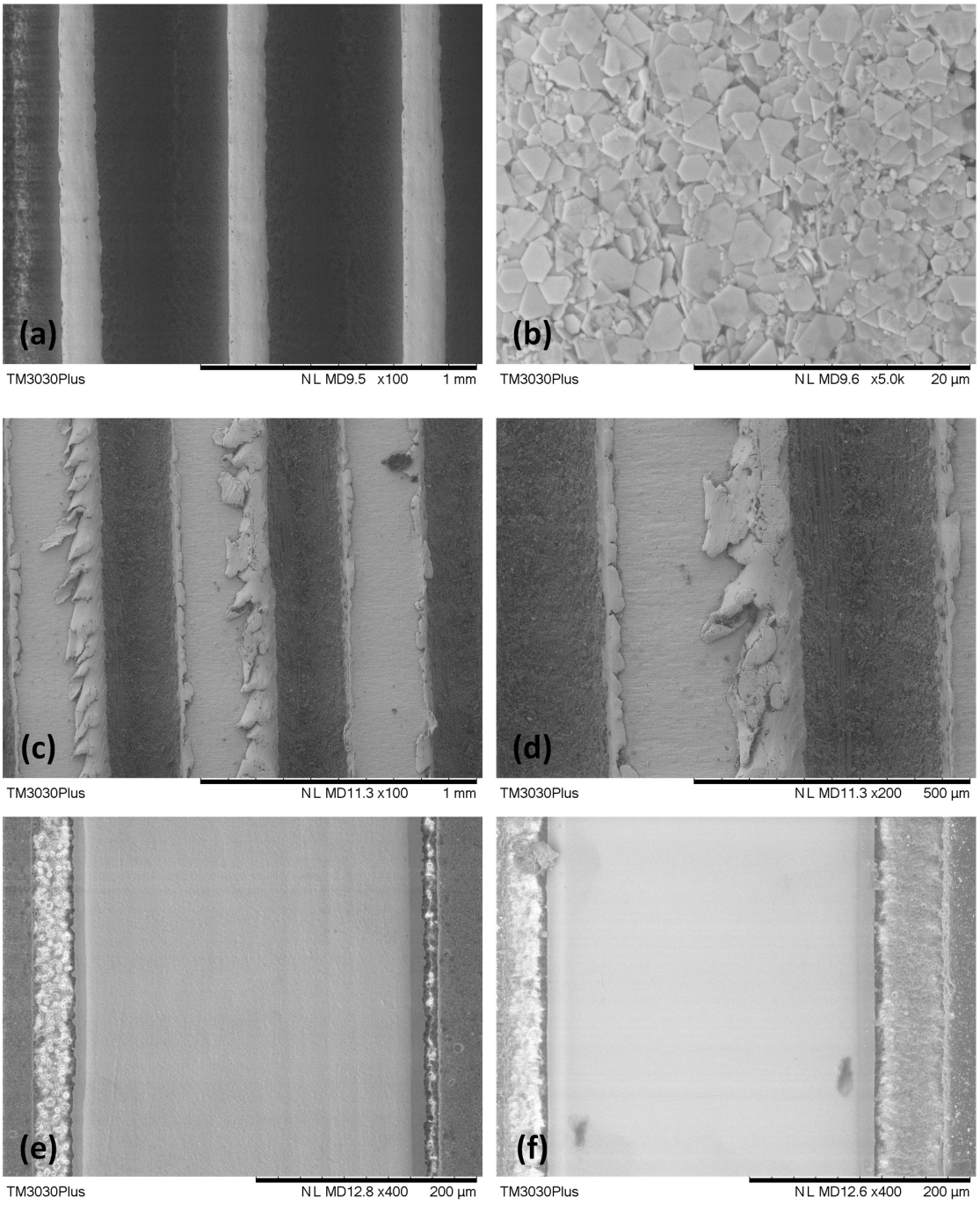

FIGURE 4.12: SEM images of silver electrodes (a,b) with magnification of x100 and x5000, respectively; copper electrodes (c,d) with x100 and x200 magnification prior to PDMS coating; gold (e) and tinned (f) electrodes, both with magnification x400.

4.3.3.2 Low Nitrate Concentration Test

We also carried out experiments for low concentration of nitrate from 0.01 to 0.1 mg/L in Waikato river sample. We chose this sample because it comprised of the highest level of turbidity as seen from the report from Hill Laboratories shown in Table 4.1

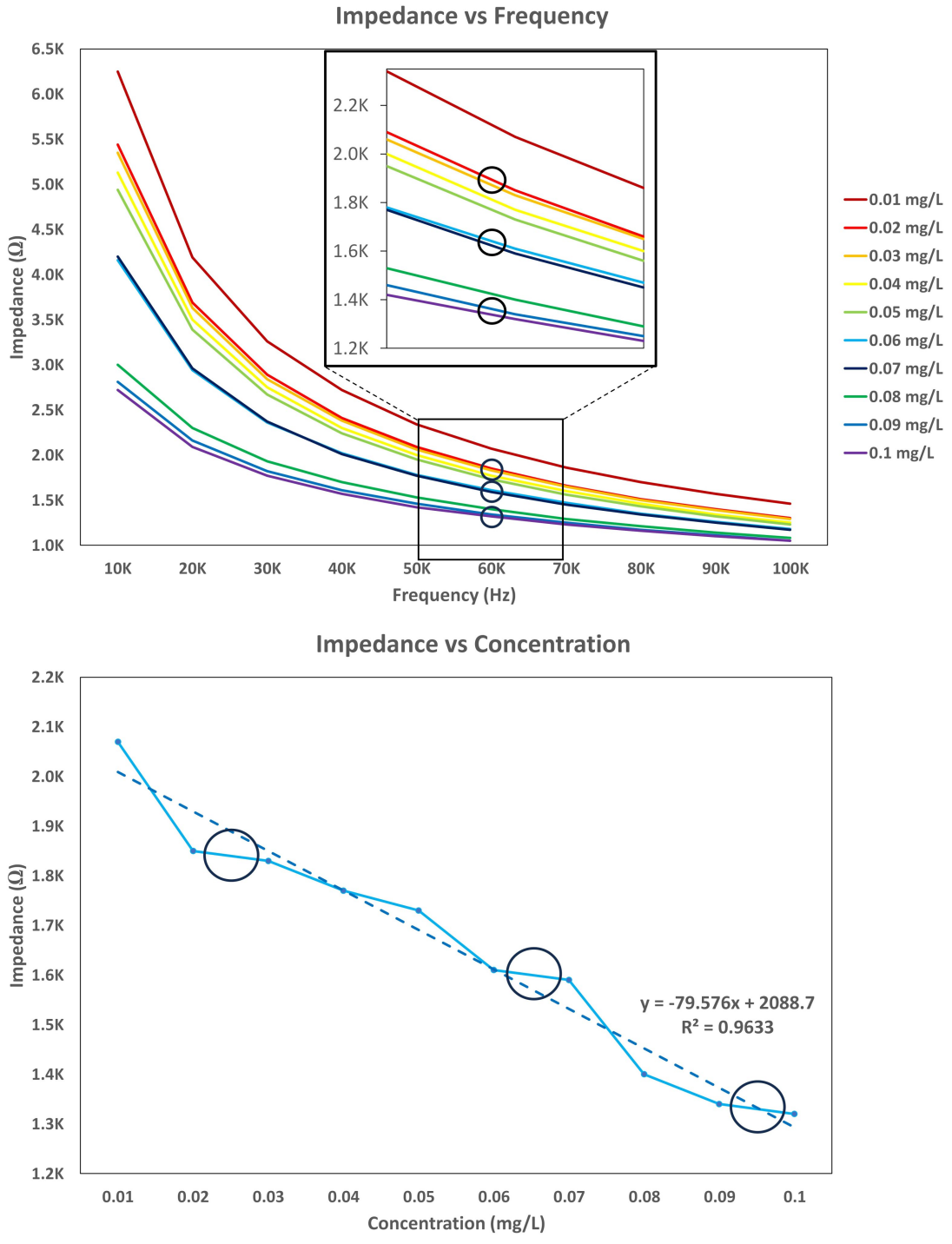

FIGURE 4.13: Results of nitrate sensing with low concentrations using Waikato river sample with Copper electrodes. Impedance vs Frequency measurement at frequencies 10 kHz to 100 kHz (top), Impedance vs Concentration (bottom) depicting linearity at 60 kHz.

and evaluate copper electrode performance to sense low levels of nitrate ions in a turbid sample. This test was carried out to assess the performance of electrodes when turbidity and total dissolved solids were high in the water. Furthermore, copper electrodes were used because they were fabricated using a printed circuit board fabricator or a CNC milling machine which is commonly available at workshops.

Referring to impedance vs frequency graph in Figure 4.13(top), that shows the impedance response for low concentration of nitrate for frequency sweeps from 10 kHz to 100 kHz. Looking at the marked regions, the impedance measurements taken at 60 kHz, show a clear separation in the correct sequence of various nitrate concentration levels. Isolating the impedance response for 60 kHz shown in bottom image in the same figure, the corresponding marked areas show minimal impedance variation between distinct ascending concentration levels from 0.01 to 0.1 mg/L. The impedance measurements at this frequency seem to have a higher gradient compared to other frequencies, resulting in a linear relationship with R^2 value of 0.9633. Set of results shown in figure indicates that impedance measurements with IDEs could also detect small variations in nitrate levels in turbid samples.

4.3.3.3 Drift Tests

Concurrent and drift tests are crucial factors in water quality monitoring to ensure sensor efficiency and accuracy over a period of time. We included Sn, Au, and Cu electrodes for these tests. Concurrent testing was carried out using five interdigitated electrodes of the same material, that were systematically mounted inside a 400 mL beaker, containing 50 mL of Waikato river sample. Nitrate ion solution was added to the sample solution, resulting in an initial nitrate concentration of 0.1 mg/L. The sensors remained dipped in the solution while the concentration of nitrate ions was increased sequentially in 0.1 mg/L increments until the solution reached maximum nitrate concentration of 1 mg/L. Impedance measurements were taken after every increment, with frequency sweeps from 100 Hz to 100 kHz. Concurrent testing of the electrodes is particularly important to assess the variation between the electrodes themselves. This is important in ensuring the quality and consistency of the electrode performance. For example, if all the five sensors of the same electrode material produce similar results, it would establish confidence in sensor performance and accuracy. Ideally, five sensors of the same electrode material

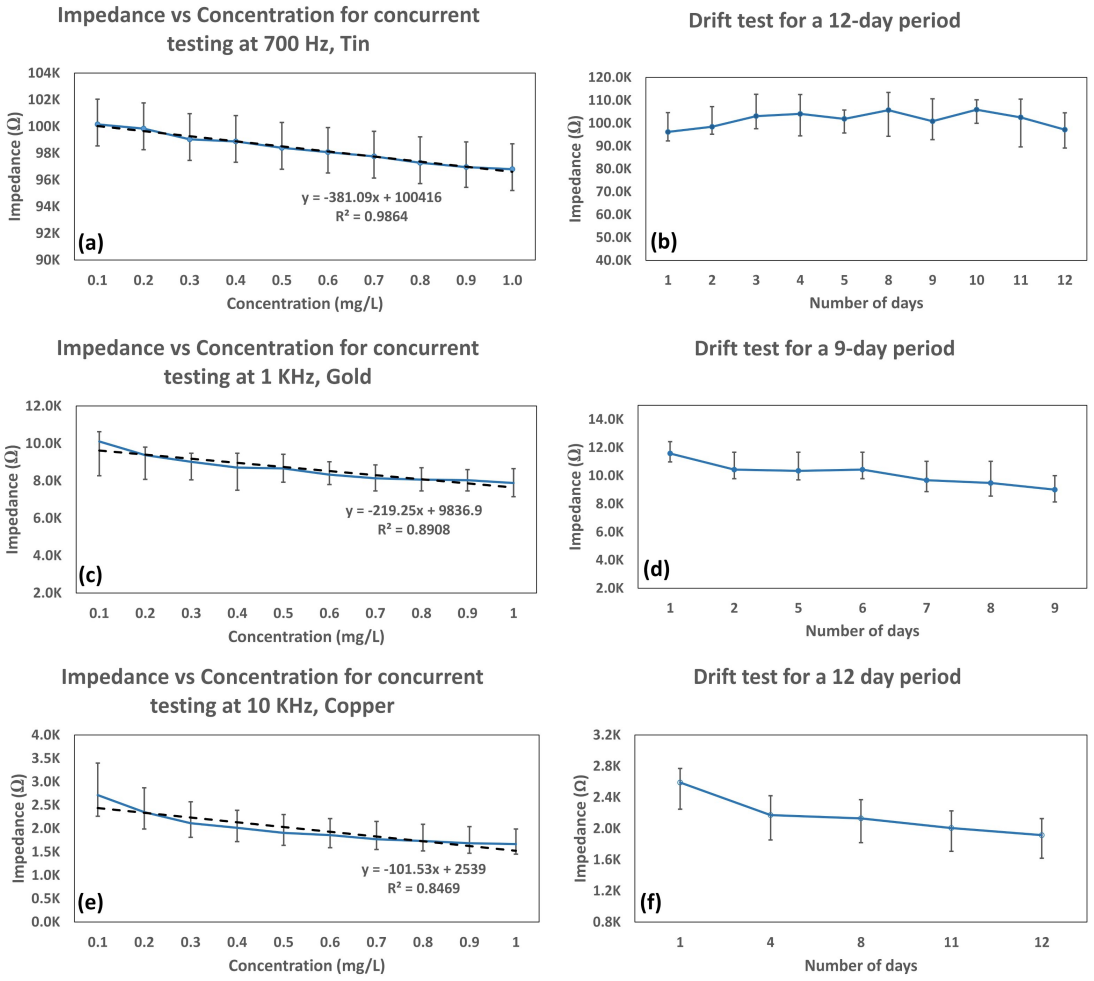

FIGURE 4.14: Results showing the concurrent and drift tests. Graphs (a,c,e) depict concurrent testing of Sn, Au, and Cu electrodes respectively, while, graphs (b,d,f) show drift tests for the respective Sn, Au, and Cu electrodes.

would produce the same result. However, results presented in Figure 4.14 (a), (c), and (e) indicates that the variation among different electrode materials can be used for calibration. Referring back to Figures 4.10, 4.9, and 4.8, a close examination of the resulting impedance measurement for each electrode material was focused on the frequencies of 700 Hz, 1 kHz, and 10 kHz for the respective Sn, Au, and Cu electrodes, as these specific frequencies yielded the most favorable impedance measurements.

Following the concurrent testing using five separate electrodes of each material, we carried out the drift tests over a period of 12, 9, and 12 days for Sn, Au, and Cu electrodes, respectively. The nitrate concentration level of 1 mg/L from concurrent testing, the sensors remained dipped in the sample solution for the aforementioned number of days. During the drift test, the sensor was exposed to a stable environment, that included optimal room temperature and humidity. The purpose of this test was

to monitor and record any gradual changes in the sensor's impedance measurement in response to degradation of PDMS coating or electrode oxidation. To measure variations in temperature and humidity while the sample solution remained in the laboratory, we measured humidity and temperature in 30 minute intervals, for forty eight hours. The results are depicted in Figure 4.5. Each day, prior to impedance measurement, the sample was stirred for five seconds, with frequency sweeps from 100 Hz to 100 kHz for each of the five sensors. The results of the drift tests are shown in Figure 4.14 (b), (d), and (f) for Sn, Au, and Cu electrodes, respectively.

The concurrent test results show a direct correlation between concentration and impedance, where they display an inverse relationship. This correlation is displayed for all the three electrode materials, with tinned electrodes performing better than other materials with R^2 value of 0.9864 compared to gold and copper achieving 0.8908 and 0.861, respectively. Regarding drift tests, tinned electrodes performed well, with an impedance variation of approximately 10 kΩ, similar to gold electrodes. However, copper electrodes showed the best performance, with a minimal impedance variation of only 800 Ω.

4.3.3.4 Hysteresis

Hysteresis is a phenomenon where the sensor's output that is measured as impedance in this case, exhibits a delay when the analyte concentration in the sample changes from higher value to lower and vice versa and how the sensor responds to this change. An ideal sensor's response would be the same for an increasing or decreasing concentration which results in a loop-like curve when the data is viewed graphically. However, hysteresis introduces a discrepancy in the sensor's behaviour which should be minimised to ensure accurate and consistent measurements [184].

Hysteresis data shown in Figure 4.15, was collected using Waikato River sample with tinned electrodes. Initially, a 50 mL sample was placed in a 500 mL beaker, and nitrate solution was systematically introduced in increments ranging from 0.1 mg/L to 1 mg/L, with 0.1 mg/L increments. Impedance measurements were taken at every step with frequency sweeps from 100 Hz - 100 kHz. Upon reaching 1 mg/L of nitrate concentration in initial 50 mL of sample, additional water sample was introduced into the existing solution, resulting in a dilution of the concentration from 1 mg/L back to 0.1 mg/L with 0.1 mg/L decrements. The resulting hysteresis at 700 Hz is shown in Figure 4.15.

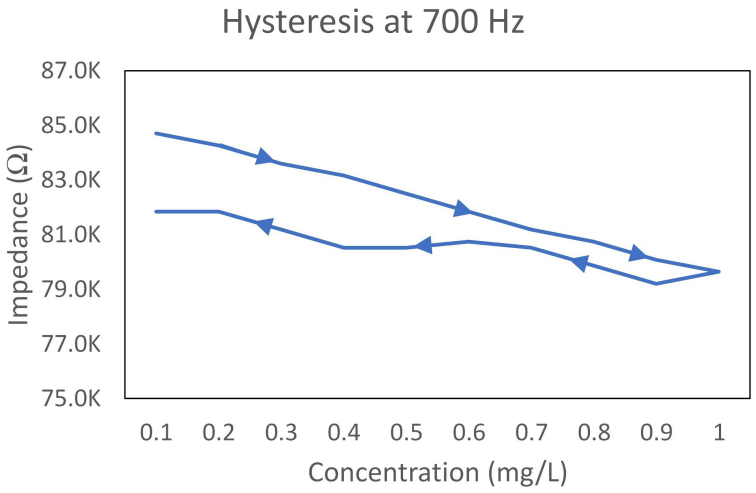

FIGURE 4.15: Hysteresis data using Waikato River sample with tinned electrodes.

4.4 Discussion

The frequency sweeps and the resulting impedance measurements were depicted in Figures 4.7, 4.8, 4.9, and 4.10, for the respective silver, copper, gold, and tin materials of electrodes. Referring to the results using silver electrodes, it is clear that the electrodes did not meet the expected performance levels in real-world samples. As a result, a specific frequency range at which the electrodes perform effectively, could not be determined for any of the three locations. To account for human error, synthesis of nitrate samples, instrument calibration error and other factors, we repeated the experiments with fresh set of silver electrodes. This could be due to the nature of silver ink that was used to prepare the electrodes. A close inspection of the electrode surface was then performed using Scanning Electron Microscope (SEM). The results obtained from SEM are shown in Figure 4.12. Images (a) and (b) depict the silver electrode surface, which is made up of fine flakes of silver, and could be a contributing factor to high point-to-point resistance of silver electrodes as shown in Table 4.2. Referring to the same figure, compared to silver electrode surface, surfaces of copper, gold, and tin electrodes, appeared smooth and continuous, thereby exhibiting low point-to-point resistance. We could see the outcome of the milling process of copper electrodes on the images (c) and (d). The new set of results for silver electrodes were not much different to what was presented in Figure 4.7. Furthermore, upon examining the graphs for copper electrodes in Figure 4.8, it is apparent that frequencies between 10kHz to 100 kHz produce impedance measurements that display a noticeable, step-wise progression across different nitrate concentration levels

for all three locations. However, it is worth noting that the dynamic range is relatively limited, with a maximum of 500 Ω for all the three locations.

Upon analyzing gold and tin electrodes, distinct sequential order for various concentration levels was also noticed. Frequencies in the range of 1 kHz to 5 kHz were most effective for gold electrodes, while tin electrodes demonstrated optimal impedance measurements between 500 Hz to 800 Hz with a wide dynamic range of impedance. However, the impedance variation between consecutive concentration levels using gold electrodes was relatively minimal when compared to tin electrodes. This would make it challenging to measure slight changes in nitrate levels, which was elaborated in Figure 4.11. The figure displays the results of the concurrent and drift tests that we also performed. From concurrent tests using five of each material of electrodes, it is evident that impedance measurements for gold electrodes exhibit a relatively flat line for the optimal performing frequencies of 1-3 kHz, indicating a low gradient. Therefore, a small change in nitrate concentration would incur a minimal change in impedance. However, copper and tin electrodes show a slope that would be ideal to detect slight changes in nitrate concentration in the sample.

Referring to the results from Hill laboratories in Table 4.1, Lucas Creek and Waikato River samples originally had marginally higher level of Nitrate-N ions at 0.28 mg/L and 0.48 mg/L, respectively, compared to Lake Pupuke with under 0.002 mg/L of nitrate content. A similar trend was also observed with Sulphate ion level. However, Total Sodium and Chloride ions were in much larger proportion in Lake Pupuke compared to other two water bodies. Upon analyzing the water quality parameters that include Turbidity, pH, Electrical Conductivity (EC), and Total Dissolved Solids (TDS) for all the three water samples, we found that pH level was near neutral and TDS values were relatively consistent across all the three samples. Furthermore, water clarity was notably better at Lake Pupuke, compared to other two locations, as also indicated by Turbidity results. However, EC values were a lot higher at Lake Pupuke. Referring to Figure 4.10, due to a higher initial concentration of nitrate level at the river, 0.6 mg/L at the river is equivalent to 0.1 mg/L at the lake. Looking at the impedance value at 500 Hz, the value is very close at the two concentration levels at approximately 104 kΩ. This is an indication that the sensor detects appropriate impedance for the relevant concentration of nitrate content in water.

Future work will involve deploying the sensor as part of our water quality assessment system for on-site nitrate concentration levels. Additionally, further studies will involve testing and evaluating the performance of different coatings on the sensing electrodes, for example, nitrate sensitive coating and its performance with real-world samples. Furthermore, evaluation of electrode performance in a more diverse matrix of impurities and gauging the performance of nitrate detection would be beneficial in producing good impedance characteristics which would enable a more accurate nitrate sensor.

4.5 Conclusion

The primary focus of this study was to evaluate the performance of four distinct materials of electrodes, particularly: silver, copper, gold, and tin. These electrodes were used to determine concentration of nitrate ions in real-world water samples. This research carries on from our previous work on detection of various concentrations of nitrate ions in deionised water, where we studied the physical aspects of different materials of electrodes in various geometric patterns. We explored how the electric field density, generated by various geometric patterns, influences the sensitivity and speed of detection. Additionally, we aimed to establish a reference point for the electrodes and evaluate their performance characteristics using EIS. We also evaluated different electrode fabrication processes, to develop a sensor that was cost-effective and easy to fabricate. Based on the findings of the study, it was evident that interdigitated pattern of electrodes (IDE) outperformed other patterns. Hence, we chose to use interdigitated geometric pattern for the work conducted in this study. Silver and copper electrodes were fabricated using in-house facilities on PMMA and fiberglass substrates, respectively. In addition to the use of silver and copper electrodes, we also conducted an evaluation of gold and tin electrodes, that were fabricated professionally from JLC on fiberglass substrate. All four materials of electrodes were coated with a thin layer of PDMS polymer to prevent direct contact with water, thereby, protecting the electrodes from oxidation.

As our focus was on detection of nitrate ions in freshwater, water samples were collected from three different freshwater sources, namely, Lucas Creek, Waikato River, and Lake Pupuke. The samples and the sensing electrodes were stored in our in-house sensors laboratory at room temperature where we monitored changes in humidity and temperature for 48 hours by employing a DHT22 sensor to measure fluctuations in these parameters.

As this study involved the use of real-world water samples containing various ionic, molecular compounds, and other impurities, our first step was to send one liter of sample from each location to Hill laboratories. This laboratory conducted a comprehensive analysis of the samples to identify the specific impurities present in them. The results are shown in Table 4.1. The experiments were then conducted in the sensors laboratory at our university, where synthetic nitrate solutions were prepared using water samples that were collected. Each material of electrode was tested with varying levels of nitrate ions, added to the water samples, ranging from 0.1 mg/L up to 1 mg/L in 0.1 mg/L increments. Each time nitrate ions were added to the sample solution, impedance measurements were taken and recorded on an LCR meter for a range of frequency sweep from 100 Hz to 100 kHz with increments based on the logarithmic scale. By sweeping through a wide range of frequencies, we established impedance characteristics to identify the frequencies at which optimal performance was achieved that resulted in clear differentiation between impedance measurements for various nitrate ion concentrations.

The water samples were collected during a period of several days of rainfall, and as a result, it was expected that water parameters and impurities would vary under different weather conditions. During rainfall, the surface water typically tends to be somewhat fresher than the deeper water.

Chapter 5

Low-cost IoT based system for lake water quality monitoring

5.1 Abstract

Water quality monitoring is a critical process in maintaining the well-being of aquatic ecosystems and ensuring growth of the surrounding environment. Clean water supports and maintains the health, livelihoods, and ecological balance of the ecosystem as a whole. Regular assessment of water quality is essential to ensure clean and reliable water is available to everyone. This requires regular measurement of pollutants or contaminants in water that can be monitored in real-time. Hence, this research showcases a system that consists of low-cost sensors used to measure five basic parameters of water quality that are: turbidity, total dissolved solids, temperature, pH, and dissolved oxygen. The system incorporates electronics and IoT technology that are powered by a solar charged lead acid battery. The data gathered from the sensors was stored locally on a micro-SD card with live updates that could be viewed on a mobile device when in proximity to the system. Data was gathered from three different bodies of water over a span of three weeks, precisely during the seasonal transition from autumn to winter. We adopted a water sampling technique since our low-cost sensors were not designed for continuous submersion. The results show that the temperature drops gradually during this period and an inversely proportional relationship between pH and temperature could be observed. The concentration of total dissolved solids decreased during rainy periods

with a variation in turbidity. The deployed system was robust and autonomous that effectively monitored the quality of water in real-time with scope of adding more sensors and employing Industry 4.0 paradigm to predict variations in water quality.

5.2 Introduction

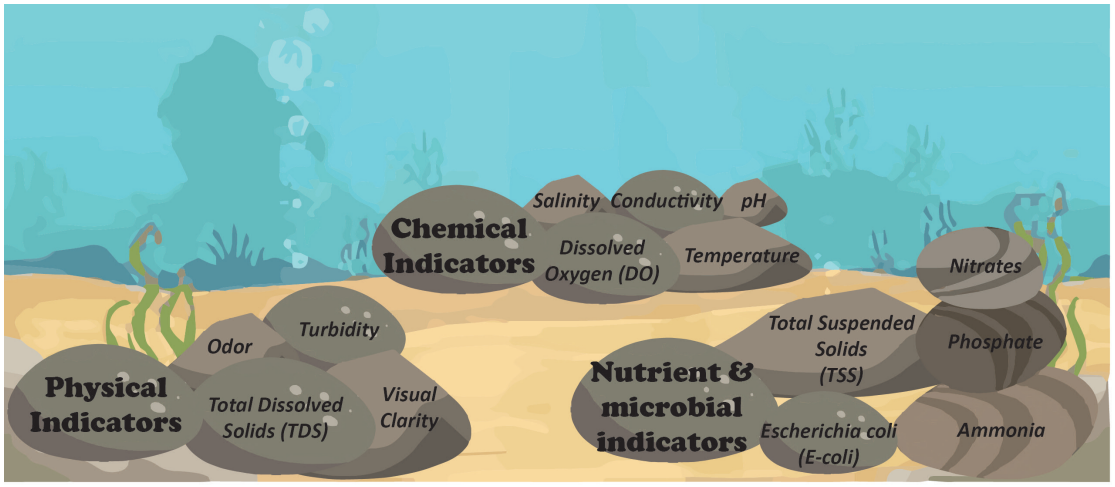

FIGURE 5.1: Physical, chemical, nutrient and microbial indicators of water quality.

The determination of water quality is desirable for a wide range of reasons. Firstly, water quality has a significant impact on aquatic life, plant growth, and human health. There are key indicators that can be used to clearly define water quality that are primarily broken into four categories: 1) biological indicators; 2) chemical indicators; 3) physical indicators; and 4) recreational indicators. Some of the indicators that are within these categories are: water conductivity, salinity, acidification, wastewater chemicals like E-coli and ammoniacal nitrogen, chlorophyll, water clarity, sediment enzymes, sediment mercury, algal toxins, Nitrogen, Phosphorus, dissolved Oxygen, Cyanobacteria, Atrazine, and Oxidation Reduction Potential (ORP) [185, 186]. Fig. 5.1 depicts a diverse range of indicators that provide information about different aspects of water quality. The physico-chemical attributes, such as dissolved oxygen and temperature have a large impact on aquatic life, the nutrient elements, such as nitrogen and phosphorus, greatly benefit plant growth; whereas, faecal microbial contaminants, such as E-coli, can have an adverse effect on human health [187]. Freshwater sources are facing a worldwide scarcity due to significant human utilization and pollution. Only 0.6% of the world's water is considered freshwater, and currently, 85% of this small percentage is used in agriculture.

TABLE 5.1: Water quality parameters with WHO standard of clean water

Parameter	WHO standard	Units
pH	7 - 8.5	
Turbidity	1 - 5	NTU
Dissolved Oxygen (DO)	5 - 6	mg/L
Total Dissolved Solids (TDS)	500	ppm
Temperature	15	°C

To determine the condition of a body of water, aforementioned indicators or parameters have been established to collectively determine the water quality, from which five are considered to be the most fundamental parameters that include pH (power of Hydrogen), turbidity, Dissolved Oxygen (DO), Total Dissolved Solids (TDS) and temperature. These fundamental parameters are important to learn from the natural processes in the environment and determine human impacts on the ecosystem [188]. These parameters also provide valuable information about the physical, chemical, and biological characteristics of water while ensuring environmental standards are being met [189]. For instance, pH refers to the level of acidity or alkalinity of water, which is measured by the concentration of hydrogen ions present, providing a numerical pH value. pH scale varies from 0 to 14. A value of 7 denotes a neutral state, while values above and below this state determine the alkaline or acidic nature of water. Turbidity refers to the degree of cloudiness of water, which arises from solids or materials suspended in water. For example, healthy water for drinking should have turbidity less than one Nephelometric Turbidity Unit (NTU). Temperature refers to how hot or cold water is, measured in degree Celsius. Temperature is associated with affecting the physical and biological processes in aquatic environments. DO refers to the quantity of oxygen dissolved in water which determines the quality of life led by aquatic organisms which greatly depends on temperature. For instance, low dissolved oxygen can flourish aquatic beings such as fish. Low dissolved oxygen can arise from pollution or poor water circulation. Warm water holds less DO than cold water, and some compounds are more toxic to aquatic life at higher temperatures [190]. Furthermore, TDS refers to the amount of suspended particles in water. This can be in the form of silt, clay, organic matter, or other pollutants. Table 5.1 indicates water quality parameters that are relevant to this study and the standards set by the World Health Organization (WHO) that defines typical values for ensuring good water quality.

Due to natural and anthropogenic release of contaminants into water, need for instantaneous measurement of water quality has become imperative. Cost-effective and real-time assessment of water quality over a certain period of time would allow end users such as government agencies and city council to access detailed evidence and trends that can support informed decisions toward managing the quality of water. With the advancement in sensing technologies and long range wireless communication networks, a low-cost water quality monitoring system can be developed to provide real-time data on condition of water quality [191]. This data can be remotely monitored and analyzed by the end users, which would be helpful in initiating any necessary interventions to keep water parameters within the required standard [192], as defined in Table 5.1.

Several laboratory-based methods are available that offer precise measurements with high sensitivity. Research in the field of water quality testing predominantly takes place using traditional sampling and laboratory methods that suffer from limitation. These drawbacks include monotonous process of sample collection which is time consuming and require a specialized facility with sophisticated laboratory equipment and trained personnel to operate [193]. This process can be very costly that also involves high overheads. Table 5.2 summarises strengths and weaknesses of laboratory-based and on-site testing methods.

TABLE 5.2: Advantages and disadvantages of on-site and lab-based water quality testing

On-Site Water Quality Monitoring		
Advantages	**Disadvantages**	**Ref**
Real-time results	Offer limited Parameters	[194]
Cost-effective	Lower accuracy	
Rapid-response	Regular calibration of sensors maybe required	
Automated data analysis	Complex analysis maybe limited	
Laboratory-Based Water Quality Testing		
Advantages	**Disadvantages**	**Ref**
Comprehensive list of parameters can be included	Time consuming	[195]
Highly accurate	Costly	
Sensitive detection using specialized equipment	Delay in receiving results	

Ample research has taken place all over the world in studying the quality of water that largely involves sample collection and testing in a laboratory. Few studies have come

to light that can provide regular updates on water quality, either through direct text messaging or cloud based monitoring but still rely on collection of sample and testing them on a system built with sensors and the IoT communications technologies. Most of the systems signal the user when any of the parameters are outside the preset thresholds.

Related solutions

Studies around water quality assessment have been carried out by numerous researchers worldwide, utilizing low-cost sensors integrated into various systems such as buoys and custom designed flotation devices. The systems not only monitor five basic parameters, but also measure Oxidation-Reduction Potential (ORP), Electrical Conductivity (EC), Total Suspended Solids (TSS), and more. Additionally, these studies leverage long-range communications and cloud services for effective data transmission and monitoring.

Demetillo et al. [196] developed two buoys and monitored water temperature, DO, and pH in a pre-programmed time interval. All sensors are connected to a microcontroller that stored information in a database. Zigbee modules were used for communication between the two nodes while a GSM module was used for sending text messages to the end-user. The information was displayed graphically on a web page that could be accessed through preregistered mobile phone for quick monitoring for only selected end-users. Similarly, Prasad et al. [197] built a system housed with four sensors namely temperature, pH, ORP and conductivity. The sensors, SD card module, and GSM module, interfaced to an Arduino Uno board that took readings from the sensors at interval of 15 minutes. Water quality was tested in tap water, creek, coast, and sea water samples. The data showed a relationship between temperature, pH and conductivity of the sample. Temperature was proportional to conductivity and inversely proportional to pH. The system was programmed to send a text message to the user if any of the parameters were detected beyond the water quality standard. Another study conducted by Rao et al. [198] demonstrated a continuous water quality monitoring system in a laboratory environment by incorporating low-cost sensors including temperature, light intensity, TDS, pH, salinity, DO, Electrical Conductivity (EC), and ORP. These parameters provided physio-chemical insights into the current condition of water and potentially identify sources of pollution. They collected samples at regular intervals for chemical analysis in the laboratory to ensure a healthy environment for aquatic life. Geetha et

al. developed a system to monitor turbidity, temperature, conductivity, and pH level of water sources around their university. The sensors connected to a microcontroller with built-in Wi-Fi. The data was sent to the cloud and real-time sensor readings were displayed on an on-board LCD. A GSM module also sent text messages to user when the quality of water was detected outside predefined range. Similarly, Chowdury et al. [199] proposed a low-cost, power efficient system with 4 sensors namely pH, turbidity, temperature, and ORP sensor. They collected river sample and tested on the system that integrated an ESP-8266 Wi-Fi module and sensor data could be viewed on LCD screen mounted on a printed circuit board or a mobile phone. Pasika et al. [200] built a system by incorporating pH, turbidity, water level sensor, along with temperature and humidity for the surrounding atmosphere. Their system revolved around filling a tank with water procured from a metropolitan water supply, taking sensor readings every 10 seconds and then uploading to Thingspeak cloud service. Although their system is capable of providing real-time sensor data, it is not field-deployable.

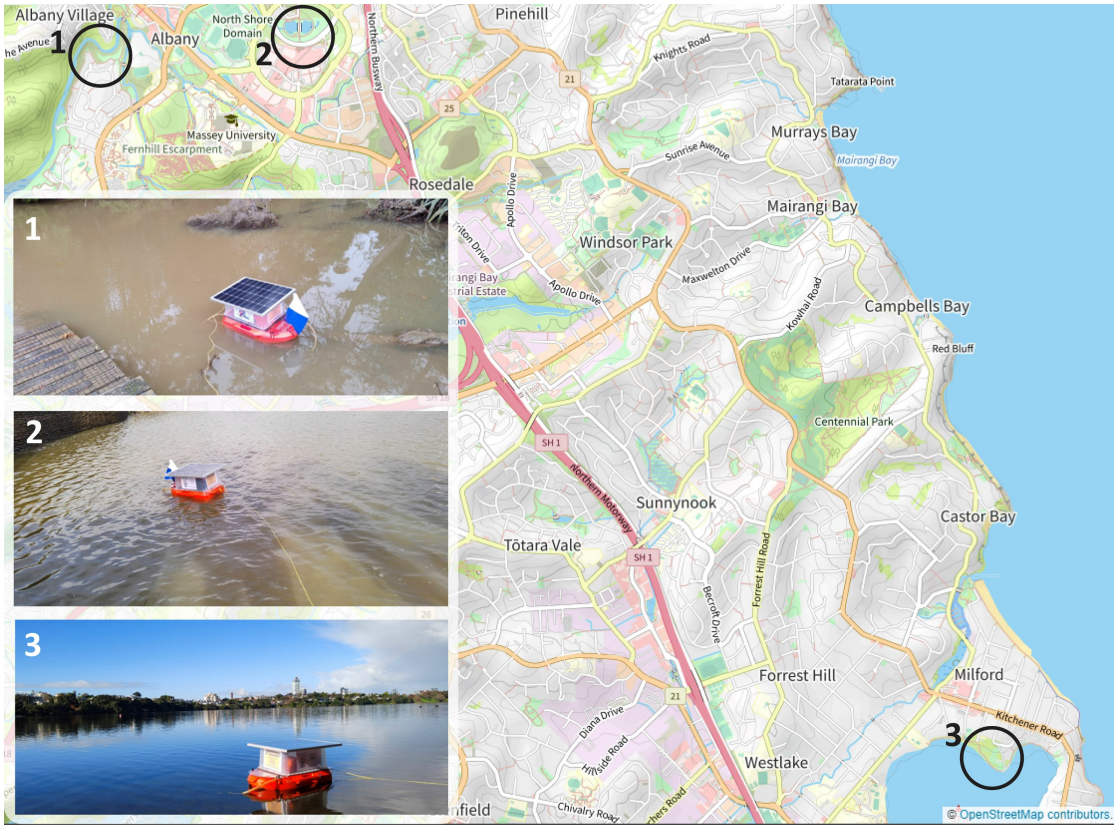

FIGURE 5.2: The labelled areas highlight three testing sites. 1. Lucas Creek, 2. Lake Albany, 3. Lake Pupuke. *Note.* Map sourced from OpenStreetMap.org

Studies show that anthropogenic and natural activities have a big impact on the quality

of water and its influence on the water quality parameters when it rains. There are systems that perform machine learning on the collected data to predict changes in water quality [201]. While these studies have provided informative results, current water monitoring systems still suffer from challenges with laborious sample collection. This kind of system would be incapable of establishing the quality of water in real-time and how that varies over a period of time. Hence, an in-situ real-time monitoring system was built that involved a flotation device, installed with five low-cost water quality sensors. The system was deployed in three different water bodies located in the suburb of Albany in Auckland, New Zealand. The locations are marked on the Google maps screenshot shown in Fig. 5.2. Our objective was to measure water quality of freshwater sources and how it was influenced by weather conditions. Lakes are known to have freshwater that is ever-changing due to inflows and outflows [202]. Inflows occur from rain, overland runoff, and groundwater seepage while outflows are caused by seepage, into groundwater and evaporation. However, inflow and outflow occur at a very slow pace. Lakes are great habitats to study physio-chemical dynamics of ecosystem. Lakes are immobile bodies of water which means they preserve their natural characteristics and keep nutrients relatively stable without abrupt changes. To build a cost-effective water quality system, we utilized inexpensive sensors that require a stable environment for detection. Table 5.3 outlines common laboratory-based detection techniques for water quality parameters. To conduct the experiments, we chose lake water because water quality parameters are expected to be fairly constant with negligible variation as compared to a river or ocean, which was suitable for our low-cost sensors.

5.2.1 Water quality assessment models

Water quality assessment models are the criteria that grade the quality of any given body of water; this is typically done using a Water Quality Index (WQI) that is used to evaluate the overall water quality of a body of water that can be compared against city council approved index [209]. There are multiple water quality assessment models that are used throughout the world to evaluate different types of parameters, from chemical pollutants in water to micro-invertebrate contamination [210]. The water quality index is a score that is established by ranking water quality parameters according to their level of importance as defined by the water quality standards. Most countries have their own modelling systems that are used to determine the water quality of bodies of

TABLE 5.3: Common laboratory-based detection techniques for fundamental water quality parameters

Parameter	**Measurement techniques**	**Ref**
Temperature	Thermocouples Thermistors Infrared (IR) Resistance Temperature Detectors (RTDs) Liquid glass tube thermometer Digital Temperature probes*	[203]
Dissolved Oxygen	Optical - luminescence quenching Winkler titration Membrane electrode*	[204]
Total Dissolved Solids	Conductivity meter* Gravimetric (filtration of residual solids) Optical - light scattering and absorption	[205]
Turbidity	Optical - light scattering* Optical - laser diffraction Optical - light absorption	[206, 207]
pH	Glass electrode method* pH test strip or litmus paper Potentiometry	[208]

water. Two examples of WQIs used by governments today are the Canadian Council of Ministers for Environment (CCME) [211] and Aggregation Functions [212]. The CCME is primarily used in New Zealand and Canada while the use of aggregation functions has been popularised in the United States of America (USA). The CCME WQI requires that there be a minimum of four water quality parameters being measured, but puts no restriction on what those parameters might be; therefore, appropriate parameters can be used in varying environments [213]. While, there are a wide range of parameters that provide the physical, chemical, nutrient and microbial aspects of water, among them, five are considered absolute fundamental parameters as illustrated in Fig. 5.1.

5.3 Methodology

The objective of this study was to monitor the quality of local bodies of water using five fundamental parameters of water namely pH, turbidity, TDS, DO and temperature. We built a system that could collect water samples as regular intervals and measure the condition of water. The design process was divided into several phases. The first

phase was to evaluate off-shore and on-shore system that would greatly influence the design process. The second phase involved choosing sensors that would measure the fundamental water quality parameters. Subsequent stages include calculations for power consumption to select the appropriate battery capacity and solar panel, the hardware design, followed by development of firmware, and lastly, functional testing.

5.3.1 Analysis of deployment methods

A field deployable water quality monitoring system could either be floating in water or secured on the coast. There are benefits and drawbacks to both. Sampling close to the coast could provide insights into the coastal environment and potential sources of pollution. It can also provide localized variations in water quality parameters compared to sampling away from the coast that can present a generalized condition of the water quality in the body of water [214]. Sampling away from the coast could also reduce the influence of coastal processes and potential contamination. This could be particularly helpful in studying widespread contamination and trends in water quality parameters, compared to sampling close to the coast [215, 216]. To study the general quality of the body of water, the ideal approach is to sample water away from the coast. Therefore, we evaluated different ways of deploying the sensors. Our first concept consisted of a system attached to a winch, which would only be lowered into the water to take measurements. The challenge with this approach was to find an appropriate place at every location to mount the heavy winch system along with heavy power demand involved with the use a winch system. Another concept was to build an enclosure that could be securely located on the shore with a long hose connected to a pump which would sample the water at regular intervals. Although, this was a credible system, which could also be cost effective, the concern was the variance in quality of water close to the shore compared to quality of water further away. Lastly, we settled on a flotation device, which would travel a few meters away from the shore and sample water. To do so, a system was developed which could house all the required components, that includes sensors, water sampling setup, and power management system.

5.3.2 Sensor selection

Sensors are the backbone of the water quality monitoring system. There are a few factors to consider when choosing the right sensor, which are: measurement range, level of accuracy, sensitivity, stability, physical limitations, output signal type, and ease of operation [217]. Considering the stability and physical limitations of the sensor are crucial because a sensor that requires frequent calibration or maintenance for accurate functioning would rely on regular human intervention, which would make it less suitable for field-deployment.

DFRobot specializes in developing low-cost, sensitive, and field deployable sensors. In addition to being cost-effective, these were desirable due to their seamless compatibility with a variety of Arduino boards. Moreover, there are well established software drivers that are compatible with Arduino, which simplified the process of integrating the sensors with Arduino. Five sensors were incorporated into the final system. The sensors and their technical specifications are shown in Table 5.4. The DO sensor's probe is galvanic and does not need polarization time. The sensor came with the signal converter module for easy interface to Arduino board through ADC. The turbidity sensor is able to detect suspended particles in water by measuring the light transmittance and scattering rate, which changes with the amount of TSS in water. TSS is direclty proportional to turbidity. The sensor comes with the signal converter module that connects to Arduino board through ADC. TDS sensor probe comprises of two needle like electrodes. The excitation source is an AC signal, which can effectively prevent the probe from polarization and prolong the life of sensor thereby achieving a stable output signal. The probe is encased in a waterproof housing with electrodes exposed, which enables the sensor to be immersed in water for long periods of time. The pH sensor probe that houses a glass bulb electrode that maximizes the surface area of the sensor. This probe too comes with the signal converter module. The probe is laboratory grade and cannot stay immersed in water for prolonged periods of time. Temperature sensor probe houses DS18B20 thermistor chip that provides a 12-bit temperature reading. Since it has only one data line, it can easily interface with Arduino boards without the need for a signal converter module.

TABLE 5.4: Five water quality sensors with technical specifications

Sensor	**Measurement Range**	**Resolution**	**Cost (USD)**
pH	0 ∼10	± 0.1	$99.00
Temperature	-10°C ∼ 85°C	± 0.5°C	$7.50
Dissolved oxygen	0 ∼20 mg/L		$169.00
Total dissolved solids	0 ∼1000 ppm	± 10%	$11.80
Turbidity	0 - 4 NTU	± 7.5%	$9.90

Power consumption and battery capacity calculation

Pumps are rated at 12V, 3A(peak), which is 36W of power. The electronics and sensors consume 500mA at 5V, totaling to 2.5W. This leads to a total power requirement of the system at 38.5W per hour.

However, the electronics side stays turned on continuously, but pumps were used only at intervals of 5 minutes. Therefore, the pumps are activated a total of 12 times in 60 minutes (1 hour). If the pumps run for one minute every time they are turned on, the calculation below displays the total power consumed by the pumps in an hour:

$$\left(\frac{36W}{hr} \div \frac{60}{12}\right) = \frac{7.2W}{hr} \tag{5.1}$$

A maximum of 7.2W of power is consumed every hour by the pumps and 2.5W of power consumed by electronics. Subsequently, 9.7W of power is consumed by the entire system every hour.

In order to run the system overnight for, approximately, 10 hours, the required power is 9.7W x 10 = 97W. Therefore, for a 12V battery, 97W/12V = 8.08AH capacity will be required. Since, lead acid batteries are not recommended to be discharged below 50% capacity, we will required at least 16.16AH battery. As a result, one 18AH or two 9AH or 10AH batteries will be sufficient to run the system for 10 hours without solar charge. The mono-crystalline solar panel is rated at 80W with 4.55A of peak current generated on a bright sunny day. If the battery is depleted and charged using an 80W solar panel, it will take the battery approximately four hours to fully charge. Sealed lead-acid batteries or absorbent glass mat (AGM) deep cycle batteries are common choice for solar-powered systems. Since the pumps used in this system are rated at 12V, a 12V sealed lead-acid battery is appropriate and an economical choice. The Powertech solar charge controller provides up to 120W (12V x 10A) of power and connects in between the solar panel

and the batteries to regulate the charge going into the batteries. It also ensures that the batteries are charged efficiently and prevents overcharging and over-discharging that prolongs the life of the battery. A block diagram of all the peripherals that connect to Arduino along with battery charging through solar charger is shown in Fig. 5.3.

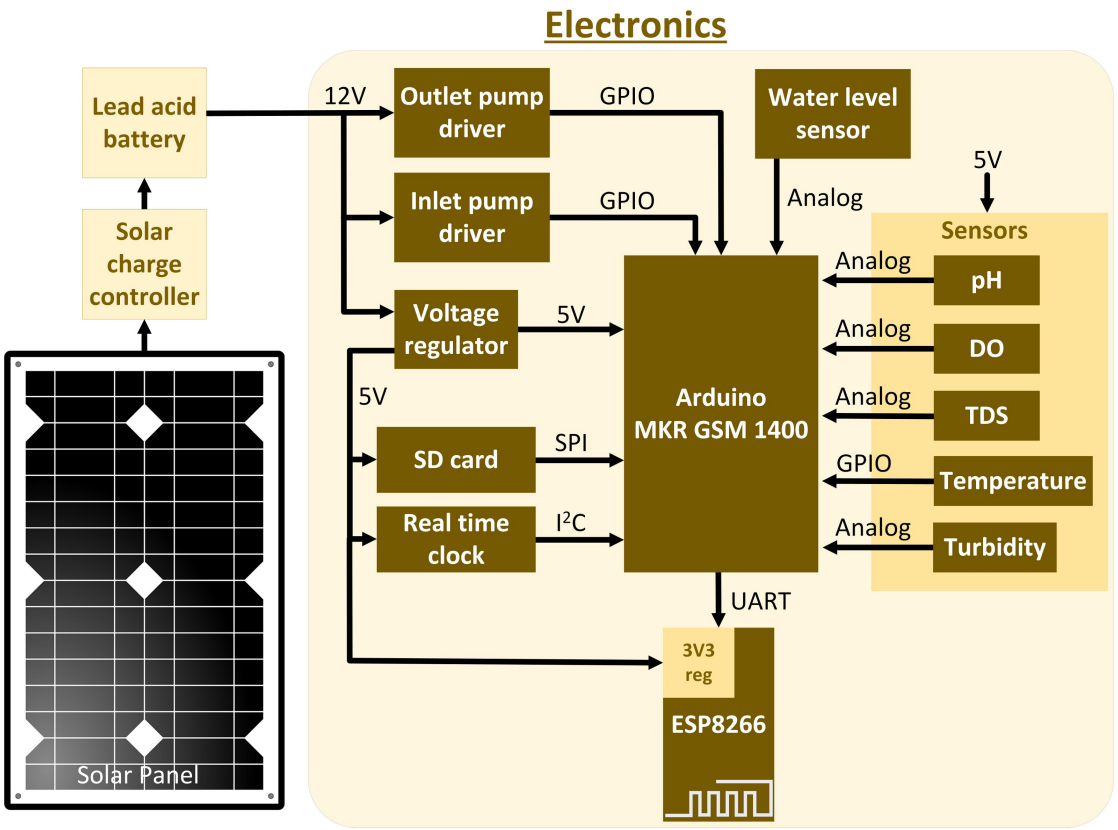

FIGURE 5.3: Overview of the hardware design

5.3.3 System architecture

During the initial stages of system development, Arduino IoT cloud was incorporated, but soon started running into issues with intermittent disconnection from cloud service. As an alternative, the text messaging service could be used, but instead, external Wi-Fi module was used to get quick system updates on a mobile device was thought to be cost-effective.

A water quality monitoring system has four primary components. First, there are sensors that measure various physical properties of the environment; as well as, 1100 GPH (Gallons per Hour) pumps, rated at 12V that were used for water sampling. Second, the use of electronics and programming that are responsible for enabling and collecting data

from the sensors. The sensor could be transmitted to a cloud service and stored locally on some form of memory, such as SD card. Furthermore, keeping a track of date and time is also incorporated, using a Real-Time Clock (RTC), which is required to record date and time to capture timestamps of crucial events. Moreover, the system includes a solar power management system that ensures self-reliant operation of the system. And lastly, wireless communication module that establishes a connection between the system, the end-user, and the world. For a system that is deployed outdoors, weather conditions also need to be considered to ensure there is no sun or water damage.

The hardware architecture of the entire system is depicted in Fig. 5.3 that shows the battery charging process through solar and the interaction of various peripherals with Arduino board. Among all the five sensors that we used, the pH sensor is the only laboratory grade sensor that was not designed for continuous immersion in water. Since, we could not continuously immerse the sensors in water, we adopted the water sampling method. The system uses Arduino MKR GSM 1400 board, which has a GSM module built-in. ARM cortex-M0 at its core, running at 48 MHz and provides enough analog and digital input/output pins to run the entire system with ease. The module supports 3G network connectivity which is capable of accessing the internet through GPRS data network as well send text messages to end user. It can also connect to Arduino IoT cloud or other cloud services. As previously mentioned, we did not use the GSM part of the board because initial tests suffered from frequent disconnection from Arduino IoT cloud, which was inefficient. This could be due to intermittent disconnection from the local 3G network. To build a robust system. An alternative communication method was chosen by using an ESP-8266 Wi-Fi module running a web server. The primary aim of a web page running on a server was to receive vital updates from the deployed system to ensure proper functioning if all the peripherals. This approach would also minimize the need for physical inspections, which would be challenging for a system positioned in water, a few meters away from the shore. Lastly, the inlet and outlet pumps were driven using logic level MOSFETs that use that supported a gate drive voltage as low as 1V. Fig. 5.4 depicts an overview of the water quality monitoring system, showcasing a boat that is equipped with a water sampling container, electronics, and a solar panel positioned on top.

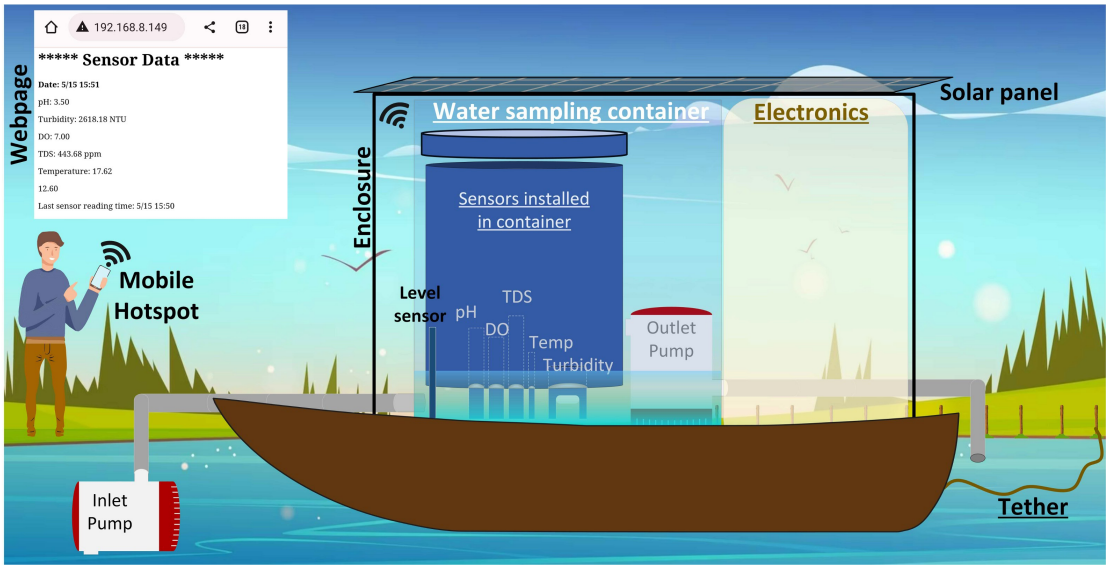

FIGURE 5.4: Illustration of the water quality monitoring system on a float boat

5.3.4 Software architecture

Upon completion of the hardware design, programming the Arduino MKR board was subsequently completed. The drivers were programmed on Arduino IDE v2.0. An incremental software development style was adopted to program and test different modules of the system incrementally, which were later brought together as a whole. With this approach, the structure of the program could be controlled and through continuous testing, program crashes caused by software bugs could be prevented. The testing process began by programming and testing the sensors, to gain an understanding of the data they generated and interpret the received data to meaningful characteristics. After completing the programming, preliminary testing was conducted to verify both the hardware and the software.

Fig. 5.3 represents the system architecture that shows the flow of signals between Arduino and the peripherals and Fig. 5.5 illustrates the flow of the firmware. Upon system startup, all the peripherals connected to Arduino are initialized. These include five water quality sensors configured as inputs to Arduino, pumps as outputs using PWM signal, micro-SD card module connected to the SPI bus, Real-Time Clock (RTC) connected to the I2C bus, and lastly, ESP-8266 Wi-Fi module that connected through UART. After the initialization process, the program enters a wait period of 10 minutes to allow the user enough time to deploy the system in water.

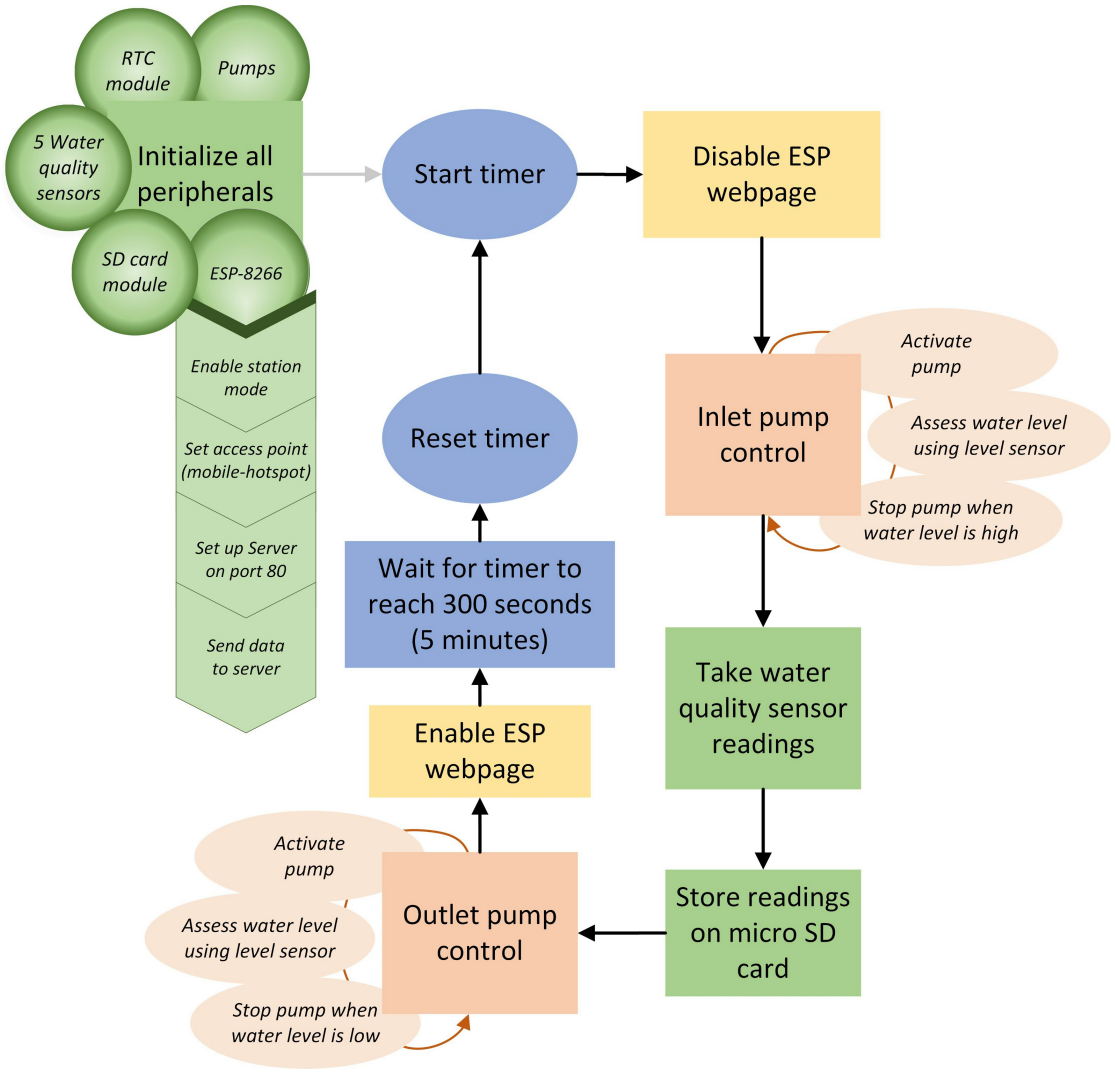

FIGURE 5.5: The flow chart illustrates the process of water sampling, sensor reading, and datalogging

Thereafter, the program sequentially iterated through a series of instructions by first, activating the inlet pump only at a duty cycle 50% because of the pump's rating of 1100 GPH. Turning on the pump at maximum power could pose a potential risk of flooding the water sampling container or even the boat. Continuously measured the water level was carried out by the water level sensor that turned off the inlet pump when the level sensor detected water level at its peak. With a fresh sample of water, the program continued to measure the parameters using the five water quality sensors. The data collected from the sensors was then stored on micro-SD card as a CSV file which it created on system startup. Upon successful storage of data, the program proceeded to activate the outlet pump at maximum power to flush the water out of the sampling container. Subsequently, the level sensor ensured that there was no residual water left

behind. This prevented the new water sample from getting contaminated due to remnant of previous sample, thereby, ensuring the system was prepared for the next iteration of sampling and data collection which was set to 5 minutes.

The software also provides the user with the functionality of a web page that can be viewed on a mobile device. This was made possible with ESP-8266 Wi-Fi module which was configured as station mode that configures the device as a client, waiting to connect to an access point. The module was also configured as a server, accessible through port 80. A Wi-Fi hotspot was created on a mobile device that acts as an access point. The Wi-Fi module connects to the access point which then gets assigned an IP address in the form of 192.168.xxx.xxx. The user can access the web page that is running on the ESP server through this IP address. The information that was intended to be displayed on this web page was the current time that was directly accessed from the RTC, the time of last sensor reading, latest sensor data, battery voltage, as well as status updates, such as, malfunction of any of the sensors,pumps, or any issues with data storage on micro-SD card. Access to web page was disabled while the system collected water sample and gathered data from sensors, so that there is no conflict between ESP and the rest of the program operation.

It is worth noting that the process of activating pumps, reading sensor data, and data storage takes between 15-20 seconds to complete. The duration of this time period is subjective as it relies on the amount of water being pumped in, which depends on the state of the filter that is attached to the inlet pump. If the filter is dirty or clogged, the process of filling the water sampling container will be prolonged.

5.4 Preliminary testing

Preliminary testing was carried out in the water tank of the water-jet cutter as a preliminary test of the system as a whole. Since, this is a field-deployed system, the pumps, the sensing and the monitoring systems were thoroughly checked, to establish confidence of correct functioning of the system. This was achieved by running the system in the pool of the water-jet cutter at our mechanical engineering workshop. The water in the water-jet pool typically consists of small scraps or fragments of metal, primarily stainless steel and aluminium, along with grains of sand that resulted in a significant amount of

suspended solids. A water-jet cutter pool was chosen to carry out initial testing of the system because it represented a worst-case scenario of the water conditions. This allowed us to test if the system could withstand the challenging water quality of the pool. Fig. 5.6 displays the pool of the water-jet cutter with the boat floating, along with the box of electronics and container for water sampling, sheltered inside a transparent enclosure with the solar panel mounted on top.

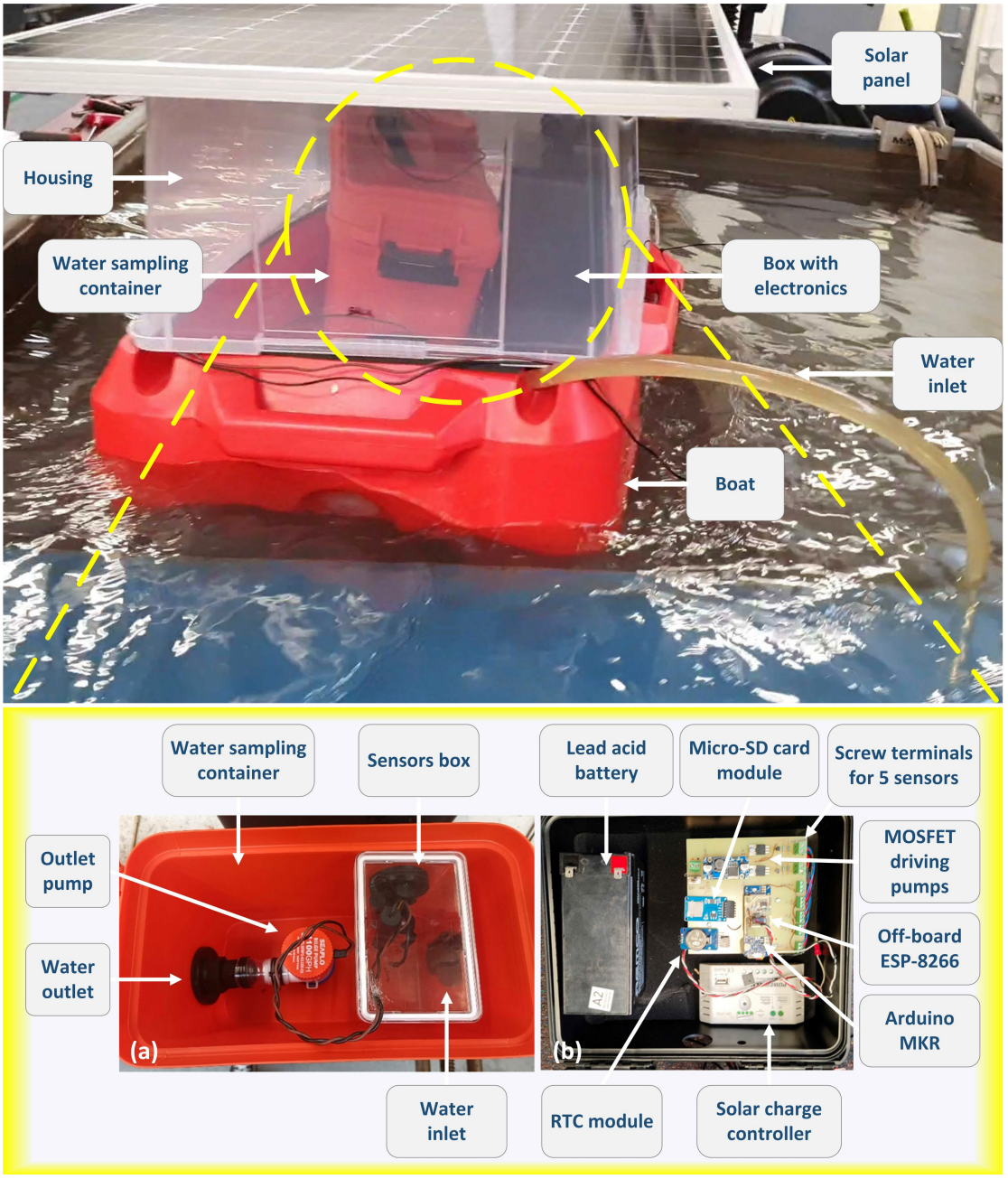

FIGURE 5.6: Initial testing of the system in pool the of water-jet cutter (Top); the system's water sampling container and the electrodes (Bottom)

5.5 Results and discussion

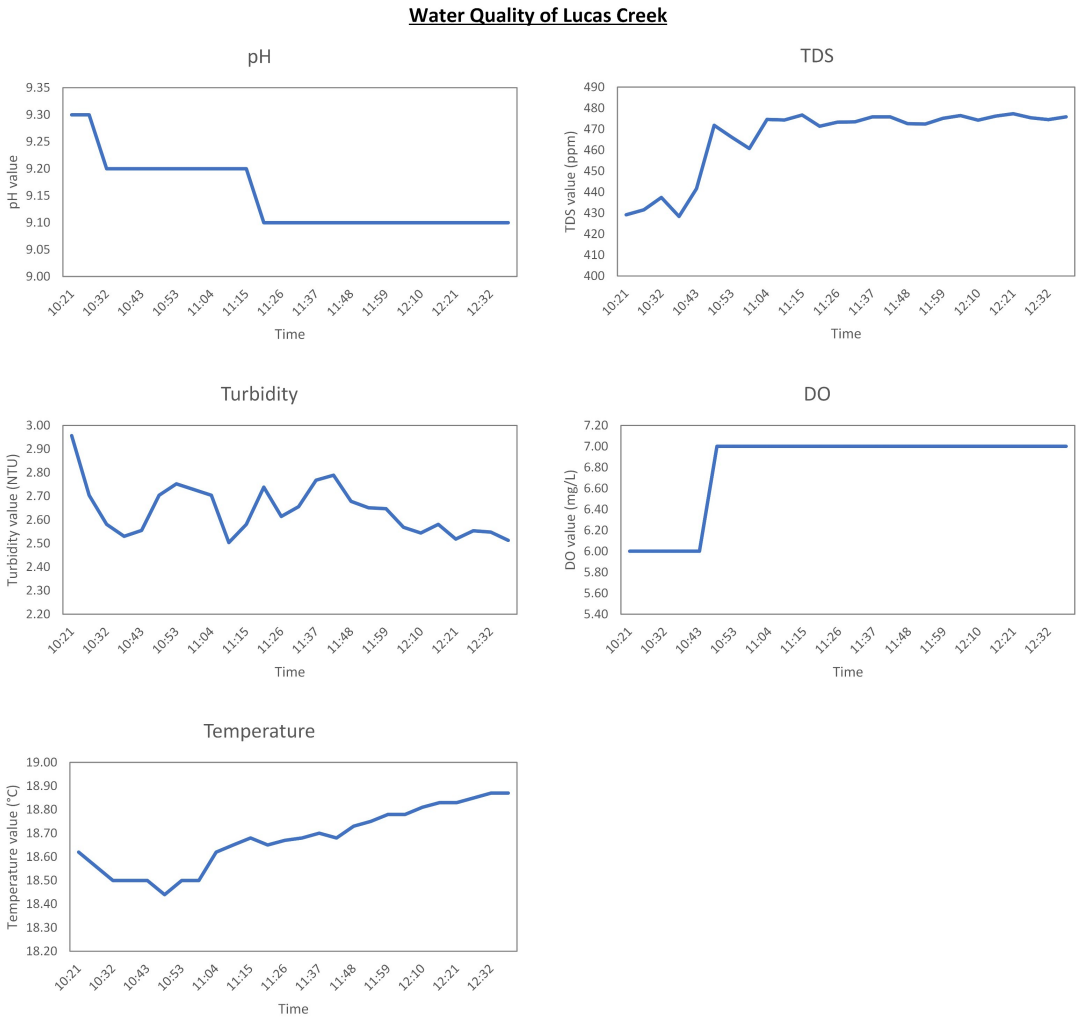

FIGURE 5.7: Results for Lucas Creek

The data gathered for this study provides valuable insights into the overall health of water around the local area. Fig. 5.7, 5.8, and 5.9 present data graphically from individual sensors for each location. As it can be seen from the graphs, the time period of the data gathered from Lucas creek and Lake Albany is quite short due to the water level being too low for any further tests. However, water level at Lake Pupuke was consistent which resulted in almost three weeks of data. Nevertheless, the results altogether yielded over three weeks of insightful data from three bodies of water.

Referring to the graphically depicted results for all the three locations, Lucas creek shows the highest turbidity level compared to the other two sites. Visually, Lucas creek had the cloudiest water as it can also be seen from Fig. 5.2(1), compared to the clarity of water

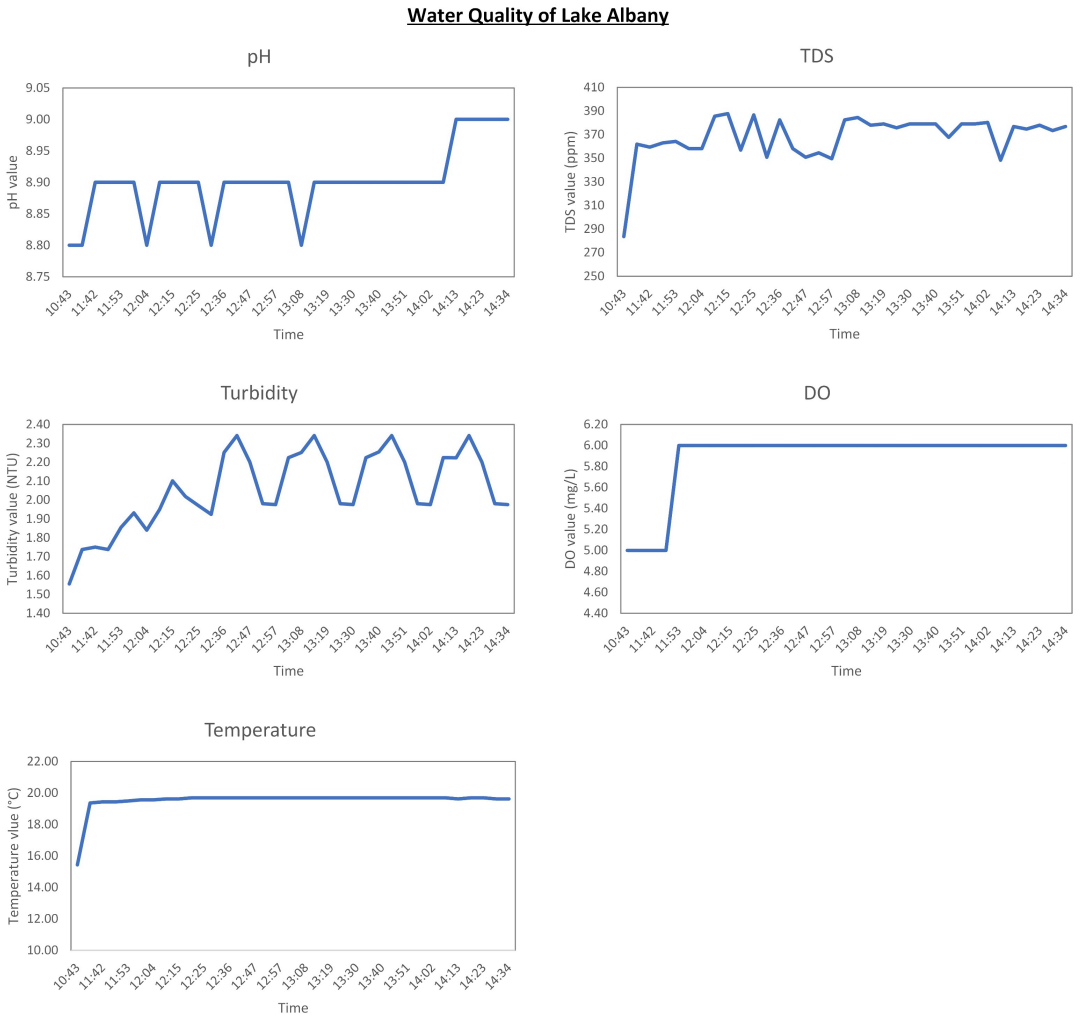

FIGURE 5.8: Results for Lake Albany

at Lake Pupuke that yielded low turbidity level. To thoroughly analyse the data, it is important to know the weather when the system was deployed at the two sites. At Lucas creek, it had rained a couple of hours prior to deploying the system, resulting in ample water, slowly flowing through the creek which was very muddy and polluted. On the other hand, it was a sunny day when data was gathered at Lake Albany. Looking at the results presented graphically in Fig. 5.7 and 5.8, water at Lucas creek had higher level of alkalinity compared to Lake Albany, even though creek is a stream of water flowing continuously. Due to high cloudiness of water at the creek, the TDS value was higher compared to Lake Albany, peaking at 480 ppm and 390 ppm, respectively. This clearly states that creek water comprised of a higher level of dissolved solids. A similar trend can be seen from the high turbidity levels at the creek. The higher TDS and turbidity levels observed at the creek are evident due to the natural presence of muddy water.

FIGURE 5.9: Results for Lake Pupuke

Furthermore, when examining the DO levels for both sites, it is evident that creek water, although it was turbid, carried more oxygen which can be seen from the high levels of dissolved oxygen of around 7 mg/L compared to 6 mg/L at Lake Albany. Regarding temperature, flowing water at the creek resulted in slightly lower temperatures compared to those observed at Lake Albany. After analyzing the quality of water at both sites, it is evident that despite the water being turbid, the oxygen levels remain relatively high compared to water at the lake.

Furthermore, analysing the results specifically for Lake Pupuke reveals a noticeable variation for a period of nearly three weeks from 16 May - 8 June 2023. This is an ideal period because the season transitions from autumn to winter in New Zealand, and three weeks of data provided some insight on how the quality of water varies over time with seasonal changes as well as changes in weather conditions. A daily average was

computed for all the sensors to present the mean values each day during the entire data collection period. These variations could either be influenced by weather or recreational activities that take place at the Lake. It rained between the periods 22-24 May which is indicated by a fall in temperature by 1.5°C, while pH value drops slightly from 8.8 to 8.2. A falling trend can also be seen from TDS data from 470 ppm to 450 ppm during this period. Between 1 June to 5 June, another noticeable event took place. During this period, the temperature dropped by approximately 0.5°C, while turbidity, TDS and pH data show an upward trend and DO demonstrated a declining trend. From the trends, it is clear that this is not a rain related event because it did not rain during this period.

Temperature and pH are inversely proportional to each other as it can be seen during periods 22-24 May, 24-26 May, and 30 May - 1 June. Although, a contrary relationship is visible during 5-7 June period when the temperature and pH both have reduced. Analysing the overall temperature data, it can be seen that the temperature gradually dropped from 18.5°C to 16.5°C. This observation clearly indicates a seasonal change, transitioning to winter.

Some sensors were not recommended for continuous immersion in water. Therefore, a water sampling method was adopted, achieved by two pumps that circulated water in and out of a water sampling container. This container housed five water quality sensors as well as a water level sensor. The inlet pump was covered with a gauze filter to minimize the amount of dirt entering the container. Alternatively, an effort was made to utilize a filter mat, but it was found to be inadequate in capturing enough dirt. Although there was some dirt in the water sampling container and the inlet pump, found by the end of the data collection period which can be see in the Fig. 5.10.

The system has been designed to be modular with scope of adding more sensors for further analysis such as monitoring and studying different types of nutrients or biological matter. This study can also be extended by building multiple systems that could be distributed around a lake or even a river. In order to cover a wider area, the boats could be equipped with propellers that will eliminate the need for tether and enable the boats to travel further away from the coast. Furthermore, all boats equipped with LoRa and low-cost Wi-Fi module can send data to IoT cloud service through LoRa gateway, if available or connect to a mobile hotspot that can collate data from all the LoRa nodes and send to IoT cloud through Wi-Fi using phone's data. An illustration

FIGURE 5.10: (left) sediment in water sampling tank, (right) small amount of dirt on inlet pump

of such a system is shown in Fig. 5.11. We can also take an alternative approach by using a single boat that would be pre-programmed to follow a path around the lake using a system called mission planner, commonly used with drones. This method would enable us to gather data from various locations within the same body of water to have a comprehensive understanding of water quality of the lake as a whole. Furthermore, using a GSM module, we could also receive real-time weather updates that can be correlated with the data to analyse weather related trends over time as well as send updates to the system such as new coordinates. Furthermore, Our system is capable of adopting an Industry 4.0 paradigm which is also known as the Fourth Industrial Revolution. It encompasses the use of automation, Big Data, Machine Learning (ML), combined with Artificial Intelligence (AI) and Internet of Things (IoT) [218]. In the age of Industry 4.0, systems are interconnected with information and communication, that results in scalability and autonomy.

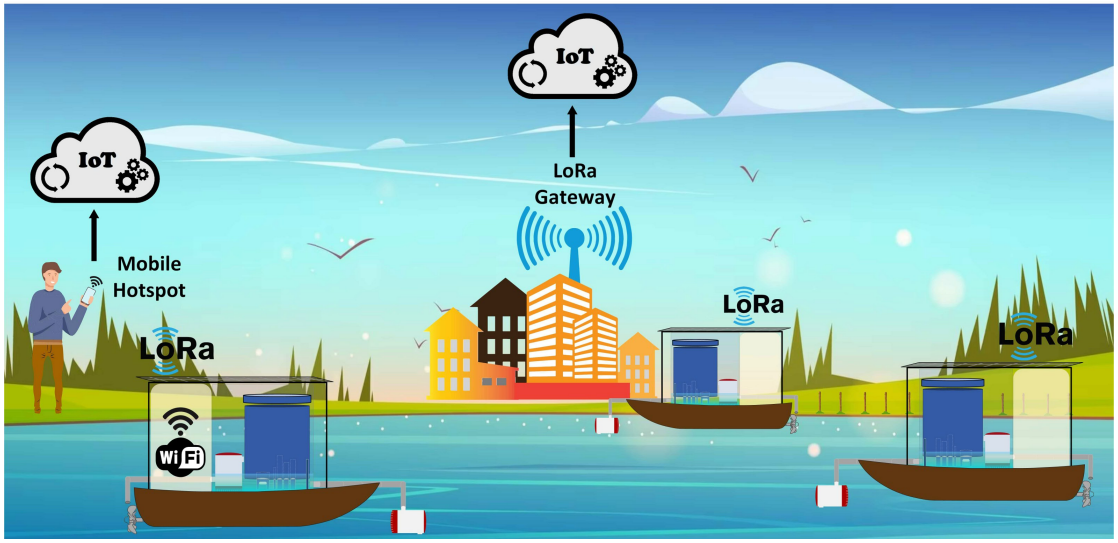

FIGURE 5.11: An extension of current work with more sensors and a few water quality systems distributed in water body, enabled with long range communications

5.6 Conclusion

Regular water quality assessment is necessary to maintain clean and reliable water for everyone. However, existing water quality monitoring systems are either bulky and expensive or not easily field-deployable.

In this research, a water quality monitoring system consisting of low-cost sensors to measure the five basic water quality parameters (turbidity, total dissolved solids, temperature, pH, and dissolved oxygen) has been developed and tested. The system includes features like IoT technology, solar power, and the ability to float in fresh water like a small boat. Since the system floats in water, a water sampling technique has been adopted to avoid continuous contact of water with the sensors, which is detrimental, especially in low-cost sensors not designed for long-term immersion in water.

The data gathered from the sensors is stored locally on a micro-SD card, and communication with the system is established through an ESP-8266 module that operates as a web server. The web page running on the server is used to view current sensor values to ensure that the system is functioning as it should without the need for physical inspection. The web page also provides information such as battery voltage and status information, including any faults encountered by the sensors or pumps.

To test the efficacy of the system, data was gathered from Lake Albany and Lake Pupuke in the local area, providing insights into how the water quality of the two lakes compares. A brief study on the water quality of Lucas Creek, with slow-moving water, was also performed. The water in this creek is considered somewhat fresh. Fast-moving rivers or oceans were excluded from the study because the variation in water quality would be too rapid for the low-cost sensors to handle.

From the results, particularly for Lake Pupuke, it can be observed that the levels of all the five parameters are quite stable with a variation of $\pm 10\%$, which was expected from a lake as it is not a moving body of water. This confirms that the developed system can be reliably used for further studies. The system operated in water bodies for several days to weeks and thus proved to be robust and autonomous in effectively monitoring the quality of water in real-time. It also carries the potential of adding more sensors and employing the Industry 4.0 paradigm to predict variations in water quality.

Chapter 6

Conclusion and Future Outlook

6.1 Conclusion

The work presented in this thesis has produced five journal articles and one book chapter. It is pertinent to mention here that each chapter of the thesis has its respective conclusion section. However, an overall brief summary of the conclusions is presented below:

- A literature survey was conducted on various detection techniques, such as optical and electrochemical methods, which are considered as two promising approaches for real-time detection of nitrate ions in water. The primary emphasis was placed on the electrochemical (EC) analytical method, as it can be integrated with planar electrodes to achieve targeted detection of nitrate ions, providing a field-deployable solution. The comprehensive review examined the benefits and limitations of two-electrode and three-electrode systems. Among these, the two-electrode system, also known as interdigitated electrodes, was identified for its simple design and implementation. This system can easily be integrated with cost-effective electronics for field deployment. Consequently, we opted to conduct experiments using two-electrode designs.

- An investigation into the performance of interdigitated electrodes was conducted to detect various concentrations of nitrate ions in deionized water ranging from 0.1 to 0.5 mg/L. Two different materials, namely silver and copper electrodes, were employed on two respective substrates - PMMA and fiberglass. Three distinct

geometric patterns of planar electrodes, namely interdigitated, square, and serpentine, were utilized. The primary focus was on studying the physics of different electrode patterns and the chemical interactions occurring between the electrode material, the analyte, and the polydimethylsiloxane (PDMS) polymer coating atop the electrodes. Additionally, the research considered the electrode fabrication process, emphasizing the use of cost-effective techniques and materials to minimize sensor costs. Silver and copper were chosen as electrode materials due to their good electrical conductivity, cost-effectiveness, and ease of procurement. The results indicated that copper electrodes outperformed silver electrodes, exhibiting a noticeable separation between various concentrations of nitrate ions.

- Upon establishing the interdigitated electrode design as the best-performing geometric pattern for nitrate detection in deionized water, additional research was conducted on the detection of nitrate ions in water samples containing a wide array of physical and chemical impurities. The study involved evaluating the performance of four distinct electrode materials: silver, copper, gold, and tin. These electrodes were employed to determine the concentration of nitrate ions in real-world water samples collected from three different freshwater sources: Lucas Creek, Waikato River, and Lake Pupuke. Synthetic nitrate samples were prepared using the collected freshwater samples. Employing Electrochemical Impedance Spectroscopy (EIS), impedance measurements were taken for each electrode material, which was tested with varying levels of nitrate ions methodically added to water samples in increments from 0.1 to 1 mg/L. Measurements were taken at every frequency, sweeping from 100 to 100 KHz with increments based on the logarithmic scale. The results indicated that copper and tin electrodes performed better in detecting varying levels of nitrate ions in a complex matrix of real-world water samples compared to gold and silver. Clear separation of impedance levels in the correct order of concentration levels could be observed.

- This research resulted in a low-cost sensor capable of detecting nitrate ions in the complex matrix of impurities present in real-world freshwater samples. The real-time aspect of the sensor enables in-situ detection and monitoring of nitrate levels. To achieve this, a water quality monitoring system was built in conjunction with our research, comprising five sensors to monitor the five basic quality parameters: turbidity, temperature, pH, dissolved oxygen, and total dissolved solids. The

system was deployed in three different freshwater sources around the local area. The aim of this system was to monitor and understand the quality of water in real-time, providing insights into the true picture of water quality in terms of the aforementioned parameters. The system was constructed in a modular fashion, with the potential to embed more sensors, such as the nitrate detection sensor we developed, and utilize the Internet of Things (IoT) to monitor variations over time.

6.2 Future Outlook

Moving forward, in-situ rigorous testing needs to be carried out when the sensor is deployed in a freshwater body for extended periods. This would be beneficial for assessing the sensor's performance when exposed to the harsh realities of a real-world environment. Furthermore, it would be advantageous to gauge sensor performance when deployed in water bodies close to agricultural land. This could be particularly crucial for water care services and city councils to assess the amount of nitrate runoff from farms and implement preventive actions.

It would also be prudent to analyze sensor performance during weather changes, as well as natural or anthropogenic processes that affect the physicochemical properties of water. Further improvements can be made by installing the nitrate sensor in the water quality system to gather data over a significant period and implementing machine learning algorithms to enhance detection efficiency.

Testing and evaluating the performance of the nitrate-sensitive coating and its behaviour with real-world samples that relate to sensitivity to nitrate ions, re-usability of the sensor, and preparation of the coating are also areas for consideration.

Appendices

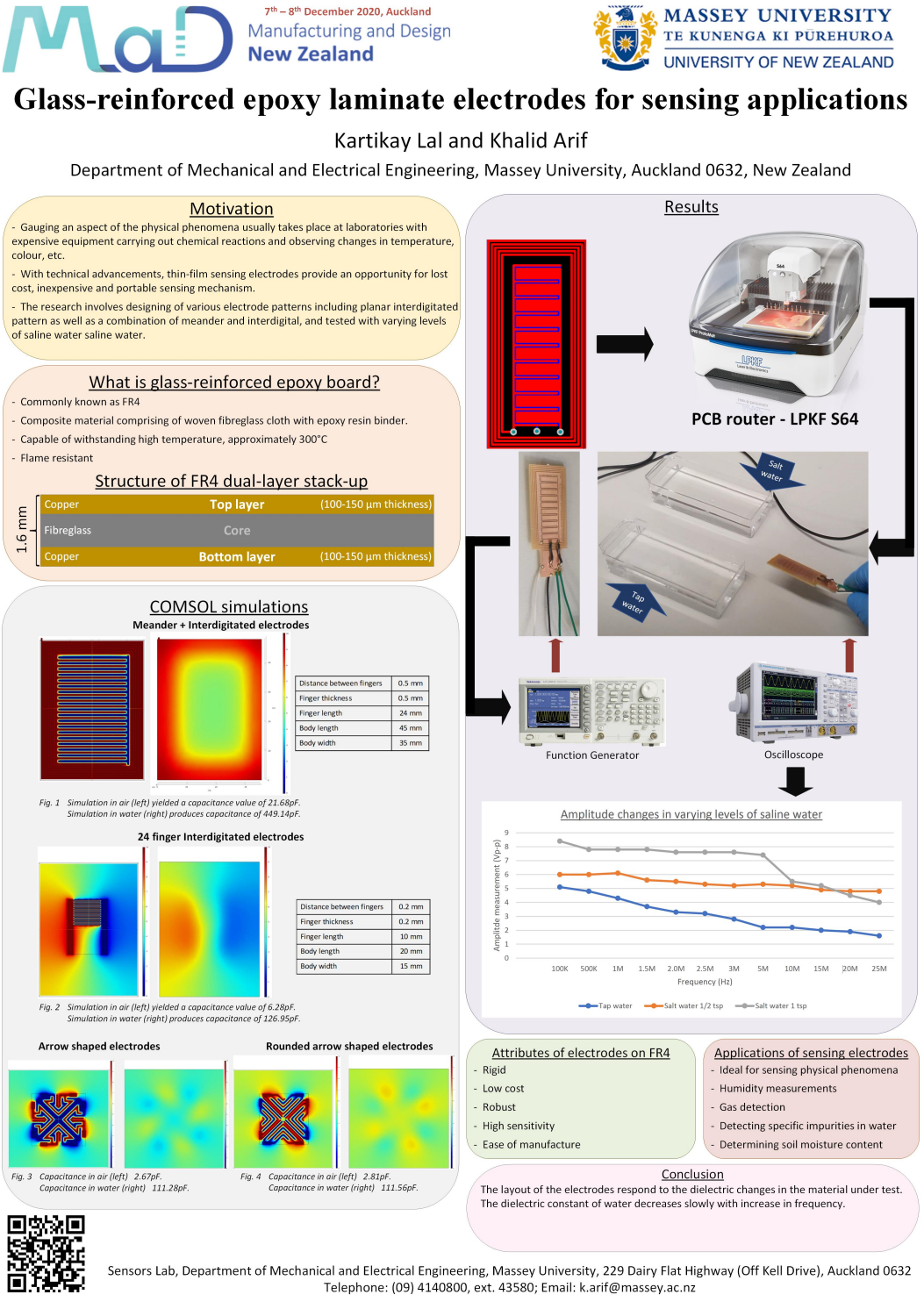

FIGURE 1: Poster presented at the MaDE2020: Synergies in New Zealand Manufacturing, Design and Entrepreneurship

Appendix A

Publication: Laser ablation assisted micropattern screen printed transduction electrodes for sensing applications

A.1 Abstract

In this work we present a facile method for the fabrication of several capacitive transduction electrodes for sensing applications. To prepare the electrodes, line widths up to 300 μm were produced on polymethyl methacrylate (PMMA) substrate using a common workshop laser engraving machine. The geometries prepared with the laser ablation process were characterised by optical microscopy for consistency and accuracy. Later, the geometries were coated with functional polymer porous cellulose decorated sensing layer for humidity sensing. The resulting sensors were tested at various relative humidity (RH) levels. In general, good sensing response was produced by the sensors with sensitivities ranging from 0.13 to 2.37 pF/%RH. In ambient conditions the response time of 10 s was noticed for all the fabricated sensors. Moreover, experimental results show that the sensitivity of the fabricated sensors depends highly on the geometry and by changing the electrode geometry sensitivity increases up to 5 times can be achieved with the same sensing layer. The simplicity of the fabrication process and higher sensitivity

resulting from the electrode designs is expected to enable the application of the proposed electrodes not only in air quality sensors but also in many other areas such as touch or tactile sensors.

A.2 Introduction

Numerous fabrication techniques have been reported in literature to form the transduction schemes for sensors attaining new functionalities, superior device responses and capabilities. However, most of the techniques require intricate processes and costly facilities to fabricate such sensors. For instance, the conventional microelectromechanical systems (MEMs) photolithography process, which is a top-down approach for fabricating sensing electrodes, requires cleanroom and chemical etching process [219, 220]. The overall process leads to chemical wastage, poses environmental issues [221–223] and customization in the electrode design is often expensive as the product cost relies heavily on the scale and batch size of fabrication. Therefore, contactless printing and contact printing, not requiring the provision of a clean room, have attained interest recently for R&D activities. Contact printing is widely used in the paper industry and print media. The upside of these printing strategies is their high throughput with accuracies up to 50 µm of printed features. Generally, all the contact printing methods use roll-to-roll technology to imprint the pattern on the substrate [224–226]. However, interconnect registration control, on account of tight tolerances and elastic nature of the substrate at high speed and pressure is intricate in nature. For large volume production the cost of printed features through roll-to-roll technology is cheaper than contactless printing method. However, for small production batches or customized imprints, the cost per item is a lot higher than contactless printing. Among contactless printing, inkjet printing has been widely used for printed electronic applications due to their low capital cost and pervasive availability. Moreover, compared to roll-to-roll printing technology the customized patterned printing can be done readily with the ability to print features or ink additively on the previously printed features. Thermal and piezoelectric inkjet techniques require formulation of ink, which needs to be compatible with the printing process. Ink often degrades in the thermal inkjet printing process if it is composed of material susceptible to thermal degradation, moreover high viscosity ink cannot be used with piezoelectric inkjet printers [227, 228]. Screen printing for a simple lab-based R&D

setup seems to be a possible solution for fabricating transduction electrodes at a much cheaper cost compared to the above-mentioned fabrication processes. Screen printing requires a stencil and although the process is simple, the low-cost customization of the transduction electrodes is a big issue and the process involves spreading a large amount of ink on the mesh. To circumvent the aforementioned issues, a simple laser ablation process for screen printing of conductive ink seems to a be an easier route for the fabrication of transduction electrodes. The laser ablation process from the commercial laser cutting machine not only provides facile implementation of transduction electrodes but also generates less ink waste when compared to the conventional screen printing of ink. In this work, printed capacitive structures to sense the electrochemical behaviour of the analyte are formed by laser ablation technique. The advantage of capacitive sensors is that they consume low energy, are less susceptible to radiation, have good sensitivity and provide fast response [229–234]. The most well-known design for measuring capacitive response is a parallel plate (PP) electrodes where the electrical terminals are isolated by a dielectric material [235, 236]. For sensing applications and particularly in thin-film capacitive sensors, interdigitated electrodes (IDEs) are perhaps the most broadly utilized electrodes mostly due to their simple design, analytical and numerical modelling [237–240].

The basic components of an electrochemical sensor are the sensing layer, transduction electrodes and the substrate. The sensing layer attracts the analyte by undergoing chemi-adsorption, which generates the electrical signal sensed by the readout circuit. The rate of adsorption dictates the response of the sensor where the desorption cycle is attributed to the recovery of the sensing layer. The sensing layer can be a single layer, bilayer or composite layer. A typical sensor layout is presented in Fig. A.1. Transduction electrodes can have different shapes or geometries such as interdigitated or meander that provide the enhanced signal for capacitive and resistive sensing schemes [241].

Capacitive sensing has been commonly used for humidity sensors with reference capacitors so to mitigate the drift due to thermal interference. However, these devices are complex due to the inclusion of additional components [242, 243]. Other methods such as heating of substrate are also used to shorten or augment the recovery of such sensors [244]. Nevertheless, with proper selection of sensing layers, electrode geometry and suitable substrate a sensitive and highly responsive environmental sensor can be

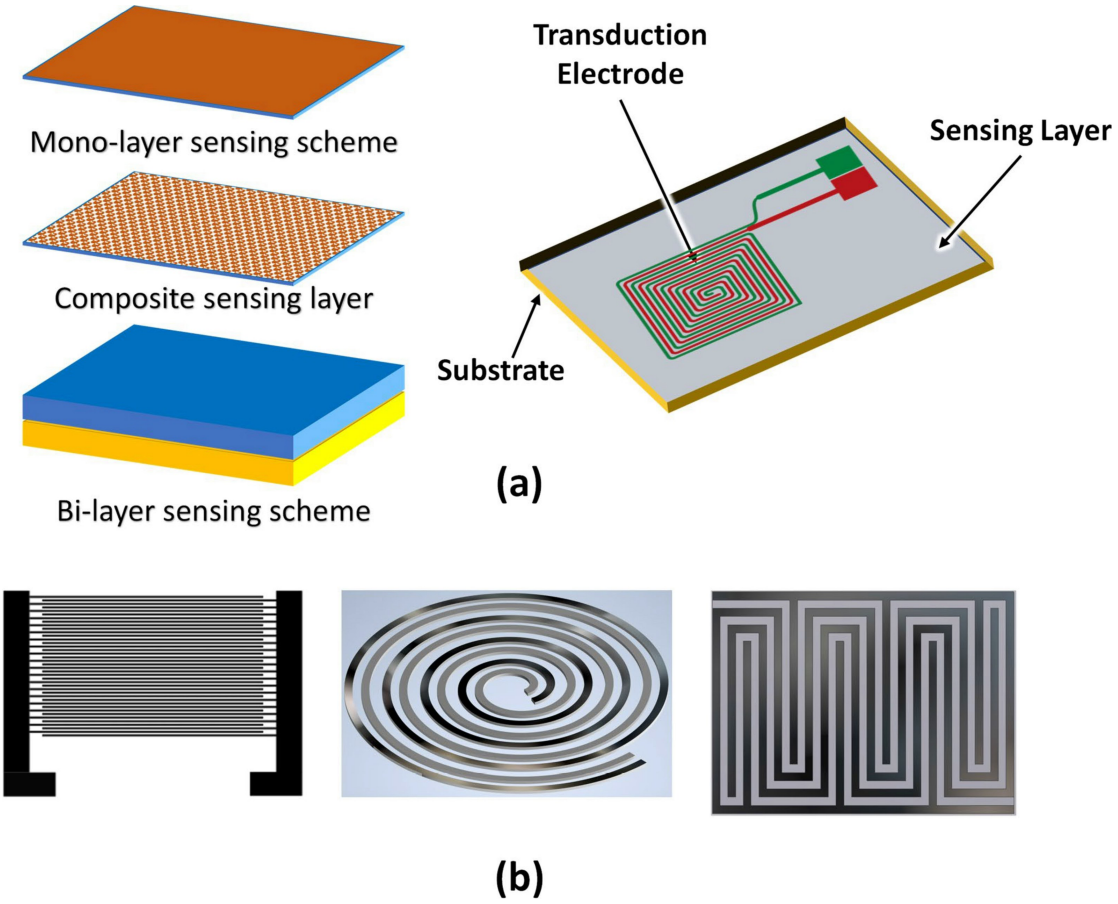

FIGURE A.1: (a) Typical sensing mechanism of an electrochemical sensor. (b) Geometric shapes of transduction electrodes.

fabricated, which operates at room temperature with low or minimal sensor drift and without needing additional components [245, 246].

Fabricating the transduction schemes on the substrate requires intricate procedure and is often subjected to available resources. In the context of the prevailing COVID-19 pandemic situation most of the fabrication facilities are either non-accessible or closed [247]. In this scenario sensor fabrication techniques based on MEMs [248–250], inkjet printing [251–253] and contact printing [254–256] methods can be expensive or unapproachable. However, a simple laser ablation technique by utilizing the desktop CO_2 laser cutter can be used to fabricate the transduction schemes for realizing the environmental sensor through screen printing the conductive ink inside the ablated tracks.

TABLE A.1: Experimental resolution of screen templating through laser engraving process

Measure	**Value μm**
Straight profiles electrode distance	
Average	289
Minimum	287
Maximum	292
Standard Deviation	2.1
Curved profiles electrode distance	
Average	377
Minimum	370
Maximum	383
Standard Deviation	5.3
Straight profile inter-electrode spacing	
Average	315
Minimum	313
Maximum	318
Standard Deviation	2.1
Curved profile inter-electrode spacing	
Average	216
Minimum	208
Maximum	223
Standard Deviation	6.1

A.3 Results and discussion

A systematic methodology followed by pursuing the steps highlighted in Figure A.2, resulted in the fabrication of laser ablated micropatterned features having an average width resolution of around 290 μm. Table A.1 shows the variation in the experimental data of the patterned features.

The microchannel is formed by the laser ablation process due to the absorption of energy induced by the laser beam. When the laser beam interacts with the workpiece it ablates the top surface of the workpiece. The rate of ablation depends upon the power, speed of the laser, wavelength of the radiation and material physical and optical properties. The resolution of the microchannel can be optimized by carefully selecting the parameters mentioned above. However, we have used the default ablation process parameters for ease of micropatterning and simplicity of fabricating micropattern, which can be utilized for sensing of humidity. In our experiments, we used 100% laser power and 100% speed for laser engraving on a 3 mm thick polymethyl methacrylate sheet. Figure A.3 shows that for curved regions the resolution of patterned microchannel was degraded. The

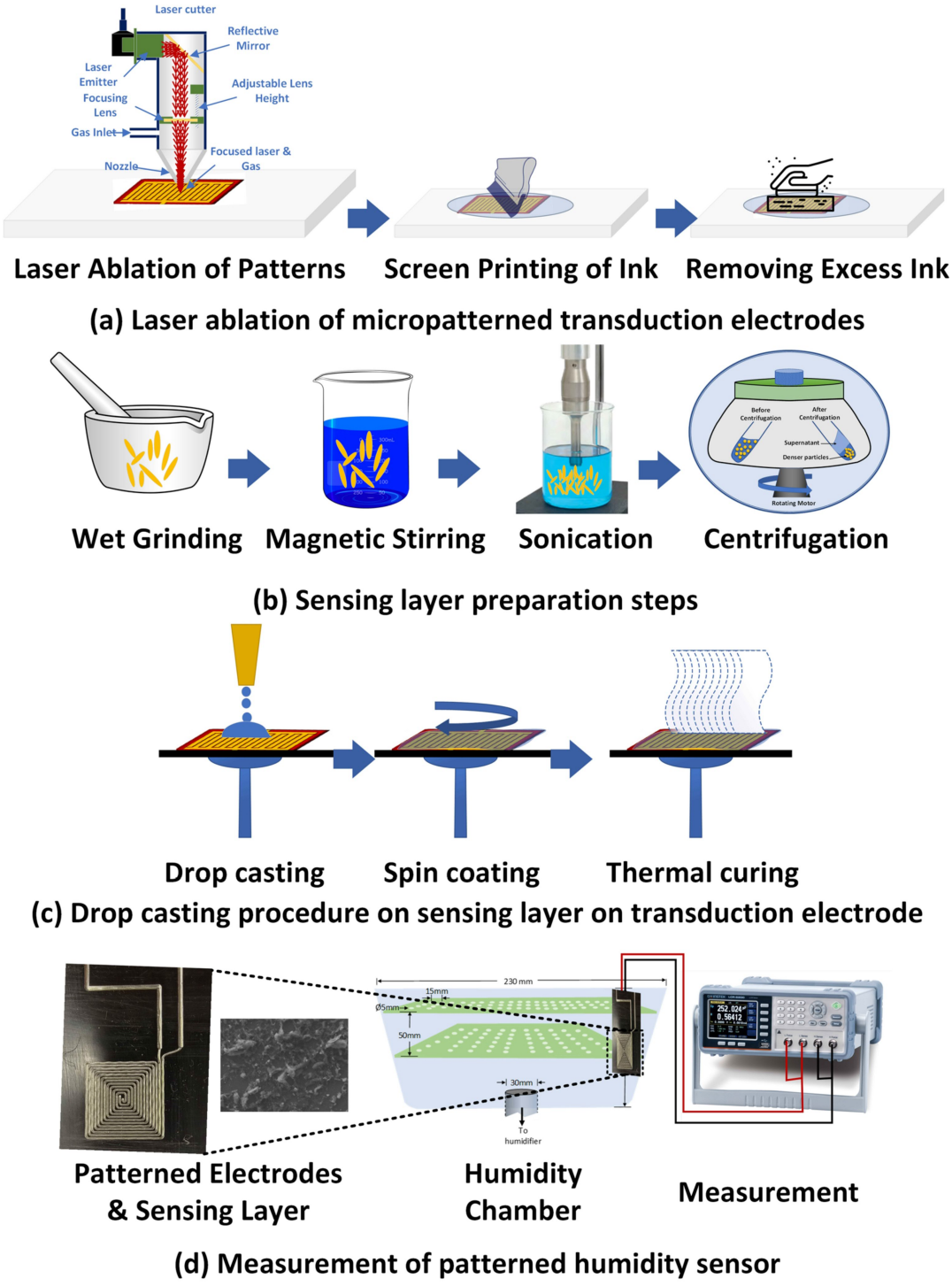

FIGURE A.2: Steps for laser ablated micropatterned sensor fabrication.

reason for degradation of the resolution is due to slower speed of the laser as compared to the straight feature. The X–Y stage of the laser scanning head uses successive straight-line interpolation and offsets to interpolate the next laser spot for a curved geometry on the workpiece. Due to this interpolation of points for a curved region the speed is slow, and more area is ablated due to the prolonged laser exposure at a particular position.

Optical images of the curved and straight features depicting the differences in the line widths are shown in Figure A.3.

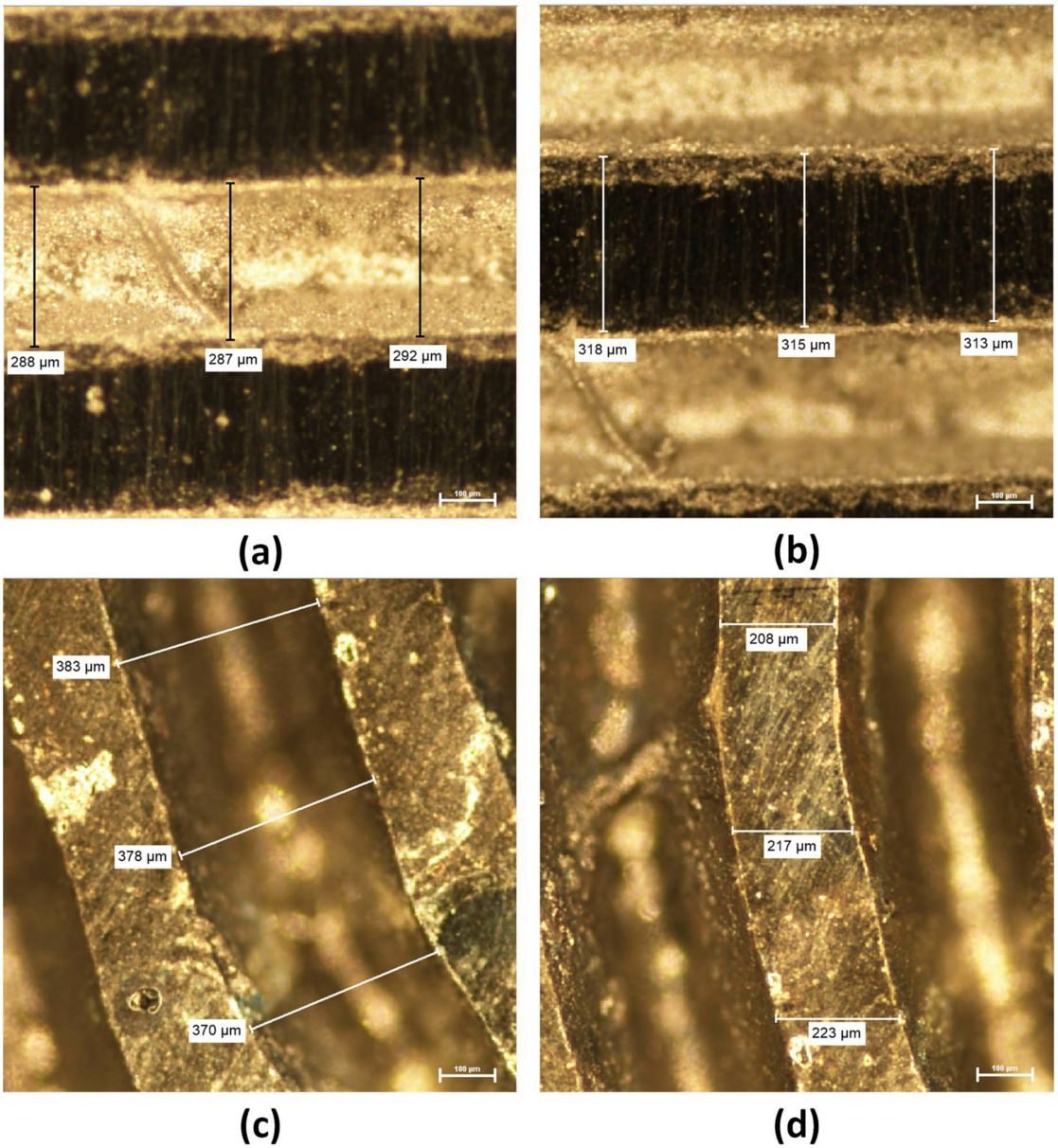

FIGURE A.3: Optical images of laser ablated transduction features. (a) Straight profile, (b) straight profile electrode inter-spacing, (c) curved profile, and (d) curved profile electrode inter-spacing.

Operations that were conducted to reduce the size of the suspended particles and to increase the activation sites can be seen from the scanning electron microscopy images in Figure A.4. The image in Figure A.4b shows the overall distribution of the cellulose after wet grinding, centrifugation and ultrasonication.

The sensing layer is based on biodegradable ink, which is mainly composed of cellulose, poly ethylene dioxythiophene: poly-styrene sulfonate (PEDOT:PSS)[257, 258] and

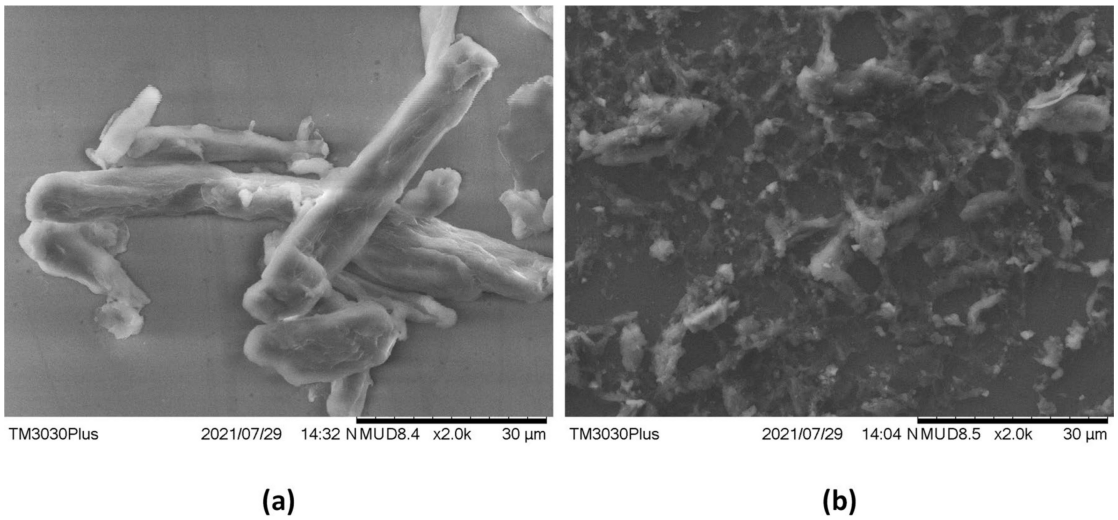

FIGURE A.4: SEM images of cellulose decorated sensing layer. (a) Decorated cellulose before ultrasonication. (b) Decorated cellulose after ultrasonication.

polyvinylpyrrolidone (PVP) coated silver nanoparticles [259, 260]. Silver nanoparticles (SNPs) are known for their antimicrobial properties as in medical applications silver catheters and silver coated catheters are used for slow-injection of solvent while providing antiseptic properties. Moreover, as the nanoparticles are coated with PVP, there are less chances of toxicity and the possibility of oxidation [261–263]. On the other hand, cellulose is a good natural insulator commonly used as a dielectric material. It has been incorporated into many applications as substrate for conductive and non-conductive applications [264, 265].

The sensing properties depend on the change in electrical properties of the sensing layer, which forms a uniform sensing region over the transduction electrodes. Once the sensing layer is exposed to humidity the porous structure of the cellulose decorated PEDOT:PSS and PVP coated SNP layer changes it's capacitance during the adsorption and desorption cycles. The change in capacitance is then recorded for various humidity levels. All the sensors were tested with a starting relative humidity level of 50% as it was the prevailing ambient condition for conducting the humidity measurements. The measurements were taken with the help of GW INSTEK LCR-6000 Precision LCR Meter by sweeping the selectable frequencies between 100 Hz and 2 kHz as tabulated in Table A.2. The formulation of the sensing layer with the addition of PVP coated SNPs has provided steric stability. The steric stability is evident in the SEM image as the cellulose fibres are well spread over the region. Not only the readings are stable but also the fluctuation of the capacitance value of the prepared sensors remains within standard

TABLE A.2: Experimental resolution of screen templating through laser cutting process

S No.	Freq	IDTs	Meander	Spiral	Swiss	Serpentine	Custom
1	100	15.87	19.43	17.30	19.65	21.23	23.10
2	200	15.52	19.09	16.88	19.21	20.84	22.75
3	300	15.28	18.95	16.71	18.90	20.58	22.48
4	400	15.24	18.63	16.70	18.77	20.43	22.34
5	500	15.14	18.66	16.56	18.6	20.32	22.32
6	750	15.14	18.42	16.39	18.22	20.31	22.39
7	1000	14.88	18.33	16.35	18.28	19.94	21.99
8	1250	14.73	18.18	16.38	18.14	19.80	21.73
9	1500	14.76	18.25	16.23	18.13	19.75	21.83
10	2000	16.68	18.16	16.16	18.00	19.60	21.75
Mean		15.12	18.61	16.56	18.59	20.28	22.27
SD		0.36	0.41	0.33	0.51	0.49	0.43
Schematic		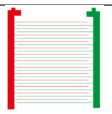				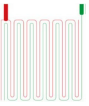	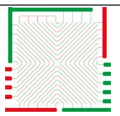

deviation of 0.52 pF. In our experiments, when only the conductive PEDOT:PSS and cellulose mixture was spin-coated on the transduction electrodes, the capacitive reading from the fabricated sensors were not stable due to highly conductive PEDOT:PSS coated layer. The mixing procedure and addition of PVP coated SNP not only reduced the conductivity of the sensing layer but also provided anti-agglomeration property to the prepared ink for sensing. We noted that, on average, for all the transduction geometries the fluctuation in the capacitance was abrupt without the inclusion of PVP coated SNP steric stabilizer.

The results of the humidity response with the transduction geometries are highlighted in Figure A.5. The highest response was recorded with a meander electrode configuration having a sensitivity of 2.37 pF/%RH whereas the lowest response was from archenemies spiral configuration of 0.13 pF/%RH. At relative humidity level above 80% there was a sharp increase in capacitive response for meander electrode configuration as compared to the other geometric configuration. Serpentine, interdigital, and custom pattern has not only shown good sensitivity but a gradual increase in capacitive response with respect to relative humidity. Therefore, these configuration may be selected for practical ranges of humidity response. The reason for the variation in the transduction response is due to the difference in the density of the sensing electrodes and inflection points in the geometries. These changes result in the difference of electric field generated by the respective geometries thus exhibiting changes in the capacitance of each geometry.

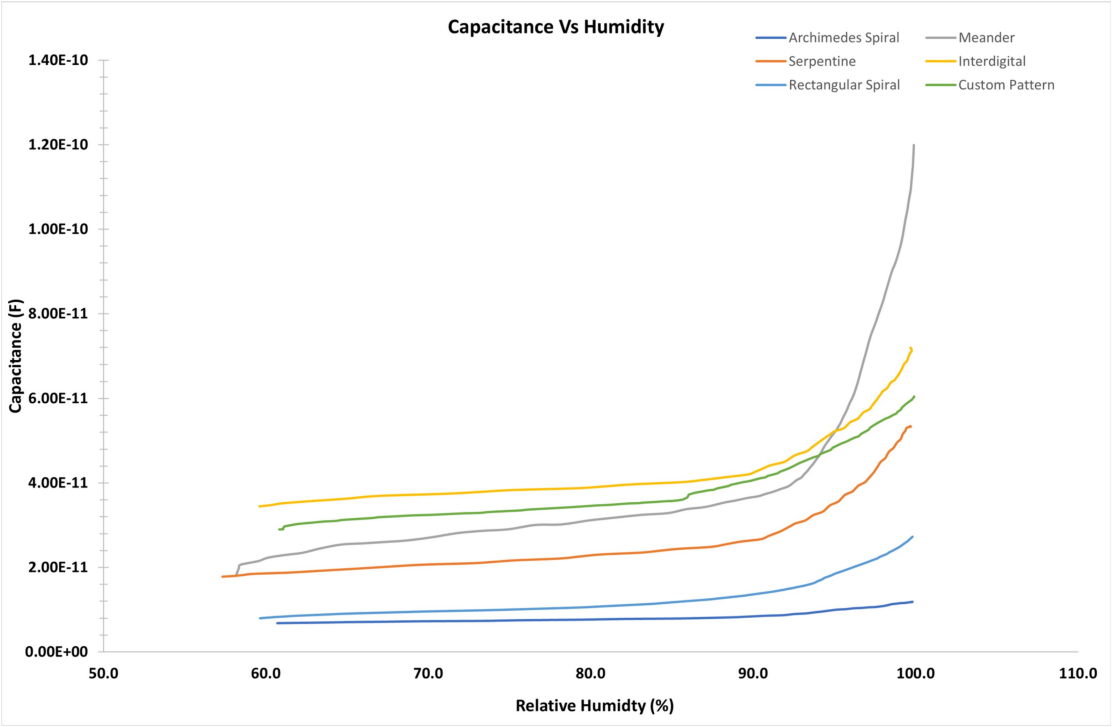

FIGURE A.5: Humidity response of patterned sensors for (a) Archemedies spiral, (b) Meander, (c) Serpentine, (d) Interdigital, (e) Rectangular spiral, and (f) Custom design.

TABLE A.3: Sensitivity of the transduction geometries

Transduction geometry	**Sensitivity pF/%RH**
Meander	2.37
Archimedes spiral	0.13
Serpentine	0.84
Interdigital	1.06
Rectangular spiral	0.31
Custom	0.88

The sensitivity of the sensor is defined as the ratio of difference of the capacitance at a specific relative humidity level designated by C_{RH} and base capacitance (C_{RHo}) of the sensor divided by the base capacitance of the sensor. Equation B.1 mathematically denotes the sensitivity of the sensor.

$$S = (C_{RH} - C_{RHo})/C_{RHo} \tag{A.1}$$

Table A.3 shows the sensitivities of the different transduction schemes. It is evident from the sensitivity values that sensing gradient highly depends on the transduction geometry. For certain sensing application a same sensing layer can offer better result with a specific geometry.

TABLE A.4: Response and recovery of the transduction geometries.

Transduction geometry	**Response (s)**	**Recovery (s)**
Meander	9.38	5.90
Archimedes spiral	0.57	5.1
Serpentine	0.38	3.13
Interdigital	0.91	4.74
Rectangular spiral	0.57	1.28
Custom	0.54	3.11

Table A.4 and Figure A.7 show the response and recovery cycles of all the patterned sensors. For each cycle of response time and recovery time of the sensor are calculated. The response time is highlighted in green and the recovery time is in red. Except the meander geometry all the other fabricated sensors have response time of less than 1 s, illustrating a quick humidity sensing application. However, the overall recovery times were below 6 seconds for all the geometries. A closer inspection of the bin sensitivities of all the transduction electrodes, as shown in Figure A.6, indicates that the meander transduction electrode geometry has exceptionally high sensitivity in the humidity bin of 90–100% when compared with the other transduction electrodes. Due to this effect the overall sensitivity of the meander geometry is higher as compared to the other geometries. Considering this factor and the gradual increase of transduction response of interdigital, serpentine, rectangular and custom geometries, it is evident that they are well suited for humidity sensing in our case.

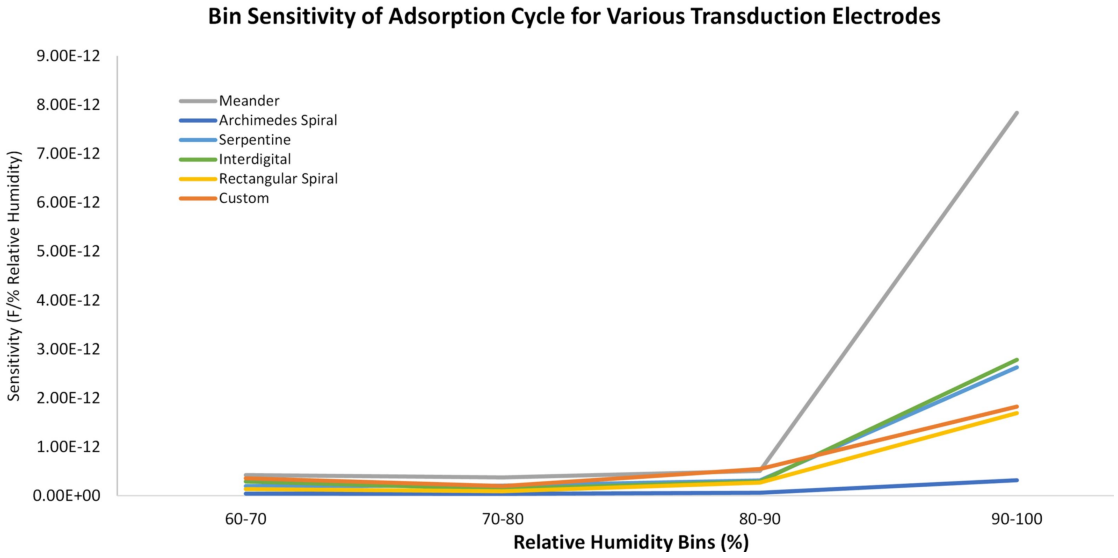

FIGURE A.6: Bin sensitivities of all six transduction electrodes.

Figure A.8 provides the adsorption and desorption cycle of patterned sensors. We found

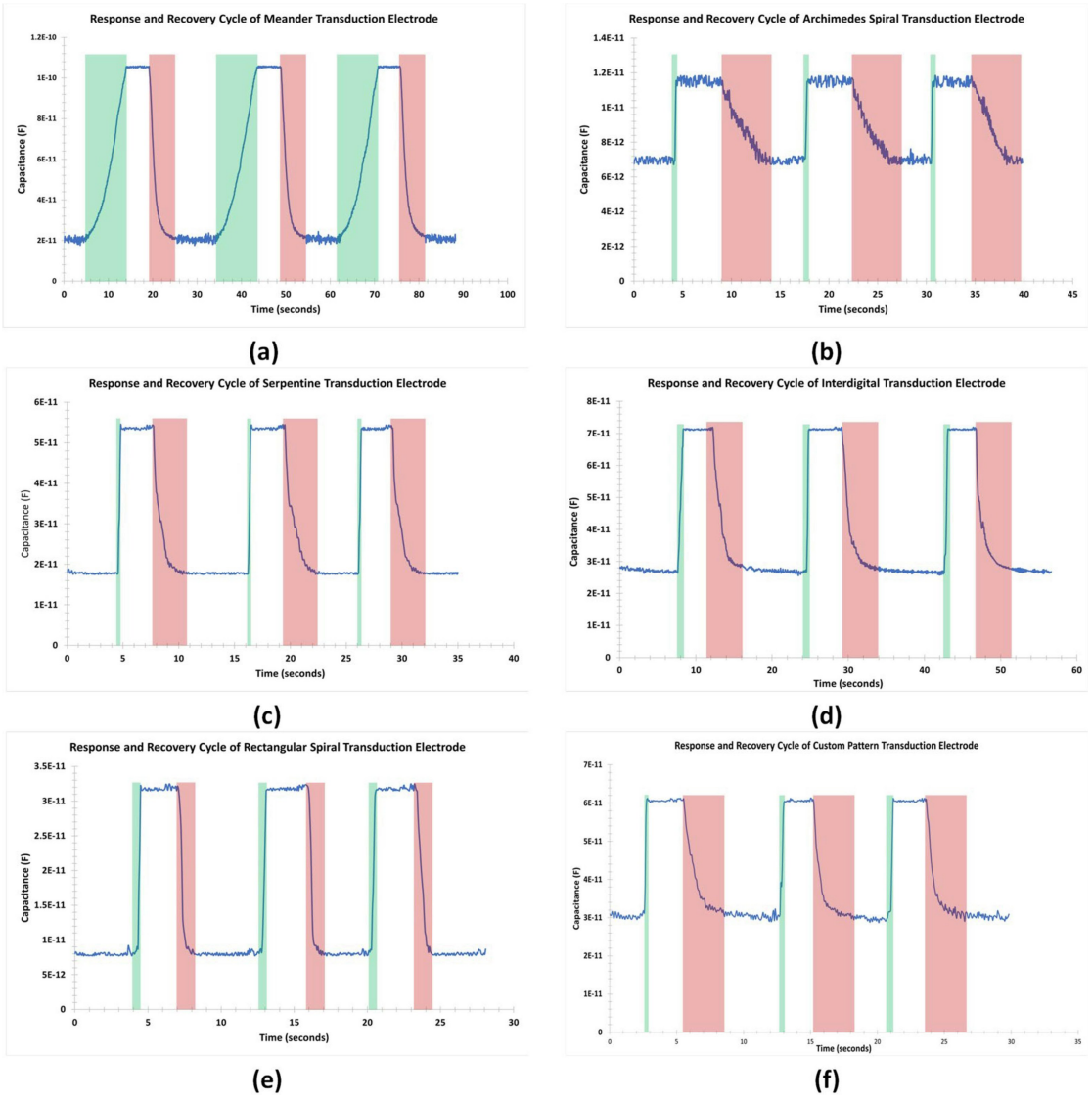

FIGURE A.7: Response and Recovery cycle of patterned sensors for (a) Meander, (b) Archimedes spiral, (c) Serpentine, (d) Interdigital, (e) Rectangular spiral, and (f) Custom design.

that there exists a hysteresis between the adsorption and desorption cycle of the patterned electrodes in all the geometry. However, for certain geometry there the hysteresis is small compared to other geometries. The reason for the hysteresis is due to two factors. The first is due to the porous nature of cellulose layers on the sensing layer, which traps the water molecules during the desorption cycle. It is evident that the capacitive response for the desorption is more than the adsorption cycle of depicting the high chances of trapping water molecules.

The other reason is the gradual decrease of humidity level in the desorption cycle as compared to the adsorption cycle, which has a steep change in the humidity level. Since,

the response of the DHT22 sensor has a higher rise due to the sudden increase of humidity in the chamber therefore, there is more hysteresis in the response stage of the sensor as compared to the recovery stage, where the hysteresis is low since the chamber humidity during this stage has a slower rate. It is anticipated that a precise measurement chamber can reduce the hysteresis between the response and recovery stage of the screen-printed sensors. It can be noted that in most of the cases the chamber starting humidity was a little higher at the end of the reading and the screen-printed response was also a little higher in the end depicting that there exists high correlation of humidity sensing of the sensors even with the slight deviation of humidity levels.

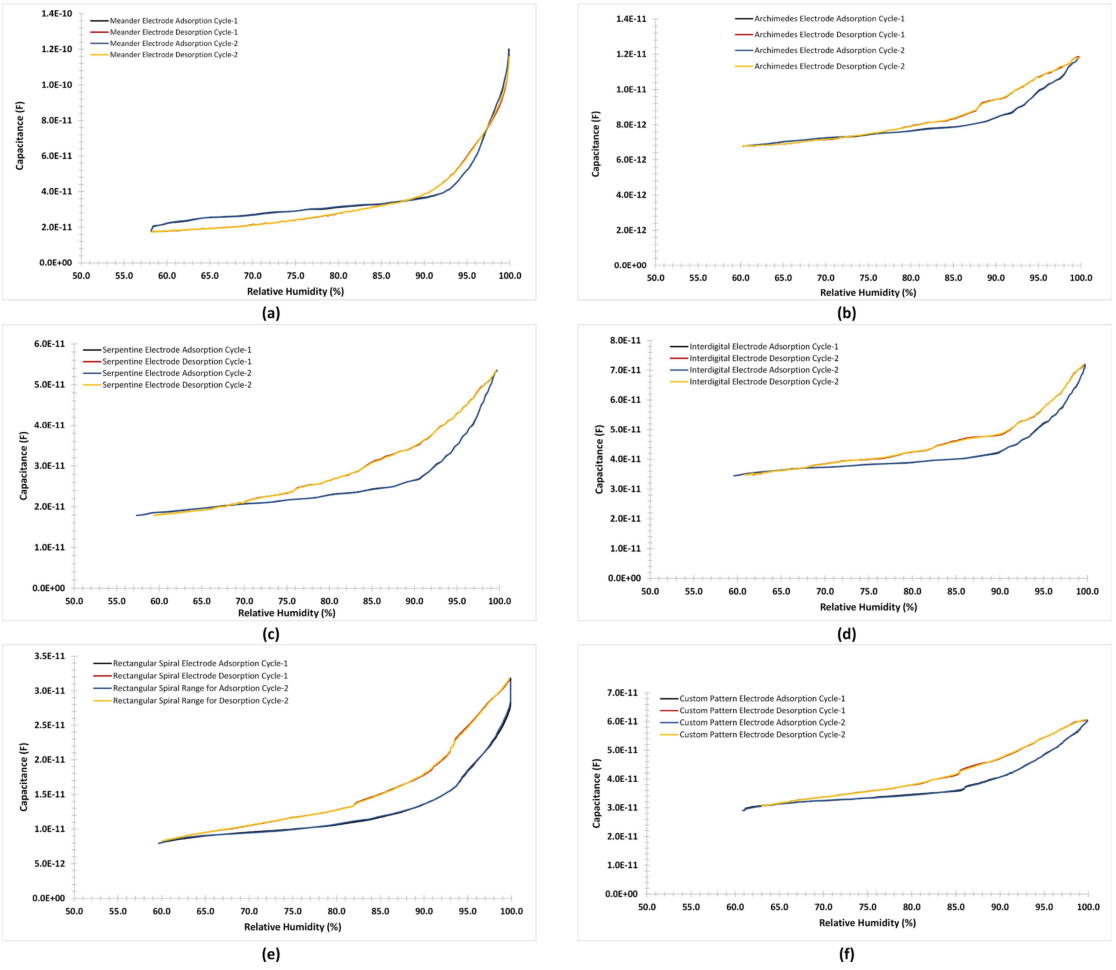

FIGURE A.8: Adsorption and desorption cycle of patterned sensors for (a) Meander, (b) Archimedes spiral, (c) Serpentine, (d) Interdigital, (e) Rectangular spiral, and (f) Custom design.

In the preceding discussion the results of the sensitivity, hysteresis, response and recovery of various transduction scheme was presented for humidity sensing. It is pertinent to note here that the sensitivity of the meander electrode was higher among all the fabricated sensors however, the response and recovery cycle was the lowest among all

the geometries. Moreover, there was an appreciable increase in the capacitance value above 80% relative humidity, which indicates highly non-linear relationship between the humidity and respective capacitive response. In this regard, the most promising electrode configuration seems to be either serpentine and custom pattern as these were the only geometries, which provided a good sensitivities and less non-linearity among all the fabricated geometry.

A.4 Methods

A.4.1 Fabrication of transduction electrodes

Laser scribing is a method to induce high laser power to produce features or cuts on the surface of the substrate. In a mechanical workshop, the laser machine is used for cutting various materials of different thickness to perform 2D cutting and engraving. The main purpose is to transform the digital design to follow a laser path, which can be used for either cutting or engraving purposes. The depth of the cut depends upon the settings of power of the laser, speed of the laser and whether the spot size of the laser is focused on the substrate. On the other hand, the width of the cut depends upon the focusing lens, laser spot speed, power of the laser and distance of the laser with the object. If the laser is adjusted so as to focus properly on the substrate, then the quality of the laser cut is precise and is slightly above the focused spot size of the laser. The power of the laser is converted into heat energy when focused on the substrate and removes the material by locally ablate or burn the material to induce the digital imprints on the substrate. In the laser cutting process, the cut width is often termed as the kerf width of the laser cutting process. In order to reap the benefits of the above-mentioned process, we followed a facile process of engraving the designed pattern on the Poly (methyl methacrylate) (PMMA) sheets of thickness 3 mm. The printing process involves the computer-aided (CAD) designs of the electrode geometry and digitally transforming those through CO_2 laser cutting beam on the PMMA sheets. Figure A.9 highlights the overall process of fabrication.

The laser ablation was done by considering the glass transition temperature of the polymer substrate, laser speed, laser power and z-height of the laser beam without the optimization of the kerf width. This technique provides a rapid production of custom

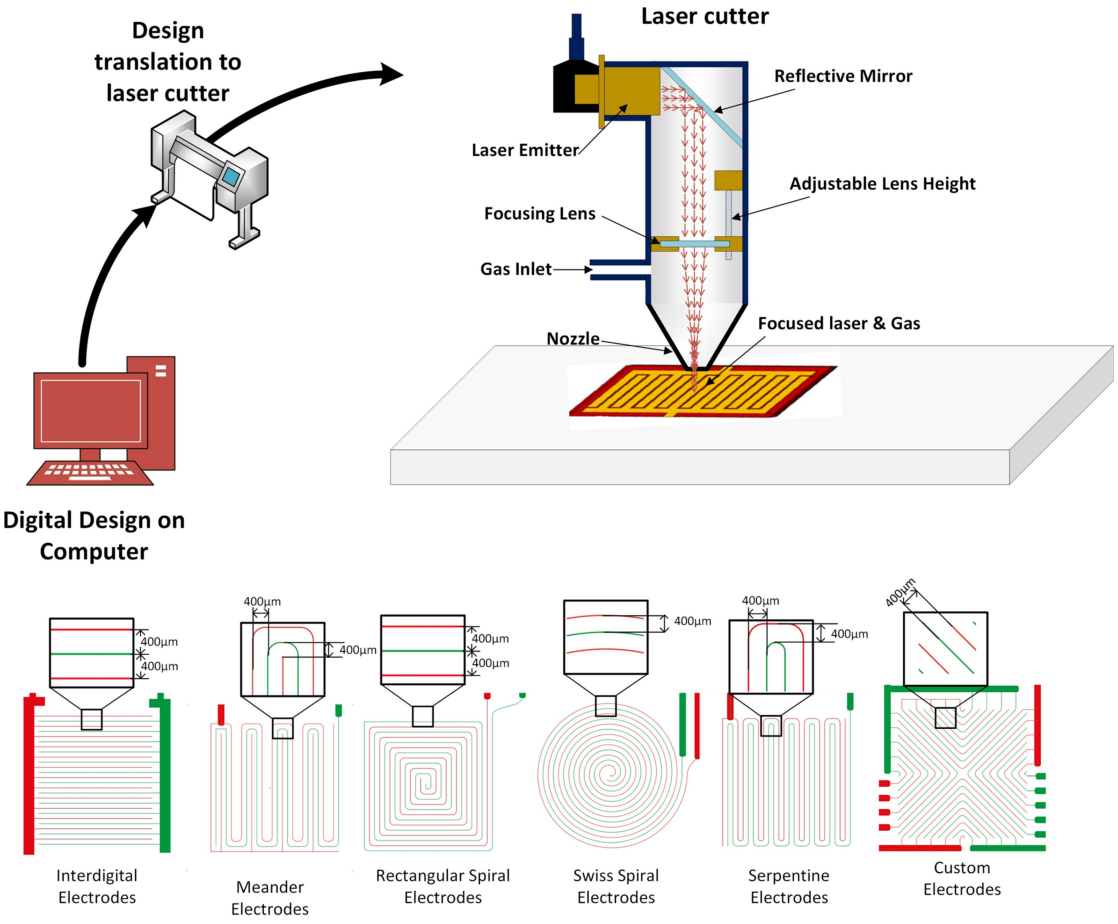

FIGURE A.9: Transduction electrode fabrication process and transduction geometries.

geometrical transduction scheme on the substrate. Due to the nature of the process, it requires no special micro fabrication process and can be done in a workshop environment to produce the transduction electrodes. Moreover, as the polymer becomes flexible close to its glass transition temperature, there is a possibility to adhere the substrate to curved surfaces. Moreover, the geometrical designs can be readily exported to the laser cutter, where the laser can be turned on and off instantly and the engraving/cutting features can be set for various layers. However, the limitation of the above technique is the resolution of the laser beam and the accuracy of stages of the CO_2 beam laser cutter. In our experiments we used six different geometrical features all with line spacing of 400 μm from the centre of the finger. Once the geometrical features were engraved on the PMMA sheets the edges of the sheets were cut out and a template for screen printing of conductive ink is ready for the next stage of conductive ink coating process. In our experiments we used the Novacentrix Metalon HPS-021LV (NOVACENTRIX, USA) screen printing ink. HPS-021LV is an electrically conductive silver flake ink designed to produce conductive traces on substrates such as paper, PET, glass, polyimide, and

TABLE A.5: Properties of HPS-021LV screen printing ink.

Measure	**Value**
Average particle size	2-4 μm
Viscosity	26,000 cP at 0.1 s^{-1}
Specific gravity	3.1
Silver loading	75%
Solvent	Water

silicon. The main properties of HPS-021LV ink are listed in Table A.5.

Once an ample amount of HPS-021LV was coated on the PMMA substrate the ink settles insides the engraved geometrical features. Later these geometrical features were subjected to heating in a convective oven to evaporate the solvent at 100°C, which is below the glass transition temperature of the PMMA sheet of 105°C. The thermal curing of the ink was done for 1 h each for all the geometrical features. After the curing process the sheet was cooled down to the ambient temperature and the excess ink was removed by uniformly scribing the surface of the PMMA sheets using a scribing knife. As the engraved features were below the level of the PMMA sheets, therefore, after the scribing process, only the ink necessary for forming the transduction electrode was left behind resulting in the functional sensing schemes. After the scribing process the conductivity of the tracks were checked through continuity measurement via a multimeter. Since, for each type of geometrical design the track lengths were different from the connection pad, the conductivity of the tracks varied for each geometrical feature.

A.4.2 Sensing layer preparation

The process of ink preparation involves the synthesis of ultrafine particles from an amorphous precursor. For this purpose, a comprehensive methodology has been devised. The methodology involves the following steps as shown in Fig. A.10.

The process starts with the wet grinding of 1g of Sigmacell Cellulose (Product Code: S3504) of Type 20 with 20μm average diameter size with 5 ml of deionized water. The wet process improves the overall particle size by reducing the lumps and agglomerations occured during the storage of the cellulose. Shearing forces reduce the particles' size, thus increasing the particles per unit weight. The reduction in particles increases the activation sites. During the 2 h grinding process the reduction in particle size in the

mortar is felt with a decrease in friction of the grinding. Wet grinding was assisted by gradually adding water to maintain the solvent quantity during the process.

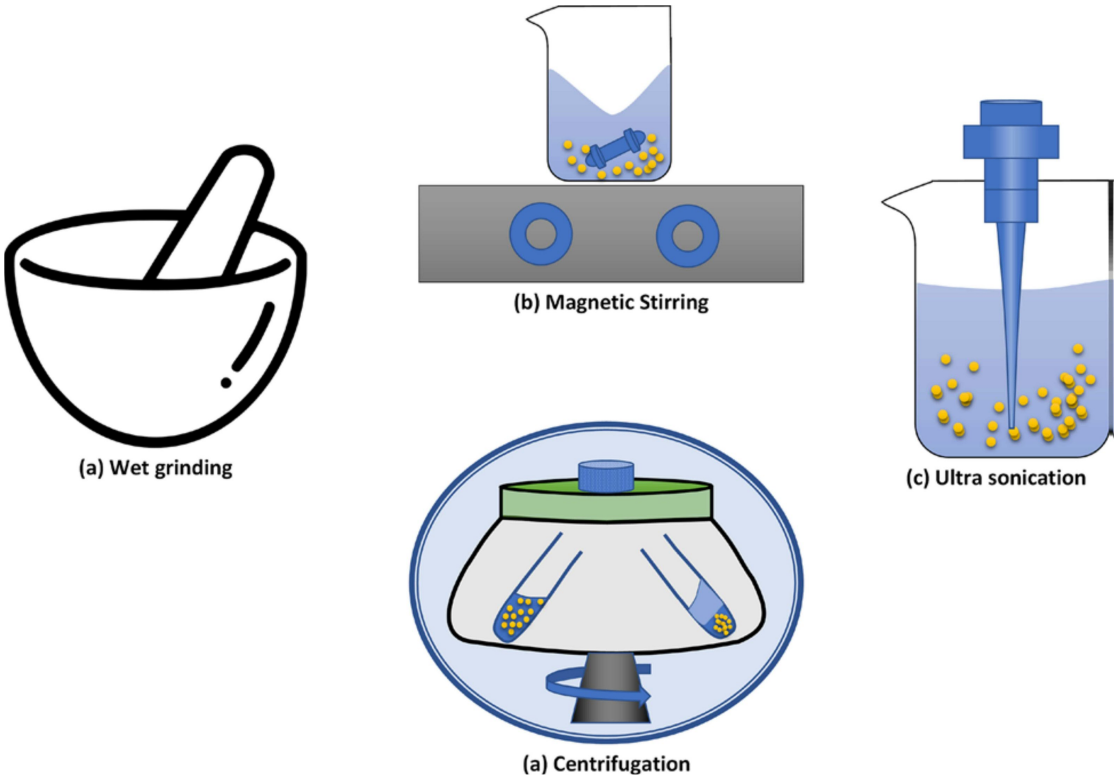

FIGURE A.10: Process of ink preparation.

Later the mixture was transferred into the beaker and was weighed to record the concentration of solvent in the mixture. Once the weight measurement was taken, 50 ml of deionized water was added so facilitate the stirring process through a magnetic stirrer. Magnetic stirring of mixture provided a uniform homogenization of amorphous solid particles in the solvent. Thus, improving the uniformity of the suspended particles in the solution. After the stirring process the mixture was heated to 100°C to attain the solvent quantity of 5 ml after the evaporation process. A 1 ml of high conductivity poly(3,4-ethylenedioxythiophene)–poly(styrenesulfonate) (PEDOT:PSS) purchased from Sigma Aldrich (Product Code: 900181) having concentration of 0.5–1 wt% of PEDOT:PSS in water along with 0.1 ml of polyvinylpyrrolidone (PVP) coated silver nanoparticle of concentration 5 mg/ml in water (PVP-coated AgNP) purchased from NanoComposix was added to adjust the conductivity and to provide the steric stability of the mixture thus avoiding agglomeration of the suspended particles. The mixture was then probe sonicated twice for an interval of 5 min each to attain the homogenized mixture of cellulose decorated conductive polymer. After sonication the liquid was then subjected to

centrifugation at 800 rpm for 30 min to remove the heavier particles from the mixture by removing the supernatant from the solution. The mentioned process provided a uniform concentration of cellulose particles when compared to the filtration process. In the filtration process only particles above a certain size are removed from the liquid. The shape of the particles remains the same, whereas the above-mentioned method shapes the particles into flakes or nanorods. This two-dimensional feature is more responsive when used for gas sensing applications [266]. Once the mixture was prepared the solution was poured on the transduction electrode and each transduction acrylic plate was then spin-coated at 1000 rpm for 120 seconds for each type of transduction geometry.

A.4.3 Measurement setup

Transduction electrodes are commonly used in sensing applications. The electrodes provide the ability to measure different kinds of gases such as Nitrous oxide, gaseous Ammonia, humidity, and many more [267]. To test the performance of various patterns of electrodes, we chose to work with the most frequently measured physical quantity i.e. humidity. This provided us with a base for assessing performance parameters of various patterns of electrodes, built using in-house facilities. Since, the humidity level in an indoor setting is quite low and stable, we carried out the experiments in an environment where humidity could be controlled to monitor the behaviour of the electrodes. Therefore, an environment was built in a plastic container that was linked to an external humidifier where the level of humidity was varied and continuously monitored. The basic layout of the experimental setup is depicted in Figure A.11.

The container was built such that the DHT22 sensors and different patterns of electrodes could be placed inside it. To achieve homogeneity of humidity inside the container, two acrylic plates were placed horizontally inside the container with holes made using a laser cutter. The holes of 5 mm in diameter were spread evenly across both plates with 15 mm spacing between them, and a 7 mm offset in holes between the top and bottom plate. The bottom plate assisted in dispersing humidity evenly while the top plate assisted in releasing excess humidity out of the chamber. Four DHT22 humidity sensors were placed on all four sides of the container such that the sensors and the electrode sensors were placed vertically around the inner walls of the container located between the top and the bottom plates. This enabled us to simultaneously test the performance of all

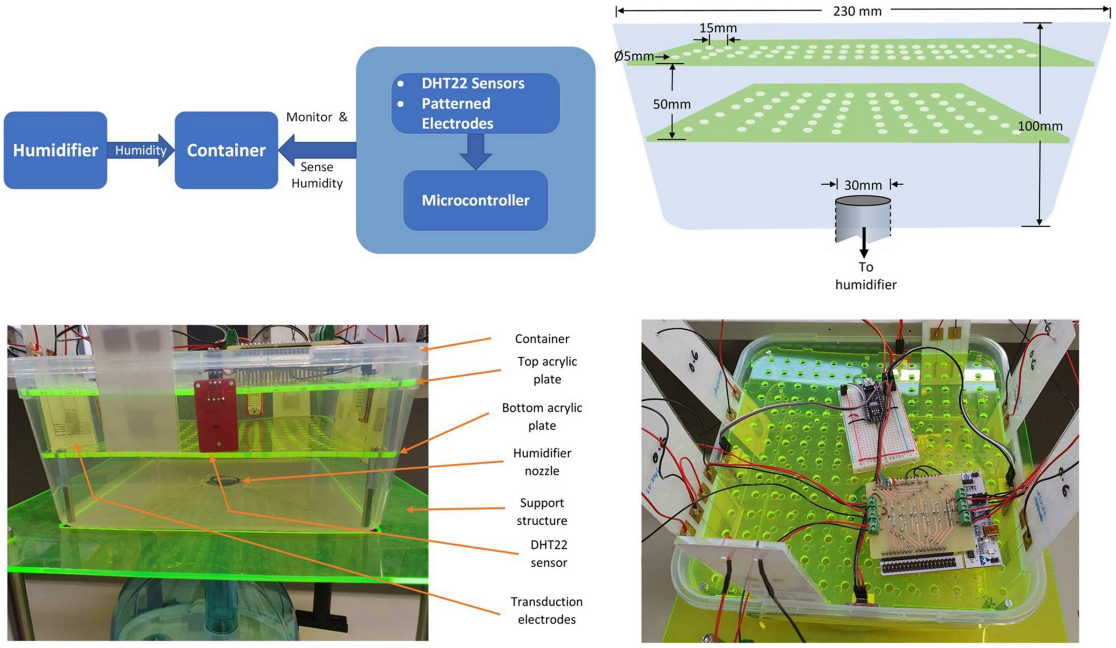

FIGURE A.11: Layout of the experimental setup.

the different patterns of transduction electrode sensors with varying levels of humidity. The two plates with holes fit inside the container with a much larger hole cut out at the centre of the container for a plastic pipe that drops down to the humidifier.

Humidity can easily be generated using an appliance called the humidifier, which is inexpensive and provides the user with the ability to control the humidity. The humidifier used in the experiment is a droplet free ultrasonic cool mist generator and has a 1.5L water tank (Kogan Mini 1.5L Humidifier). The humidifier was placed at the bottom of the container with a circular hole cut out at the bottom for a tight fit of a 30 mm wide pipe connecting to the outlet of the humidifier. A support structure was built to place the container on top of the humidifier. The humidifier exudes mist from the top into the bottom of the container through a pipe. Each transduction pattern has two square pads filled with silver ink that extends to the sensing electrodes themselves. With the help of adhesive copper tape, small pieces were fixed to the two pads, so that the thin multistrand wires could be soldered on to the tape for connectivity. As soon as the humidifier starts introducing humidity into the container, DHT22 sensors begin reading humidity levels and simultaneously the transduction electrodes start sensing the humidity levels. Humidity levels from DHT22 sensors, were read using Arduino Nano that was kept separate from the capacitive readings taken with Nucleo-F446RE board. Components of the experimental setup are labelled in Figure A.11.

The top view of the experimental setup indicates the position of the transduction electrodes of six different patterns (meander, interdigital, serpentine, circular spiral, rectangular spiral and a custom design) and four DHT22 humidity sensors, all mounted on inner walls of the container.

A.5 Conclusion

In this work, we presented a comparison among six different electrode layouts fabricated by using a laser ablation process. It has been observed that depending on the specific application and its requirements, an appropriate transduction scheme for environmental humidity sensors can be ascertained. For a large area sensing applications, the presented designs are scalable and suitable for sensing applications. The custom triangular pattern presented in this work can be a promising scheme when scalability for large area is not an issue. The fabricated sensors were tested at various relative humidity levels that achieved a good sensing response with sensitivities ranging from 0.13 to 2.37 pF/%RH in general for various transduction schemes. The meander geometric transduction scheme reported the highest sensitivity among the fabricated sensors however, there were some demerits for this geometry, such as lower response and recovery time along with associated non-linearity of capacitive response with respect to humidity. The work presented here provides a facile approach, biocompatible sensing layer and compendium of processes for fabricating sensors in a small low-cost laboratory, which can be of great advantage during the prevailing COVID-19 pandemic. Furthermore, the results obtained from the presented fabrication scheme can be extended for a high-resolution patterning electrode geometry with a suitable sensing layer.

Appendix B

DRC16 Forms

MASSEY UNIVERSITY
TE KUNENGA KI PŪREHUROA
UNIVERSITY OF NEW ZEALAND

GRADUATE RESEARCH SCHOOL

STATEMENT OF CONTRIBUTION DOCTORATE WITH PUBLICATIONS/MANUSCRIPTS

We, the student and the student's main supervisor, certify that all co-authors have consented to their work being included in the thesis and they have accepted the student's contribution as indicated below in the Statement of Originality.

Student name:	Kartikay Lal
Name and title of main supervisor:	Dr. Khalid Arif
In which chapter is the manuscript/published work?	Chapter 2

Describe the contribution that the student and members of the supervisory team have made to the manuscript/published work:[1]

Conceptualization, methodology, investigation, Kartikay Lal (K.L.), S.A.J. and K.M.A.; writing—original draft preparation, K.L. and S.A.J.; writing—review and editing, K.L., S.A.J. and K.M.A.; visualization, K.L. and S.A.J.; funding acquisition; supervision, project administration, K.M.A.

Please select one of the following three options:

- (●) The manuscript/published work is published or in press

  Please provide the full reference of the research output:

  Lal, K., Jaywant, S.A. and Arif, K.M., 2023. Electrochemical and Optical Sensors for Real-Time Detection of Nitrate in Water. Sensors, 23(16), p.7099.

- ( ) The manuscript is currently under review for publication

  Please provide the name of the journal:

- ( ) It is intended that the manuscript will be published, but it has not yet been submitted to a journal

Student's signature:	Kartikay Lal — Digitally signed by Kartikay Lal Date: 2023.11.08 13:29:00 +13'00'	Main supervisor's signature:	Khalid Arif — Digitally signed by Khalid Arif Date: 2023.11.21 14:17:29 +13'00'

This form should be placed at the beginning of each relevant thesis chapter.

[1] Refer to the Massey University Publishing and Authorship guidelines (OneMassey for staff, Stream for students) and/ or Contributor Roles Taxonomy (CRediT) guidelines for guidance.

MASSEY UNIVERSITY
TE KUNENGA KI PŪREHUROA
UNIVERSITY OF NEW ZEALAND

GRADUATE RESEARCH SCHOOL

STATEMENT OF CONTRIBUTION DOCTORATE WITH PUBLICATIONS/MANUSCRIPTS

We, the student and the student's main supervisor, certify that all co-authors have consented to their work being included in the thesis and they have accepted the student's contribution as indicated below in the Statement of Originality.

Student name:	Kartikay Lal
Name and title of main supervisor:	Dr. Khalid Arif
In which chapter is the manuscript/published work?	Chapter 3

Describe the contribution that the student and members of the supervisory team have made to the manuscript/published work:[1]

Conceptualization, experimentation, data analyses - Kartikay Lal (K.L.). Writing - original draft preparation, K.L., Khalid M. Arif (K.M.A.). Funding acquisition, supervision, project administration, K.M.A.

Please select one of the following three options:

- ○ The manuscript/published work is published or in press
  Please provide the full reference of the research output:
- ◉ The manuscript is currently under review for publication
  Please provide the name of the journal:
  Springer - Sensing and Imaging
- ○ It is intended that the manuscript will be published, but it has not yet been submitted to a journal

Student's signature:	Kartikay Lal — Digitally signed by Kartikay Lal Date: 2023.11.08 13:33:17 +13'00'	Main supervisor's signature:	Khalid Arif — Digitally signed by Khalid Arif Date: 2023.11.21 14:16:45 +13'00'

This form should be placed at the beginning of each relevant thesis chapter.

[1] Refer to the Massey University Publishing and Authorship guidelines (OneMassey for staff, Stream for students) and/ or Contributor Roles Taxonomy (CRediT) guidelines for guidance.

MASSEY UNIVERSITY
TE KUNENGA KI PŪREHUROA
UNIVERSITY OF NEW ZEALAND

GRADUATE RESEARCH SCHOOL

STATEMENT OF CONTRIBUTION DOCTORATE WITH PUBLICATIONS/MANUSCRIPTS

We, the student and the student's main supervisor, certify that all co-authors have consented to their work being included in the thesis and they have accepted the student's contribution as indicated below in the Statement of Originality.

Student name:	Kartikay Lal
Name and title of main supervisor:	Dr. Khalid Arif
In which chapter is the manuscript/published work?	Chapter 4

Describe the contribution that the student and members of the supervisory team have made to the manuscript/published work:[1]

Conceptualization, experimentation, data analyses - Kartikay Lal (K.L.). Writing - original draft preparation, K.L., Khalid M. Arif (K.M.A.). Funding acquisition, supervision, project administration, K.M.A.

Please select one of the following three options:

- ○ The manuscript/published work is published or in press
  Please provide the full reference of the research output:
- ◉ The manuscript is currently under review for publication
  Please provide the name of the journal:
  Elsevier - Sensors and Actuators A: Physical
- ○ It is intended that the manuscript will be published, but it has not yet been submitted to a journal

Student's signature:	Kartikay Lal — Digitally signed by Kartikay Lal Date: 2023.11.08 13:37:13 +13'00'	Main supervisor's signature:	Khalid Arif — Digitally signed by Khalid Arif Date: 2023.11.21 14:17:13 +13'00'

This form should be placed at the beginning of each relevant thesis chapter.

[1] Refer to the Massey University Publishing and Authorship guidelines (OneMassey for staff, Stream for students) and/ or Contributor Roles Taxonomy (CRediT) guidelines for guidance.

MASSEY UNIVERSITY
TE KUNENGA KI PŪREHUROA
UNIVERSITY OF NEW ZEALAND

GRADUATE RESEARCH SCHOOL

STATEMENT OF CONTRIBUTION DOCTORATE WITH PUBLICATIONS/MANUSCRIPTS

We, the student and the student's main supervisor, certify that all co-authors have consented to their work being included in the thesis and they have accepted the student's contribution as indicated below in the Statement of Originality.

Student name:	Kartikay Lal
Name and title of main supervisor:	Dr. Khalid Arif
In which chapter is the manuscript/published work?	Chapter 5

Describe the contribution that the student and members of the supervisory team have made to the manuscript/published work:[1]

Conceptualization, experimentation, data analyses - Kartikay Lal (K.L.) and Sanoj Menon (S.M.). Writing - original draft preparation, K.L., S.M. Frazer Noble (F.N.) and Khalid M. Arif (K.M.A.) read and approved the final draft. Funding acquisition; supervision, project administration, K.M.A.

Please select one of the following three options:

- ○ The manuscript/published work is published or in press
  Please provide the full reference of the research output:
- ◉ The manuscript is currently under review for publication
  Please provide the name of the journal:
  PLOS One
- ○ It is intended that the manuscript will be published, but it has not yet been submitted to a journal

Student's signature:	Kartikay Lal — Digitally signed by Kartikay Lal Date: 2023.11.08 13:39:10 +13'00'	Main supervisor's signature:	Khalid Arif — Digitally signed by Khalid Arif Date: 2023.11.21 14:17:00 +13'00'

This form should be placed at the beginning of each relevant thesis chapter.

[1] Refer to the Massey University Publishing and Authorship guidelines (OneMassey for staff, Stream for students) and/ or Contributor Roles Taxonomy (CRediT) guidelines for guidance.

MASSEY UNIVERSITY
TE KUNENGA KI PŪREHUROA
UNIVERSITY OF NEW ZEALAND

GRADUATE RESEARCH SCHOOL

STATEMENT OF CONTRIBUTION DOCTORATE WITH PUBLICATIONS/MANUSCRIPTS

We, the student and the student's main supervisor, certify that all co-authors have consented to their work being included in the thesis and they have accepted the student's contribution as indicated below in the Statement of Originality.

Student name:	Kartikay Lal
Name and title of main supervisor:	Dr. Khalid Arif
In which chapter is the manuscript/published work?	Appendix A

Describe the contribution that the student and members of the supervisory team have made to the manuscript/published work:[1]

M.A.A.R., Kartikay Lal (K.L.), A.S. and K.M.A. designed the research; M.A.A.R. and K.L. performed the experiments and analyzed the data; K.M.A. acquired funding, provided resources, and supervised the research; M.A.A.R., A.S. and K.L. wrote the first draft.

Please select one of the following three options:

- (●) The manuscript/published work is published or in press
  Please provide the full reference of the research output:
  Rehmani, M.A.A., Lal, K., Shaukat, A. and Arif, K.M., 2022. Laser ablation assisted micropattern screen printed transduction electrodes for sensing applications. Scientific Reports, 12(1), p.6928.
- ( ) The manuscript is currently under review for publication
  Please provide the name of the journal:
- ( ) It is intended that the manuscript will be published, but it has not yet been submitted to a journal

Student's signature:	Kartikay Lal — Digitally signed by Kartikay Lal Date: 2023.11.08 13:39:10 +13'00'	Main supervisor's signature:	Khalid Arif — Digitally signed by Khalid Arif Date: 2023.11.21 14:15:48 +13'00'

This form should be placed at the beginning of each relevant thesis chapter.

[1] Refer to the Massey University Publishing and Authorship guidelines (OneMassey for staff, Stream for students) and/ or Contributor Roles Taxonomy (CRediT) guidelines for guidance.

MASSEY UNIVERSITY
TE KUNENGA KI PŪREHUROA
UNIVERSITY OF NEW ZEALAND

GRADUATE RESEARCH SCHOOL

STATEMENT OF CONTRIBUTION DOCTORATE WITH PUBLICATIONS/MANUSCRIPTS

We, the student and the student's main supervisor, certify that all co-authors have consented to their work being included in the thesis and they have accepted the student's contribution as indicated below in the Statement of Originality.

Student name:	Kartikay Lal
Name and title of main supervisor:	Dr. Khalid Arif
In which chapter is the manuscript/published work?	Appendix A

Describe the contribution that the student and members of the supervisory team have made to the manuscript/published work:[1]

Conceptualization, methodology, investigation, Lal, K., Thomas, T., Arif, K.; writing—original draft preparation, Lal, K., Thomas, T.; writing—review and editing, Lal, K., Thomas, T., Arif, K.; visualization, Lal, K., Thomas, T.; funding acquisition; supervision, project administration, Arif, K.

Please select one of the following three options:

- (●) The manuscript/published work is published or in press

  Please provide the full reference of the research output:

  Lal, K., Thomas, T., Arif, K. (2023). Performance Evaluation of Interdigitated Electrodes for Electrochemical Detection of Nitrates in Water. In: Suryadevara, N.K., George, B., Jayasundera, K.P., Mukhopadhyay, S.C. (eds) Sensing Technology. ICST 2022. Lecture Notes in Electrical Engineering, vol 1035. Springer, Cham.

- ( ) The manuscript is currently under review for publication

  Please provide the name of the journal:

- ( ) It is intended that the manuscript will be published, but it has not yet been submitted to a journal

Student's signature:	Kartikay Lal — Digitally signed by Kartikay Lal Date: 2023.11.08 13:39:10 +13'00'	Main supervisor's signature:	Khalid Arif — Digitally signed by Khalid Arif Date: 2023.11.21 13:02:03 +13'00'

This form should be placed at the beginning of each relevant thesis chapter.

[1] Refer to the Massey University Publishing and Authorship guidelines (OneMassey for staff, Stream for students) and/ or Contributor Roles Taxonomy (CRediT) guidelines for guidance.

References

[1] Our freshwater 2023 - ministry of the environment. https://environment.govt.nz/publications/our-freshwater-2023/#introduction, 2023. accessed on Oct 31.

[2] Jean D Brender. Human health effects of exposure to nitrate, nitrite, and nitrogen dioxide. *Just enough nitrogen: Perspectives on how to get there for regions with too much and too little nitrogen*, pages 283–294, 2020.

[3] Norman G Hord, Yaoping Tang, and Nathan S Bryan. Food sources of nitrates and nitrites: the physiologic context for potential health benefits. *The American journal of clinical nutrition*, 90(1):1–10, 2009.

[4] Mirko Lunau, Maren Voss, Matthew Erickson, Claudia Dziallas, Karen Casciotti, and Hugh Ducklow. Excess nitrate loads to coastal waters reduces nitrate removal efficiency: mechanism and implications for coastal eutrophication. *Environmental microbiology*, 15(5):1492–1504, 2013.

[5] Kartikay Lal, Swapna A Jaywant, and Khalid Mahmood Arif. Electrochemical and optical sensors for real-time detection of nitrate in water. *Sensors*, 23(16): 7099, 2023.

[6] Resham Thapa, Steven B Mirsky, and Katherine L Tully. Cover crops reduce nitrate leaching in agroecosystems: A global meta-analysis. *Journal of environmental quality*, 47(6):1400–1411, 2018.

[7] Edgar García-Torres, Rebeca Pérez-Morales, Alberto González-Zamora, and Esperanza Yasmín Calleros-Rincón. Subclinical hypothyroidism in families due to chronic consumption of nitrate-contaminated water in rural areas with intensive livestock and agricultural practices in durango, mexico. *Water*, 14(3):282, 2022.

[8] Khalid Rehman Hakeem, Muhammad Sabir, Munir Ozturk, Mohd Sayeed Akhtar, and Faridah Hanum Ibrahim. Nitrate and nitrogen oxides: sources, health effects and their remediation. *Reviews of Environmental Contamination and Toxicology Volume 242*, pages 183–217, 2017.

[9] Karyne M Rogers, Rob van der Raaij, Andy Phillips, and Mike Stewart. A national isotope survey to define the sources of nitrate contamination in new zealand freshwaters. *Journal of Hydrology*, 617:129131, 2023.

[10] Scott Fields. Global nitrogen: cycling out of control, 2004.

[11] JW Gilliam, RW Skaggs, and SB Weed. Drainage control to diminish nitrate loss from agricultural fields. Technical report, Wiley Online Library, 1979.

[12] Swapna A Jaywant and Khalid Mahmood Arif. A comprehensive review of microfluidic water quality monitoring sensors. *Sensors*, 19(21):4781, 2019.

[13] Md Eshrat E Alahi and Subhas Chandra Mukhopadhyay. Detection methods of nitrate in water: A review. *Sensors and Actuators A: Physical*, 280:210–221, 2018.

[14] Elwira Wierzbicka. Novel methods of nitrate and nitrite determination-a review. *Journal of elementology*, 25(1), 2020.

[15] Aizat Azmi, Ahmad Amsyar Azman, Sallehuddin Ibrahim, and Mohd Amri Md Yunus. Techniques in advancing the capabilities of various nitrate detection methods: A review. *International Journal on Smart Sensing and Intelligent Systems*, 10(2):1–39, 2017.

[16] RKA Amali, HN Lim, I Ibrahim, NM Huang, Z Zainal, and SAA Ahmad. Significance of nanomaterials in electrochemical sensors for nitrate detection: A review. *Trends in Environmental Analytical Chemistry*, 31:e00135, 2021.

[17] Paula Jakszyn and Carlos Alberto González. Nitrosamine and related food intake and gastric and oesophageal cancer risk: a systematic review of the epidemiological evidence. *World journal of gastroenterology: WJG*, 12(27):4296, 2006.

[18] Jean D Brender, Martha M Werler, Katherine E Kelley, Ann M Vuong, Mayura U Shinde, Qi Zheng, John C Huber Jr, Joseph R Sharkey, John S Griesenbeck, Paul A Romitti, et al. Nitrosatable drug exposure during early pregnancy and neural tube

defects in offspring: National birth defects prevention study. *American journal of epidemiology*, 174(11):1286–1295, 2011.

[19] O Korostynska, A Mason, and A Al-Shamma'a. Monitoring of nitrates and phosphates in wastewater: current technologies and further challenges. *International journal on smart sensing and intelligent systems*, 5(1):149–176, 2012.

[20] AM Stortini, LM Moretto, A Mardegan, M Ongaro, and P Ugo. Arrays of copper nanowire electrodes: Preparation, characterization and application as nitrate sensor. *Sensors and Actuators B: Chemical*, 207:186–192, 2015.

[21] World Health Organization and WHO. *Guidelines for drinking-water quality*, volume 1. World Health Organization, 2004.

[22] Md Azahar Ali, Huawei Jiang, Navreet K Mahal, Robert J Weber, Ratnesh Kumar, Michael J Castellano, and Liang Dong. Microfluidic impedimetric sensor for soil nitrate detection using graphene oxide and conductive nanofibers enabled sensing interface. *Sensors and Actuators B: Chemical*, 239:1289–1299, 2017.

[23] Chunbo Jiang, Yinghe He, and Yang Liu. Recent advances in sensors for electrochemical analysis of nitrate in food and environmental matrices. *Analyst*, 145(16): 5400–5413, 2020.

[24] Mohamed Noor An'amt, Norazriena Yusoff, Suresh Sagadevan, Yasmin Abdul Wahab, Mohd Rafie Johan, et al. Recent progress in nitrates and nitrites sensor with graphene-based nanocomposites as electrocatalysts. *Trends in Environmental Analytical Chemistry*, page e00162, 2022.

[25] DM Rosenberg, TB Reynoldson, VH Resh, et al. Establishing reference conditions in the fraser river catchment, british columbia, canada, using the beast (benthic assessment of sediment) predictive model. In *Assessing the biological quality of fresh waters: RIVPACS and other techniques. Proceedings of an International Workshop held in Oxford, UK, on 16-18 September 1997*, pages 181–194. Freshwater Biological Association (FBA), 2000.

[26] Alexander D Beaton, Jemma L Wadham, Jon Hawkings, Elizabeth A Bagshaw, Guillaume Lamarche-Gagnon, Matthew C Mowlem, and Martyn Tranter. High-resolution in situ measurement of nitrate in runoff from the greenland ice sheet. *Environmental science & technology*, 51(21):12518–12527, 2017.

[27] Sristi Majumdar, Debajit Thakur, and Devasish Chowdhury. Dna carbon-nanodots based electrochemical biosensor for detection of mutagenic nitrosamines. *ACS Applied Bio Materials*, 3(3):1796–1803, 2020.

[28] Md Eshrat E Alahi, Li Xie, Subhas Mukhopadhyay, and Lucy Burkitt. A temperature compensated smart nitrate-sensor for agricultural industry. *IEEE Transactions on industrial electronics*, 64(9):7333–7341, 2017.

[29] Muhammad Asif Ali Rehmani, Kartikay Lal, Ayesha Shaukat, and Khalid Mahmood Arif. Laser ablation assisted micropattern screen printed transduction electrodes for sensing applications. *Scientific Reports*, 12(1):6928, 2022.

[30] Jimmy Ludeña-Choez, Juan J Choquehuanca-Zevallos, Alex Yasmany-Juarez, Efraín Mayhua-López, Julia Zea, María Elena Talavera-Núñez, Jorge L Magallanes-Magallanes, and H Saúl Pérez-Montaño. Capacitance sensitivity study of interdigital capacitive sensor based on graphene for monitoring nitrates concentrations. *Computers and Electronics in Agriculture*, 202:107361, 2022.

[31] NS Mazlan, MM Ramli, Mohd Mustafa Al Bakri Abdullah, DS Che Halin, SS Mat Isa, LFA Talip, NS Danial, and SA Zainol Murad. Interdigitated electrodes as impedance and capacitance biosensors: A review. In *AIP Conference proceedings*, volume 1885, page 020276. AIP Publishing LLC, 2017.

[32] Jihong Liang, Yifan Zheng, and Zongjian Liu. Nanowire-based cu electrode as electrochemical sensor for detection of nitrate in water. *Sensors and Actuators B: Chemical*, 232:336–344, 2016.

[33] Jing Fang Tan, Amie Anastasi, and Shaneel Chandra. Electrochemical detection of nitrate, nitrite and ammonium for on-site water quality monitoring. *Current Opinion in Electrochemistry*, 32:100926, 2022.

[34] Hasan Bagheri, Ali Hajian, Mosayeb Rezaei, and Ali Shirzadmehr. Composite of cu metal nanoparticles-multiwall carbon nanotubes-reduced graphene oxide as a novel and high performance platform of the electrochemical sensor for simultaneous determination of nitrite and nitrate. *Journal of hazardous materials*, 324:762–772, 2017.

[35] Nader Amini, Afshin Maleki, and Paria Maleki. Electrochemical detection of nitrate ions via reduction of no2- and oxidation of no reactions based on cu@

tio2 coreshell/nafion/polyalizarin immobilized electrode. *Materials Chemistry and Physics*, 264:124384, 2021.

[36] Yingzheng Fan, Yuankai Huang, Will Linthicum, Fangyuan Liu, André O'Reilly Beringhs, Yanliu Dang, Zhiheng Xu, Shing-Yun Chang, Jing Ling, Bryan D Huey, et al. Toward long-term accurate and continuous monitoring of nitrate in wastewater using poly (tetrafluoroethylene)(ptfe)–solid-state ion-selective electrodes (s-ises). *ACS sensors*, 5(10):3182–3193, 2020.

[37] Y Li, JZ Sun, C Bian, JH Tong, HP Dong, H Zhang, and SH Xia. Copper nano-clusters prepared by one-step electrodeposition and its application on nitrate sensing. *AIP Advances*, 5(4):041312, 2015.

[38] Dawei Pan, Wenjing Lu, Haiyun Zhang, Li Zhang, and Jianmei Zhuang. Voltammetric determination of nitrate in water samples at copper modified bismuth bulk electrode. *International Journal of Environmental Analytical Chemistry*, 93(9): 935–945, 2013.

[39] Behnam Hafezi and Mir Reza Majidi. A sensitive and fast electrochemical sensor based on copper nanostructures for nitrate determination in foodstuffs and mineral waters. *Analytical Methods*, 5(14):3552–3556, 2013.

[40] Iranaldo S da Silva, William R de Araujo, Thiago RLC Paixão, and Lúcio Angnes. Direct nitrate sensing in water using an array of copper-microelectrodes from flat flexible cables. *Sensors and Actuators B: Chemical*, 188:94–98, 2013.

[41] Guangzhen Li, Hua Yuan, Jinjin Mou, Enhao Dai, Huayu Zhang, Zhende Li, Yankun Zhao, Yifeng Dai, and Xiaoyan Zhang. Electrochemical detection of nitrate with carbon nanofibers and copper co-modified carbon fiber electrodes. *Composites Communications*, 29:101043, 2022.

[42] Pi-Guey Su and Hung-Chiang Shieh. Flexible no2 sensors fabricated by layer-by-layer covalent anchoring and in situ reduction of graphene oxide. *Sensors and Actuators B: Chemical*, 190:865–872, 2014.

[43] Vahid Riahifar, Nahid Haghnazari, Fatemeh Keshavarzi, and Fariborz Nasri. Design a high sensitive electrochemical sensor based on immobilized cysteine on fe3o4@ au core-shell nanoparticles and reduced graphene oxide nanocomposite for nitrite monitoring. *Microchemical Journal*, 166:106217, 2021.

[44] Md Azahar Ali, Yueyi Jiao, Shawana Tabassum, Yifei Wang, Huawei Jiang, and Liang Dong. Electrochemical detection of nitrate ions in soil water using graphene foam modified by tio 2 nanofibers and enzyme molecules. In *2017 19th International Conference on Solid-State Sensors, Actuators and Microsystems (TRANSDUCERS)*, pages 238–241. IEEE, 2017.

[45] Faruk Can, Seyda Korkut Ozoner, Pinar Ergenekon, and Elif Erhan. Amperometric nitrate biosensor based on carbon nanotube/polypyrrole/nitrate reductase biofilm electrode. *Materials Science and Engineering: C*, 32(1):18–23, 2012.

[46] Xunjia Li, Jianfeng Ping, and Yibin Ying. Recent developments in carbon nanomaterial-enabled electrochemical sensors for nitrite detection. *TrAC Trends in Analytical Chemistry*, 113:1–12, 2019.

[47] RDAA Rajapaksha, U Hashim, SCB Gopinath, and CAN Fernando. Sensitive ph detection on gold interdigitated electrodes as an electrochemical sensor. *Microsystem Technologies*, 24:1965–1974, 2018.

[48] Luiza A Wasiewska, Ian Seymour, Bernardo Patella, Rosalinda Inguanta, Catherine M Burgess, Geraldine Duffy, and Alan O'Riordan. Reagent free electrochemical-based detection of silver ions at interdigitated microelectrodes using in-situ ph control. *Sensors and Actuators B: Chemical*, 333:129531, 2021.

[49] Kartikay Lal, Tinu Thomas, and Khalid Arif. Performance evaluation of interdigitated electrodes for electrochemical detection of nitrates in water. In *International Conference on Sensing Technology*, pages 407–413. Springer, 2022.

[50] Ian Seymour, Benjamin O'Sullivan, Pierre Lovera, James F Rohan, and Alan O'Riordan. Electrochemical detection of free-chlorine in water samples facilitated by in-situ ph control using interdigitated microelectrodes. *Sensors and Actuators B: Chemical*, 325:128774, 2020.

[51] Benjamin O'Sullivan, Bernardo Patella, Robert Daly, Ian Seymour, Caoimhe Robinson, Pierre Lovera, James Rohan, Rosalinda Inguanta, and Alan O'Riordan. A simulation and experimental study of electrochemical ph control at gold interdigitated electrode arrays. *Electrochimica Acta*, 395:139113, 2021.

[52] Mehdi Baghayeri, Heshmatollah Alinezhad, Maryam Fayazi, Mehrasa Tarahomi, Reza Ghanei-Motlagh, and Behrooz Maleki. A novel electrochemical sensor based

on a glassy carbon electrode modified with dendrimer functionalized magnetic graphene oxide for simultaneous determination of trace pb (ii) and cd (ii). *Electrochimica Acta*, 312:80–88, 2019.

[53] Li Fu, Aiwu Wang, Kefeng Xie, Jiangwei Zhu, Fei Chen, Henggang Wang, Huaiwei Zhang, Weitao Su, Zhenguang Wang, Cangtao Zhou, et al. Electrochemical detection of silver ions by using sulfur quantum dots modified gold electrode. *Sensors and Actuators B: Chemical*, 304:127390, 2020.

[54] Enyioma C Okpara, Omolola E Fayemi, El-Sayed M Sherif, Pattan S Ganesh, BE Kumara Swamy, and Eno E Ebenso. Electrochemical evaluation of cd2+ and hg2+ ions in water using zno/cu2onps/pani modified spce electrode. *Sensing and Bio-Sensing Research*, 35:100476, 2022.

[55] Fowzia Akhter, HR Siddiquei, Md Eshrat E Alahi, and SC Mukhopadhyay. Design and development of an iot-enabled portable phosphate detection system in water for smart agriculture. *Sensors and Actuators A: Physical*, 330:112861, 2021.

[56] Mozhgan Parsaei, Zahra Asadi, and Saeid Khodadoust. A sensitive electrochemical sensor for rapid and selective determination of nitrite ion in water samples using modified carbon paste electrode with a newly synthesized cobalt (ii)-schiff base complex and magnetite nanospheres. *Sensors and actuators B: Chemical*, 220: 1131–1138, 2015.

[57] Fowzia Akhter, HR Siddiquei, Md Eshrat E Alahi, and Subhas Chandra Mukhopadhyay. An iot-enabled portable sensing system with mwcnts/pdms sensor for nitrate detection in water. *Measurement*, 178:109424, 2021.

[58] K Scott. Electrochemical principles and characterization of bioelectrochemical systems. In *Microbial Electrochemical and Fuel Cells*, pages 29–66. Elsevier, 2016.

[59] Minh-Phuong N Bui, John Brockgreitens, Snober Ahmed, and Abdennour Abbas. Dual detection of nitrate and mercury in water using disposable electrochemical sensors. *Biosensors and Bioelectronics*, 85:280–286, 2016.

[60] Luis Fermín Capitán-Vallvey, Eduardo Arroyo-Guerrero, María Dolores Fernández-Ramos, and F Santoyo-Gonzalez. Disposable receptor-based optical sensor for nitrate. *Analytical Chemistry*, 77(14):4459–4466, 2005.

[61] Christopher MA Brett. Electrochemical sensors for environmental monitoring. strategy and examples. *Pure and applied chemistry*, 73(12):1969–1977, 2001.

[62] Arif U Alam, Dennis Clyne, Hao Jin, Nan-Xing Hu, and M Jamal Deen. Fully integrated, simple, and low-cost electrochemical sensor array for in situ water quality monitoring. *ACS sensors*, 5(2):412–422, 2020.

[63] Mehdi Baghayeri, Masoud Ghanei-Motlagh, Reza Tayebee, Maryam Fayazi, and Fatemeh Narenji. Application of graphene/zinc-based metal-organic framework nanocomposite for electrochemical sensing of as (iii) in water resources. *Analytica chimica acta*, 1099:60–67, 2020.

[64] NS Mazlan, MM Ramli, Mohd Mustafa Al Bakri Abdullah, DS Che Halin, SS Mat Isa, LFA Talip, NS Danial, and SA Zainol Murad. Interdigitated electrodes as impedance and capacitance biosensors: A review. In *AIP Conference proceedings*, volume 1885, page 020276. AIP Publishing LLC, 2017.

[65] Asif I Zia, AR Mohd Syaifudin, SC Mukhopadhyay, PL Yu, Ibrahim H Al-Bahadly, Chinthaka P Gooneratne, Jurgen Kosel, and Tai-Shan Liao. Electrochemical impedance spectroscopy based mems sensors for phthalates detection in water and juices. In *Journal of Physics: Conference Series*, volume 439, page 012026. IOP Publishing, 2013.

[66] Scott MacKay, Gaser N Abdelrasoul, Marcus Tamura, Donghai Lin, Zhimin Yan, and Jie Chen. Using impedance measurements to characterize surface modified with gold nanoparticles. *Sensors*, 17(9):2141, 2017.

[67] Md Eshrat E Alahi, Nasrin Afsarimanesh, Subhas Chandra Mukhopadhyay, and Lucy Burkitt. Development of the selectivity of nitrate sensors based on ion imprinted polymerization technique. In *2017 Eleventh International Conference on Sensing Technology (ICST)*, pages 1–6. IEEE, 2017.

[68] Zannatul Mumtarin, Mohammed M Rahman, Hadi M Marwani, and Mohammad A Hasnat. Electro-kinetics of conversion of no3- into no2- and sensing of nitrate ions via reduction reactions at copper immobilized platinum surface in the neutral medium. *Electrochimica Acta*, 346:135994, 2020.

[69] Bernardo Patella, RR Russo, Alan O'Riordan, Giuseppe Aiello, Carmelo Sunseri, and Rosslinda Inguanta. Copper nanowire array as highly selective electrochemical sensor of nitrate ions in water. *Talanta*, 221:121643, 2021.

[70] AKM Sarwar Inam, Martina A Costa Angeli, Bajramshahe Shkodra, Ali Douaki, Enrico Avancini, Luca Magagnin, Luisa Petti, and Paolo Lugli. Flexible screen-printed electrochemical sensors functionalized with electrodeposited copper for nitrate detection in water. *ACS omega*, 6(49):33523–33532, 2021.

[71] Md Eshrat EE Alahi, Najid Pereira-Ishak, Subhas Chandra Mukhopadhyay, and Lucy Burkitt. An internet-of-things enabled smart sensing system for nitrate monitoring. *IEEE Internet of Things Journal*, 5(6):4409–4417, 2018.

[72] Md Eshrat E Alahi, Subhas Chandra Mukhopadhyay, and Lucy Burkitt. Imprinted polymer coated impedimetric nitrate sensor for real-time water quality monitoring. *Sensors and Actuators B: Chemical*, 259:753–761, 2018.

[73] Md Azahar Ali, Yueyi Jiao, Shawana Tabassum, Yifei Wang, Huawei Jiang, and Liang Dong. Electrochemical detection of nitrate ions in soil water using graphene foam modified by tio 2 nanofibers and enzyme molecules. In *2017 19th International Conference on Solid-State Sensors, Actuators and Microsystems (TRANSDUCERS)*, pages 238–241. IEEE, 2017.

[74] Donatella Albanese, Marisa Di Matteo, and Crescitelli Alessio. Screen printed biosensors for detection of nitrates in drinking water. In *Computer Aided Chemical Engineering*, volume 28, pages 283–288. Elsevier, 2010.

[75] W Nur Sabrina, AP Nurul Hidayah, S Faridah, MR Rashid, Y Nurul Adibah, and I Zamri. Electroimmobilization of nitrate reductase into polypyrrole films on screen printed carbon electrode (spce) for amperometric detection of nitrate. *Procedia Chemistry*, 20:69–72, 2016.

[76] T Dam Van Anh and Marcel AG Zevenbergen. Low cost nitrate sensor for agricultural applications. In *2019 20th International Conference on Solid-State Sensors, Actuators and Microsystems & Eurosensors XXXIII (TRANSDUCERS & EUROSENSORS XXXIII)*, pages 1285–1288. IEEE, 2019.

[77] Hao Wan, Qiyong Sun, Haibo Li, Fei Sun, Ning Hu, and Ping Wang. Screen-printed gold electrode with gold nanoparticles modification for simultaneous electrochemical determination of lead and copper. *Sensors and Actuators B: Chemical*, 209: 336–342, 2015.

[78] Hao Wan, Qiyong Sun, Haibo Li, Fei Sun, Ning Hu, and Ping Wang. Design of a miniaturized multisensor chip with nanoband electrode array and light addressable potentiometric sensor for ion sensing. *Analytical Methods*, 7(21):9190–9197, 2015.

[79] Houda Essousi, Houcine Barhoumi, Malek Bibani, Nadia Ktari, Frank Wendler, Ammar Al-Hamry, and Olfa Kanoun. Ion-imprinted electrochemical sensor based on copper nanoparticles-polyaniline matrix for nitrate detection. *Journal of Sensors*, 2019, 2019.

[80] Yutong Wu, Meiqi Gao, Song Li, Yuping Ren, and Gaowu Qin. Copper wires with seamless 1d nanostructures: Preparation and electrochemical sensing performance. *Materials Letters*, 211:247–249, 2018.

[81] Juan V Capella, Alberto Bonastre, Rafael Ors, and Miguel Peris. In line river monitoring of nitrate concentration by means of a wireless sensor network with energy harvesting. *Sensors and Actuators B: Chemical*, 177:419–427, 2013.

[82] Vasit Sagan, Kyle T Peterson, Maitiniyazi Maimaitijiang, Paheding Sidike, John Sloan, Benjamin A Greeling, Samar Maalouf, and Craig Adams. Monitoring inland water quality using remote sensing: Potential and limitations of spectral indices, bio-optical simulations, machine learning, and cloud computing. *Earth-Science Reviews*, 205:103187, 2020.

[83] Priyanka Singh, Manish Kumar Singh, Younus Raza Beg, and Gokul Ram Nishad. A review on spectroscopic methods for determination of nitrite and nitrate in environmental samples. *Talanta*, 191:364–381, 2019.

[84] Katrina M Miranda, Michael G Espey, and David A Wink. A rapid, simple spectrophotometric method for simultaneous detection of nitrate and nitrite. *Nitric oxide*, 5(1):62–71, 2001.

[85] Raquel Catalan-Carrio, Janire Saez, Luis Ángel Fernández Cuadrado, Gorka Arana, Lourdes Basabe-Desmonts, and Fernando Benito-Lopez. Ionogel-based

hybrid polymer-paper handheld platform for nitrite and nitrate determination in water samples. *Analytica Chimica Acta*, 1205:339753, 2022.

[86] Alexander D Beaton, Christopher L Cardwell, Rupert S Thomas, Vincent J Sieben, François-Eric Legiret, Edward M Waugh, Peter J Statham, Matthew C Mowlem, and Hywel Morgan. Lab-on-chip measurement of nitrate and nitrite for in situ analysis of natural waters. *Environmental science & technology*, 46(17):9548–9556, 2012.

[87] Moo Yow Chong, Mohd Zubir Mat Jafri, Lim Hwee San, and Tan Chun Ho. Detection of nitrate ions in water by optical fiber. In *2012 International Conference on Computer and Communication Engineering (ICCCE)*, pages 271–273. IEEE, 2012.

[88] Qiu-Hua Wang, Li-Ju Yu, Yang Liu, Lan Lin, Ri-gang Lu, Jian-ping Zhu, Lan He, and Zhong-Lin Lu. Methods for the detection and determination of nitrite and nitrate: A review. *Talanta*, 165:709–720, 2017.

[89] JL Camas-Anzueto, AE Aguilar-Castillejos, JH Castañón-González, MC Lujpán-Hidalgo, HR Hernandez De Leon, and R Mota Grajales. Fiber sensor based on lophine sensitive layer for nitrate detection in drinking water. *Optics and Lasers in Engineering*, 60:38–43, 2014.

[90] MA Parvez Mahmud, Fatemeh Ejeian, Shohreh Azadi, Matthew Myers, Bobby Pejcic, Rouzbeh Abbassi, Amir Razmjou, and Mohsen Asadnia. Recent progress in sensing nitrate, nitrite, phosphate, and ammonium in aquatic environment. *Chemosphere*, 259:127492, 2020.

[91] Shi-gang Su, Hao-yi Cheng, Ting-ting Zhu, Hong-cheng Wang, and Ai-jie Wang. A novel bioelectrochemical method for real-time nitrate monitoring. *Bioelectrochemistry*, 125:33–37, 2019.

[92] Simon Bluett, Paul O'Callaghan, Brett Paull, and Eoin Murray. Robust off-grid analyser for autonomous remote in-situ monitoring of nitrate and nitrite in water. *Talanta Open*, 7:100173, 2023.

[93] Xiaoyan Chen, Haihui Pu, Zipeng Fu, Xiaoyu Sui, Jingbo Chang, Junhong Chen, and Shun Mao. Real-time and selective detection of nitrates in water using

graphene-based field-effect transistor sensors. *Environmental Science: Nano*, 5 (8):1990–1999, 2018.

[94] Huang-Chen Lee, Amit Banerjee, Yao-Min Fang, Bing-Jean Lee, and Chung-Ta King. Design of a multifunctional wireless sensor for in-situ monitoring of debris flows. *IEEE Transactions on Instrumentation and Measurement*, 59(11):2958–2967, 2010.

[95] Peng Jiang, Hongbo Xia, Zhiye He, and Zheming Wang. Design of a water environment monitoring system based on wireless sensor networks. *Sensors*, 9(8): 6411–6434, 2009.

[96] Theofanis P Lambrou, Christos C Anastasiou, Christos G Panayiotou, and Marios M Polycarpou. A low-cost sensor network for real-time monitoring and contamination detection in drinking water distribution systems. *IEEE sensors journal*, 14(8):2765–2772, 2014.

[97] Peter Corke, Tim Wark, Raja Jurdak, Wen Hu, Philip Valencia, and Darren Moore. Environmental wireless sensor networks. *Proceedings of the IEEE*, 98 (11):1903–1917, 2010.

[98] Yang Xu and Fugui Liu. Application of wireless sensor network in water quality monitoring. In *2017 IEEE International Conference on Computational Science and Engineering (CSE) and IEEE International Conference on Embedded and Ubiquitous Computing (EUC)*, volume 2, pages 368–371. IEEE, 2017.

[99] Kofi Sarpong Adu-Manu, Cristiano Tapparello, Wendi Heinzelman, Ferdinand Apietu Katsriku, and Jamal-Deen Abdulai. Water quality monitoring using wireless sensor networks: Current trends and future research directions. *ACM Transactions on Sensor Networks (TOSN)*, 13(1):1–41, 2017.

[100] A Bonastre, JV Capella, R Ors, and M Peris. In-line monitoring of chemical-analysis processes using wireless sensor networks. *TrAC Trends in Analytical Chemistry*, 34:111–125, 2012.

[101] Ke Xu, Qiulin Chen, Yuanyuan Zhao, Chengjun Ge, Shiwei Lin, and Jianjun Liao. Cost-effective, wireless, and portable smartphone-based electrochemical system for on-site monitoring and spatial mapping of the nitrite contamination in water. *Sensors and Actuators B: Chemical*, 319:128221, 2020.

[102] Pietro Di Gennaro, Domenico Lofú, Daniele Vitanio, Pietro Tedeschi, and Pietro Boccadoro. Waters: A sigfox-compliant prototype for water monitoring. *Internet Technology Letters*, 2(1):e74, 2019.

[103] Manas Ranjan Gartia, Björn Braunschweig, Te-Wei Chang, Parya Moinzadeh, Barbara S Minsker, Gul Agha, Andrzej Wieckowski, Laura L Keefer, and Gang Logan Liu. The microelectronic wireless nitrate sensor network for environmental water monitoring. *Journal of Environmental Monitoring*, 14(12):3068–3075, 2012.

[104] Gurkan Tuna, Bilel Nefzi, Orhan Arkoc, and Stelios M Potirakis. Wireless sensor network-based water quality monitoring system. In *Key Engineering Materials*, volume 605, pages 47–50. Trans Tech Publ, 2014.

[105] Xin Wang, Longquan Ma, and Huizhong Yang. Online water monitoring system based on zigbee and gprs. *Procedia Engineering*, 15:2680–2684, 2011.

[106] Nidal Nasser, Asmaa Ali, Lutful Karim, and Samir Belhaouari. An efficient wireless sensor network-based water quality monitoring system. In *2013 ACS international conference on computer systems and applications (AICCSA)*, pages 1–4. IEEE, 2013.

[107] JV Capella, A Bonastre, R Ors, and M Peris. A wireless sensor network approach for distributed in-line chemical analysis of water. *Talanta*, 80(5):1789–1798, 2010.

[108] S Angel Vergina, S Kayalvizhi, RM Bhavadharini, and S Kalpana Devi. A real time water quality monitoring using machine learning algorithm. *Eur. J. Mol. Clin. Med*, 7:2035–2041, 2020.

[109] Ismail Agir, Ridvan Yildirim, Mustafa Nigde, and Ibrahim Isildak. Internet of things implementation of nitrate and ammonium sensors for online water monitoring. *Analytical Sciences*, 37(7):971–976, 2021.

[110] AJ Ramadhan, AM Ali, HK Kareem, et al. Smart water-quality monitoring system based on enabled real-time internet of things. *J. Eng. Sci. Technol*, 15(6):3514–3527, 2020.

[111] Md Eshrat E Alahi, Anindya Nag, Subhas Chandra Mukhopadhyay, and Lucy Burkitt. A temperature-compensated graphene sensor for nitrate monitoring in real-time application. *Sensors and Actuators A: Physical*, 269:79–90, 2018.

[112] Alexander D Beaton, Jemma L Wadham, Jon Hawkings, Elizabeth A Bagshaw, Guillaume Lamarche-Gagnon, Matthew C Mowlem, and Martyn Tranter. High-resolution in situ measurement of nitrate in runoff from the greenland ice sheet. *Environmental science & technology*, 51(21):12518–12527, 2017.

[113] Yong Jie Wong, Rei Nakayama, Yoshihisa Shimizu, Akinori Kamiya, Shang Shen, Idlan Zarizi Muhammad Rashid, and Nik Meriam Nik Sulaiman. Toward industrial revolution 4.0: Development, validation, and application of 3d-printed iot-based water quality monitoring system. *Journal of Cleaner Production*, 324:129230, 2021.

[114] Martin Jason Luna Juncal, Timothy Skinner, Edoardo Bertone, and Rodney A Stewart. Development of a real-time, mobile nitrate monitoring station for high-frequency data collection. *Sustainability*, 12(14):5780, 2020.

[115] Yu-Ting Chen and Jill Crossman. The impacts of biofouling on automated phosphorus analysers during long-term deployment. *Science of the Total Environment*, 784:147188, 2021.

[116] Adrian M Nightingale, Sammer-ul Hassan, Brett M Warren, Kyriacos Makris, Gareth WH Evans, Evanthia Papadopoulou, Sharon Coleman, and Xize Niu. A droplet microfluidic-based sensor for simultaneous in situ monitoring of nitrate and nitrite in natural waters. *Environmental science & technology*, 53(16):9677–9685, 2019.

[117] Supakorn Harnsoongnoen, Anuwat Wanthong, Urit Charoen-In, and Apirat Siritaratiwat. Microwave sensor for nitrate and phosphate concentration sensing. *IEEE Sensors Journal*, 19(8):2950–2955, 2019.

[118] O Korostynska, A Mason, M Ortoneda-Pedrola, and A Al-Shamma'a. Electromagnetic wave sensing of no3 and cod concentrations for real-time environmental and industrial monitoring. *Sensors and Actuators B: Chemical*, 198:49–54, 2014.

[119] Sevda Mohammadi, Anupama Vijaya Nadaraja, Deborah J Roberts, and Mohammad H Zarifi. Real-time and hazard-free water quality monitoring based on microwave planar resonator sensor. *Sensors and Actuators A: Physical*, 303:111663, 2020.

[120] Muhammad Asif Ali Rehmani, Swapna A Jaywant, and Khalid Mahmood Arif. Study of microchannels fabricated using desktop fused deposition modeling systems. *Micromachines*, 12(1):14, 2020.

[121] Clear Water Sensors. Clear water sensors - nitrate + nitrite sensor. https://www.clearwatersensors.com/nitrate-sensor/, July 2023.

[122] Libelium. Waspmote smart water. https://www.libelium.com/libeliumworld/smart-water-ions-sensors-calcium-fluoride-chloride-nitrate-iodide-lead-bromide-c July 2023.

[123] Boqu Instrument Co. Iot digital multi-parameter water quality sensor. https://www.boquinstruments.com/iot-digital-multi-parameter-water-quality-sensor-product/, July 2023.

[124] Ministry for the Environment & Stats NZ. Our freshwater, 2020. *Issue 1: Our native freshwater species and ecosystems are under threat*, page 32, 2020.

[125] Drinking water nitrate limit 11 times higher than it should be - health expert. https://www.rnz.co.nz/news/national/436088/drinking-water-nitrate-limit-11-times-higher-than-it-should-be-health-expert, 2022. accessed on Dec 22.

[126] Margaret McCasland, Nancy M Trautmann, and Robert J Wagenet. Nitrate: Health effects in drinking water. *My Swiss Mountain*, 1985.

[127] Md Eshrat E Alahi and Subhas Chandra Mukhopadhyay. Detection methods of nitrate in water: A review. *Sensors and Actuators A: Physical*, 280:210–221, 2018.

[128] Jiri Barek. How to improve the performance of electrochemical sensors via minimization of electrode passivation. *Chemosensors*, 9(1):12, 2021.

[129] Md Eshrat EE Alahi, Najid Pereira-Ishak, Subhas Chandra Mukhopadhyay, and Lucy Burkitt. An internet-of-things enabled smart sensing system for nitrate monitoring. *IEEE Internet of Things Journal*, 5(6):4409–4417, 2018.

[130] MA Farehanim, U Hashim, N Azizah, MF Fatin, and AH Azman. Fabrication of interdigitated electrodes (ides) using basic conventional lithography for ph measurement. In *AIP Conference Proceedings*, volume 1808, page 020029. AIP Publishing LLC, 2017.

[131] Cacie Hart and Swaminathan Rajaraman. Low-power, multimodal laser micromachining of materials for applications in sub-5 μm shadow masks and sub-10 μm interdigitated electrodes (ides) fabrication. *Micromachines*, 11(2):178, 2020.

[132] Harish Gnanasambanthan and Debashis Maji. Reusable thin stainless steel shadow mask fabrication using electron discharge machining. In *2022 IEEE 7th International conference for Convergence in Technology (I2CT)*, pages 1–4. IEEE, 2022.

[133] Duy Dam Le, Thi Ngoc Nhien Nguyen, Duc Chanh Tin Doan, Thi My Dung Dang, and Mau Chien Dang. Fabrication of interdigitated electrodes by inkjet printing technology for apllication in ammonia sensing. *Advances in Natural Sciences: Nanoscience and Nanotechnology*, 7(2):025002, 2016.

[134] Shawkat Ali, Saleem Khan, and Amine Bermak. Inkjet-printed human body temperature sensor for wearable electronics. *IEEE Access*, 7:163981–163987, 2019.

[135] Binu Baby Narakathu, Sai Guruva Reddy Avuthu, Ali Eshkeiti, Sepehr Emamian, and Massood Zandi Atashbar. Development of a microfluidic sensing platform by integrating pcb technology and inkjet printing process. *IEEE sensors journal*, 15 (11):6374–6380, 2015.

[136] Joon S Shim, Michael J Rust, and Chong H Ahn. A large area nano-gap interdigitated electrode array on a polymer substrate as a disposable nano-biosensor. *Journal of Micromechanics and Microengineering*, 23(3):035002, 2013.

[137] Philipp Schäffner, Martin Zirkl, Gerburg Schider, Jonas Groten, Maria Regina Belegratis, Peter Knoll, and Barbara Stadlober. Microstructured single-layer electrodes embedded in p (vdf-trfe) for flexible and self-powered direction-sensitive strain sensors. *Smart Materials and Structures*, 29(8):085040, 2020.

[138] Pen-Cheng Wang, Rollin E Lakis, and Alan G MacDiarmid. Morphology-correlated electrical conduction in micro-contact-printed polypyrrole thin films grown by in situ deposition. *Thin Solid Films*, 516(8):2341–2345, 2008.

[139] Manish Rishi, Khairunnisa Amreen, Khush Gohel, Arshad Javed, Satish Kumar Dubey, and Sanket Goel. Three different rapidly prototyped polymeric substrates with interdigitated electrodes for escherichia coli sensing: A comparative study. *IEEE Transactions on NanoBioscience*, 2022.

[140] Muhammad Asif Ali Rehmani, Kartikay Lal, Ayesha Shaukat, and Khalid Mahmood Arif. Laser ablation assisted micropattern screen printed transduction electrodes for sensing applications. *Scientific Reports*, 12(1):1–15, 2022.

[141] Muhammad Asif Ali Rehmani and Khalid Mahmood Arif. High resolution electrohydrodynamic printing of conductive ink with an aligned aperture coaxial printhead. *The International Journal of Advanced Manufacturing Technology*, 115(9): 2785–2800, 2021.

[142] Niina J Ronkainen, H Brian Halsall, and William R Heineman. Electrochemical biosensors. *Chemical Society Reviews*, 39(5):1747–1763, 2010.

[143] Dirk Johannes De Beer and Trudi-Heleen Joubert. Validation of low-cost impedance analyzer via nitrate detection. *Sensors*, 21(19):6695, 2021.

[144] Elyana Kosri, Fatimah Ibrahim, Aung Thiha, and Marc Madou. Micro and nano interdigitated electrode array (idea)-based mems/nems as electrochemical transducers: A review. *Nanomaterials*, 12(23):4171, 2022.

[145] Hend S Magar, Rabeay YA Hassan, and Ashok Mulchandani. Electrochemical impedance spectroscopy (eis): Principles, construction, and biosensing applications. *Sensors*, 21(19):6578, 2021.

[146] N Nedyalkov, Ru Nikov, Ro Nikov, A Nikolov, P Atanasov, Y Nakajima, M Terakawa, M Sawczak, K Grochowska, and G Sliwinski. Gold nanostructures for detection of pesticides, nitrates and drugs using surface enhanced raman spectroscopy. In *19th International Conference and School on Quantum Electronics: Laser Physics and Applications*, volume 10226, pages 85–92. SPIE, 2017.

[147] Jungyoon Kim, Qingyuan Liu, and Tianhong Cui. Graphene-based ion sensitive-fet sensor with porous anodic aluminum oxide substrate for nitrate detection. *Journal of Microelectromechanical Systems*, 29(5):966–971, 2020.

[148] Meng Xu, Dora Obodo, and Vamsi K Yadavalli. The design, fabrication, and applications of flexible biosensing devices. *Biosensors and Bioelectronics*, 124: 96–114, 2019.

[149] Quanling Li, Jiayan Zhang, Qianhao Li, Guihong Li, Xiyue Tian, Zewei Luo, Fei Qiao, Xing Wu, and Jian Zhang. Review of printed electrodes for flexible devices. *Frontiers in Materials*, 5:77, 2019.

[150] Alireza Shamsi, Ali Amiri, Payam Heydari, Hasan Hajghasem, Mansour Mohtashamifar, and Mehrnaz Esfandiari. Low cost method for hot embossing of microstructures on pmma by su-8 masters. *Microsystem technologies*, 20:1925–1931, 2014.

[151] "polymethyl methacrylate". https://www.britannica.com/science/polymethyl-methacrylate, 2023. accessed on 27 January.

[152] Muhammad Asif Ali Rehmani and Khalid Mahmood Arif. Capacitive transduction schemes for environmental humidity sensors. In *2019 13th International Conference on Sensing Technology (ICST)*, pages 1–5. IEEE, 2019.

[153] Espen Tunhøvd Haugan and Per Dalsjø. Characterization of the material properties of two fr4 printed circuit board laminates. *ffi-publikasjoner.archive.knowledgearc.net*, 2014.

[154] Jintao Zhang, Thangavel Lakshmipriya, and Subash CB Gopinath. Electroanalysis on an interdigitated electrode for high-affinity cardiac troponin i biomarker detection by aptamer–gold conjugates. *ACS omega*, 5(40):25899–25905, 2020.

[155] Ian Seymour, Benjamin O'Sullivan, Pierre Lovera, James F Rohan, and Alan O'Riordan. Elimination of oxygen interference in the electrochemical detection of monochloramine, using in situ ph control at interdigitated electrodes. *ACS sensors*, 6(3):1030–1038, 2021.

[156] Shan He, Shilun Feng, Anindya Nag, Nasrin Afsarimanesh, Md Eshrat E Alahi, Siying Li, Subhas Chandra Mukhopadhyay, and Jonathan Woon Chung Wong. Iot-based laser-inscribed sensors for detection of sulfate in water bodies. *IEEE Access*, 8:228879–228890, 2020.

[157] Christopher S Storer, Zachary Coldrick, Daniel J Tate, Jack Marsden Donoghue, and Bruce Grieve. Towards phosphate detection in hydroponics using molecularly imprinted polymer sensors. *Sensors*, 18(2):531, 2018.

[158] Shumin Zheng, Hong Zhang, Thangavel Lakshmipriya, Subash CB Gopinath, and Na Yang. Gold nanorod integrated electrochemical sensing for hyperglycaemia on interdigitated electrode. *BioMed research international*, 2019, 2019.

[159] Yan Gu, Lijie Liu, Jian Guo, Shun Xiao, Fang Fang, Xiaoyun Yu, Subash CB Gopinath, Jianlie Wu, and Xunqiang Liu. Biomolecular assembly on interdigitated electrode nanosensor for selective detection of insulin-like growth factor-1. *Artificial cells, nanomedicine, and biotechnology*, 49(1):30–37, 2021.

[160] Md Eshrat E Alahi, Xie Li, Subhas Mukhopadhyay, and L Burkitt. Application of practical nitrate sensor based on electrochemical impedance spectroscopy. *Sensors for Everyday Life: Environmental and Food Engineering*, pages 109–136, 2017.

[161] Shanshan Zhao, Jianhua Tong, Yang Li, Jizhou Sun, Chao Bian, and Shanhong Xia. Palladium-gold modified ultramicro interdigital array electrode chip for nitrate detection in neutral water. *Micromachines*, 10(4):223, 2019.

[162] Xiaoyan Chen, Haihui Pu, Zipeng Fu, Xiaoyu Sui, Jingbo Chang, Junhong Chen, and Shun Mao. Real-time and selective detection of nitrates in water using graphene-based field-effect transistor sensors. *Environmental Science: Nano*, 5 (8):1990–1999, 2018.

[163] Jin Wook Jeong, Jin Woo Huh, Jeong Ik Lee, Hye Yong Chu, James Jungho Pak, and Byeong Kwon Ju. Interdigitated electrode geometry effects on the performance of organic photoconductors for optical sensor applications. *Thin Solid Films*, 518 (22):6343–6347, 2010.

[164] KP Srinivasan and T Muthuramalingam. Fabrication and performance evolution of agnp interdigitated electrode touch sensor for automotive infotainment. *Sensors*, 21(23):7961, 2021.

[165] Md Eshrat E Alahi, Subhas Chandra Mukhopadhyay, and Lucy Burkitt. Imprinted polymer coated impedimetric nitrate sensor for real-time water quality monitoring. *Sensors and Actuators B: Chemical*, 259:753–761, 2018.

[166] Md Eshrat E Alahi, Anindya Nag, Subhas Chandra Mukhopadhyay, and Lucy Burkitt. A temperature-compensated graphene sensor for nitrate monitoring in real-time application. *Sensors and Actuators A: Physical*, 269:79–90, 2018.

[167] Yonggang Liu, Aoke Zeng, Shuliang Zhang, Ruixiang Ma, and Zhe Du. An experimental investigation on polarization process of a pzt-52 tube actuator with interdigitated electrodes. *Micromachines*, 13(10):1760, 2022.

[168] Guokang Fan, Peng Sun, Jie Zhao, Dongxue Han, Li Niu, and Guofeng Cui. Alleviating concentration polarization: a micro three-electrode interdigitated glucose sensor based on nanoporous gold from a mild process. *RSC advances*, 9(19):10465–10472, 2019.

[169] Yan-Feng Sun, Yuming Guo, Chi Xu, Ying Liu, Xu Zhao, Qian Liu, Erik Jeppesen, Haijun Wang, and Ping Xie. Will "air eutrophication" increase the risk of ecological threat to public health? *Environmental Science & Technology*, 57(29): 10512–10520, 2023.

[170] Xin Zhang, Yan Zhang, Peng Shi, Zhilei Bi, Zexuan Shan, and Lijiang Ren. The deep challenge of nitrate pollution in river water of china. *Science of the Total Environment*, 770:144674, 2021.

[171] Eric Craswell. Fertilizers and nitrate pollution of surface and ground water: an increasingly pervasive global problem. *SN Applied Sciences*, 3(4):518, 2021.

[172] Schreckenbach, Knösche, and Ebert. Nutrient and energy content of freshwater fishes. *Journal of Applied Ichthyology*, 17(3):142–144, 2001.

[173] RKA Amali, HN Lim, I Ibrahim, NM Huang, Z Zainal, and SAA Ahmad. Significance of nanomaterials in electrochemical sensors for nitrate detection: A review. *Trends in Environmental Analytical Chemistry*, 31:e00135, 2021.

[174] Kartikay Lal and Khalid Arif. Investigation of planar electrodes for electrochemical impedance spectroscopy-based detection of nitrate in water. *Sensors and Actuators A: Physical*, in press.

[175] Woo Jae Cho, Dong-Wook Kim, Dae Hyun Jung, Sang Sun Cho, and Hak-Jin Kim. An automated water nitrate monitoring system based on ion-selective electrodes. *Journal of Biosystems Engineering*, 41(2):75–84, 2016.

[176] N Paniel, J Baudart, A Hayat, and L Barthelmebs. Aptasensor and genosensor methods for detection of microbes in real world samples. *Methods*, 64(3):229–240, 2013.

[177] Abid A Ansari, Gill Sarvajeet Singh, Guy R Lanza, and Walter Rast. *Eutrophication: causes, consequences and control*, volume 1. Springer, 2010.

[178] JoAnn M Burkholder, David A Tomasko, and Brant W Touchette. Seagrasses and eutrophication. *Journal of experimental marine biology and ecology*, 350(1-2): 46–72, 2007.

[179] David M Harper et al. *Eutrophication of freshwaters*. Springer, 1992.

[180] M Nasir Khan and Firoz Mohammad. Eutrophication: challenges and solutions. *Eutrophication: Causes, Consequences and Control: Volume 2*, pages 1–15, 2014.

[181] Deionized water vs distilled water. https://www.uswatersystems.com/deionized-water-vs-distilled-water#:~:text=Deionized%20(DI)%20water%20is%20water,methods%20for%20creating%20pure%20water., 2023. accessed on 03 September 2023.

[182] Md Galal Uddin, Stephen Nash, and Agnieszka I Olbert. A review of water quality index models and their use for assessing surface water quality. *Ecological Indicators*, 122:107218, 2021.

[183] Zijun Li, Qingchun Yang, Chuan Xie, and Xingyu Lu. Source identification and health risks of nitrate contamination in shallow groundwater: a case study in subei lake basin. *Environmental Science and Pollution Research*, 30(5):13660–13670, 2023.

[184] Admin Husic, James F Fox, Evan Clare, Tyler Mahoney, and Amirreza Zarnaghsh. Nitrate hysteresis as a tool for revealing storm-event dynamics and improving water quality model performance. *Water Resources Research*, 59(1):e2022WR033180, 2023.

[185] William A Jury and Henry J Vaux Jr. The emerging global water crisis: managing scarcity and conflict between water users. *Advances in agronomy*, 95:1–76, 2007.

[186] BS Abed, MARIAM H Daham, and ALHASSAN H Ismail. Water quality modelling and management of diyala river and its impact on tigris river. *J. Eng. Sci. Technol*, 16:122–135, 2021.

[187] Robert J Davies-Colley et al. River water quality in new zealand: an introduction and overview. *Ecosystem services in New Zealand: conditions and trends. Manaaki Whenua Press, Lincoln*, pages 432–447, 2013.

[188] P Payment, M Waite, and A Dufour. Introducing parameters for the assessment of drinking water quality. *Assessing microbial safety of drinking water*, 4:47–77, 2003.

[189] SP Gorde and MV Jadhav. Assessment of water quality parameters: a review. *J Eng Res Appl*, 3(6):2029–2035, 2013.

[190] Jorge G Ibanez, Margarita Hernandez-Esparza, Carmen Doria-Serrano, Arturo Fregoso-Infante, Mono Mohan Singh, Jorge G Ibanez, Margarita Hernandez-Esparza, Carmen Doria-Serrano, Arturo Fregoso-Infante, and Mono Mohan Singh. Dissolved oxygen in water: Reference chapters: 6, 7, 8, 2008.

[191] Kofi Sarpong Adu-Manu, Cristiano Tapparello, Wendi Heinzelman, Ferdinand Apietu Katsriku, and Jamal-Deen Abdulai. Water quality monitoring using wireless sensor networks: Current trends and future research directions. *ACM Transactions on Sensor Networks (TOSN)*, 13(1):1–41, 2017.

[192] Rizqi Putri Nourma Budiarti, Anang Tjahjono, Mochamad Hariadi, and Mauridhi Hery Purnomo. Development of iot for automated water quality monitoring system. In *2019 International Conference on Computer Science, Information Technology, and Electrical Engineering (ICOMITEE)*, pages 211–216. IEEE, 2019.

[193] Soundarya Pappu, Prathyusha Vudatha, AV Niharika, T Karthick, and Suresh Sankaranarayanan. Intelligent iot based water quality monitoring system. *International Journal of Applied Engineering Research*, 12(16):5447–5454, 2017.

[194] Tengyue Fang, Hangqian Li, Guangyong Bo, Kunde Lin, Dongxing Yuan, and Jian Ma. On-site detection of nitrate plus nitrite in natural water samples using smartphone-based detection. *Microchemical Journal*, 165:106117, 2021.

[195] Agnieszka Gałuszka, Zdzisław M Migaszewski, and Jacek Namieśnik. Moving your laboratories to the field–advantages and limitations of the use of field portable instruments in environmental sample analysis. *Environmental research*, 140:593–603, 2015.

[196] Alexander T Demetillo, Michelle V Japitana, and Evelyn B Taboada. A system for monitoring water quality in a large aquatic area using wireless sensor network technology. *Sustainable Environment Research*, 29:1–9, 2019.

[197] AN Prasad, K Al Mamun, FR Islam, and Haq Haqva. Smart water quality monitoring system. In *2015 2nd Asia-Pacific World Congress on Computer Science and Engineering (APWC on CSE)*, pages 1–6. IEEE, 2015.

[198] Aravinda S Rao, Stephen Marshall, Jayavardhana Gubbi, Marimuthu Palaniswami, Richard Sinnott, and Vincent Pettigrovet. Design of low-cost autonomous water quality monitoring system. In *2013 International Conference on Advances in Computing, Communications and Informatics (ICACCI)*, pages 14–19. IEEE, 2013.

[199] Mohammad Salah Uddin Chowdury, Talha Bin Emran, Subhasish Ghosh, Abhijit Pathak, Mohd Manjur Alam, Nurul Absar, Karl Andersson, and Mohammad Shahadat Hossain. Iot based real-time river water quality monitoring system. *Procedia computer science*, 155:161–168, 2019.

[200] Sathish Pasika and Sai Teja Gandla. Smart water quality monitoring system with cost-effective using iot. *Heliyon*, 6(7), 2020.

[201] Andres Felipe Zambrano, Luis Felipe Giraldo, Julian Quimbayo, Brayan Medina, and Eduardo Castillo. Machine learning for manually-measured water quality prediction in fish farming. *Plos one*, 16(8):e0256380, 2021.

[202] Chengfeng Le, Y Zha, Y Li, D Sun, H Lu, and B Yin. Eutrophication of lake waters in china: cost, causes, and control. *Environmental management*, 45:662–668, 2010.

[203] David Holler, Rodolfo Vaghetto, and Yassin Hassan. Water temperature measurements with a rayleigh backscatter distributed sensor. *Optical Fiber Technology*, 55:102160, 2020.

[204] Haijiang Tai, Yuting Yang, Shuangyin Liu, and Daoliang Li. A review of measurement methods of dissolved oxygen in water. In *Computer and Computing Technologies in Agriculture V: 5th IFIP TC 5/SIG 5.1 Conference, CCTA 2011, Beijing, China, October 29-31, 2011, Proceedings, Part II 5*, pages 569–576. Springer, 2012.

[205] Kevin R Gilmore and Huan V Luong. Improved method for measuring total dissolved solids. *Analytical letters*, 49(11):1772–1782, 2016.

[206] Ben GB Kitchener, John Wainwright, and Anthony J Parsons. A review of the principles of turbidity measurement. *Progress in Physical Geography*, 41(5):620–642, 2017.

[207] KC Yang and Richard Hogg. Estimation of particle size distributions from turbidimetric measurements. *Analytical Chemistry*, 51(6):758–763, 1979.

[208] Miao Yuqing, Chen Jianrong, and Fang Keming. New technology for the detection of ph. *Journal of biochemical and biophysical methods*, 63(1):1–9, 2005.

[209] Sayka Jahan and Vladimir Strezov. Water quality assessment of australian ports using water quality evaluation indices. *PloS one*, 12(12):e0189284, 2017.

[210] Adamu Mustapha and Ado Abdu. Application of principal component analysis & multiple regression models in surface water quality assessment. *Journal of environment and earth science*, 2(2):16–23, 2012.

[211] D Ballantine. Developing a composite index to describe river condition in new zealand. *A composite river condition index for New Zealand: Prepared for the Ministry for the Environment by the National Institute of Water and Atmospheric Research, Hamilton. HAM2012-131*, 2012.

[212] P Walsh and W Wheeler. Water quality index aggregation and cost benefit analysis. us environmental protection agency. *National Center for Environmental Economics, Washington*, 2012.

[213] Canadian Council of Ministers of the Environment. Canadian water quality guidelines for the protection of aquatic life: Ccme water quality index 1.0 user's manual, 2001.

[214] Malinali Sánchez, Javier Alcocer, Elva Escobar, and Alfonso Lugo. Phytoplankton of cenotes and anchialine caves along a distance gradient from the northeastern coast of quintana roo, yucatan peninsula. *Hydrobiologia*, 467:79–89, 2002.

[215] K Zakowski, M Narozny, M Szocinski, and Kazimierz Darowicki. Influence of water salinity on corrosion risk—the case of the southern baltic sea coast. *Environmental monitoring and assessment*, 186:4871–4879, 2014.

[216] Eleanor A Weideman, Vonica Perold, Vincenzo Donnarumma, Giuseppe Suaria, and Peter G Ryan. Proximity to coast and major rivers influence the density of floating microplastics and other litter in east african coastal waters. *Marine Pollution Bulletin*, 188:114644, 2023.

[217] Frederic Baret and Samuel Buis. Estimating canopy characteristics from remote sensing observations: Review of methods and associated problems. *Advances in land remote sensing: System, modeling, inversion and application*, pages 173–201, 2008.

[218] Mohd Javaid, Abid Haleem, Ravi Pratap Singh, Rajiv Suman, and Ernesto Santibañez Gonzalez. Understanding the adoption of industry 4.0 technologies in improving environmental sustainability. *Sustainable Operations and Computers*, 3:203–217, 2022.

[219] Weng Hong Lim, Yuen Kiat Yap, Wu Yi Chong, and Harith Ahmad. All-optical graphene oxide humidity sensors. *Sensors*, 14(12):24329–24337, 2014.

[220] Mahdiar Ghadiry, Mehrdad Gholami, Lai Choon Kong, Chong Wu Yi, Harith Ahmad, and Yatima Alias. Nano-anatase tio2 for high performance optical humidity sensing on chip. *Sensors*, 16(1):39, 2015.

[221] Miyeon Jang, Chungsik Yoon, Jihoon Park, and Ohhun Kwon. Evaluation of hazardous chemicals with material safety data sheet and by-products of a photoresist used in the semiconductor-manufacturing industry. *Safety and health at work*, 10 (1):114–121, 2019.

[222] Angela Yu-Chen Lin, Sri Chandana Panchangam, and Chao-Chun Lo. The impact of semiconductor, electronics and optoelectronic industries on downstream perfluorinated chemical contamination in taiwanese rivers. *Environmental Pollution*, 157(4):1365–1372, 2009.

[223] Yaoming Wang, Zenghui Zhang, Chenxiao Jiang, and Tongwen Xu. Electrodialysis process for the recycling and concentrating of tetramethylammonium hydroxide (tmah) from photoresist developer wastewater. *Industrial & Engineering Chemistry Research*, 52(51):18356–18361, 2013.

[224] Sílvia Manuela Ferreira Cruz, Luís A Rocha, and Júlio C Viana. Printing technologies on flexible substrates for printed electronics. In *Flexible electronics*. IntechOpen, 2018.

[225] Rd K Khirotdin, Nurhafizzah Hassan, Hi H Siang, and Muhamad H Zawahid. Printing and curing of conductive ink track on curvature substrate using fluid dispensing system and oven. *Engineering Letters*, 25(3), 2017.

[226] Erika Hrehorova, Marian Rebros, Alexandra Pekarovicova, Bradley Bazuin, Amrith Ranganathan, Sean Garner, Gary Merz, John Tosch, and Robert Boudreau. Gravure printing of conductive inks on glass substrates for applications in printed electronics. *Journal of Display Technology*, 7(6):318–324, 2011.

[227] Claudio S Ravasio, Stephen D Hoath, Graham D Martin, Peter Boltryk, and Marko Dorrestijn. Meniscus motion inside a dod inkjet print-head nozzle. *repository.cam.ac.uk*, 2016.

[228] Shlomo Magdassi. *The chemistry of inkjet inks*. World scientific, 2009.

[229] Tatsumi Ishihara and Shogo Matsubara. Capacitive type gas sensors. *Journal of electroceramics*, 2:215–228, 1998.

[230] Hanns-Erik Endres, Ralf Hartinger, Markus Schwaiger, Gerhard Gmelch, and Mathias Roth. A capacitive co2 sensor system with suppression of the humidity interference. *Sensors and Actuators B: Chemical*, 57(1-3):83–87, 1999.

[231] SC Lee and Maureen Chang. Indoor air quality investigations at five classrooms. *Indoor air*, 9(2):134–138, 1999.

[232] B Ivanov, O Zhelondz, L Borodulkin, and H Ruser. Distributed smart sensor system for indoor climate monitoring. In *KONNEX Scientific Conf., Mnchen*, pages 10–11, 2002.

[233] Florian Bender, Kerstin Länge, Achim Voigt, and Michael Rapp. Improvement of surface acoustic wave gas and biosensor response characteristics using a capacitive coupling technique. *Analytical chemistry*, 76(13):3837–3840, 2004.

[234] Jung-Yoon Kim, Chao-Hsien Chu, and Sang-Moon Shin. Issaq: An integrated sensing systems for real-time indoor air quality monitoring. *IEEE Sensors Journal*, 14(12):4230–4244, 2014.

[235] Yi Liu, Tianhong Cui, and Kody Varahramyan. All-polymer capacitor fabricated with inkjet printing technique. *Solid-State Electronics*, 47(9):1543–1548, 2003.

[236] Anglique Tetelin, Claude Pellet, Cline Laville, and Gilles N'Kaoua. Fast response humidity sensors for a medical microsystem. *Sensors and Actuators B: Chemical*, 91(1-3):211–218, 2003.

[237] OK Varghese, PD Kichambre, D Gong, KG Ong, EC Dickey, and CA Grimes. Gas sensing characteristics of multi-wall carbon nanotubes. *Sensors and Actuators B: Chemical*, 81(1):32–41, 2001.

[238] Peter Van Gerwen, Wim Laureyn, Wim Laureys, Guido Huyberechts, Maaike Op De Beeck, Kris Baert, Jan Suls, Willy Sansen, Philippe Jacobs, Lou Hermans, et al. Nanoscaled interdigitated electrode arrays for biochemical sensors. *Sensors and Actuators B: Chemical*, 49(1-2):73–80, 1998.

[239] M Kitsara, D Goustouridis, S Chatzandroulis, M Chatzichristidi, I Raptis, Th Ganetsos, R Igreja, and CJ Dias. Single chip interdigitated electrode capacitive chemical sensor arrays. *Sensors and Actuators B: Chemical*, 127(1):186–192, 2007.

[240] H-E Endres and S Drost. Optimization of the geometry of gas-sensitive interdigital capacitors. *Sensors and Actuators B: Chemical*, 4(1-2):95–98, 1991.

[241] Xiaohui Hu and Wuqiang Yang. Planar capacitive sensors–designs and applications. *Sensor Review*, 30(1):24–39, 2010.

[242] A Oprea, J Courbat, N Bârsan, D Briand, NF De Rooij, and U Weimar. Temperature, humidity and gas sensors integrated on plastic foil for low power applications. *Sensors and Actuators B: Chemical*, 140(1):227–232, 2009.

[243] J Courbat, YB Kim, D Briand, and NF De Rooij. Inkjet printing on paper for the realization of humidity and temperature sensors. In *2011 16th International*

Solid-State Sensors, Actuators and Microsystems Conference, pages 1356–1359. IEEE, 2011.

[244] A Vásquez Quintero, F Molina-Lopez, G Mattana, D Briand, and NF De Rooij. Self-standing printed humidity sensor with thermo-calibration and integrated heater. In *2013 Transducers & Eurosensors XXVII: The 17th International Conference on Solid-State Sensors, Actuators and Microsystems (TRANSDUCERS & EUROSENSORS XXVII)*, pages 838–841. IEEE, 2013.

[245] Almudena Rivadeneyra, José Fernández-Salmerón, Manuel Agudo, Juan A López-Villanueva, Luis Fermín Capitan-Vallvey, and Alberto J Palma. Design and characterization of a low thermal drift capacitive humidity sensor by inkjet-printing. *Sensors and Actuators B: Chemical*, 195:123–131, 2014.

[246] F Molina-Lopez, D Briand, and NF De Rooij. All additive inkjet printed humidity sensors on plastic substrate. *Sensors and Actuators B: Chemical*, 166:212–222, 2012.

[247] Catrin Sohrabi, Ginimol Mathew, Thomas Franchi, Ahmed Kerwan, Michelle Griffin, Jennick Soleil C Del Mundo, Syed Ahsan Ali, Maliha Agha, and Riaz Agha. Impact of the coronavirus (covid-19) pandemic on scientific research and implications for clinical academic training–a review. *International Journal of Surgery*, 86: 57–63, 2021.

[248] G Jeffrey Snyder, James R Lim, Chen-Kuo Huang, and Jean-Pierre Fleurial. Thermoelectric microdevice fabricated by a mems-like electrochemical process. *Nature materials*, 2(8):528–531, 2003.

[249] L Li, Filipe Vilela, J Forgie, Peter J Skabara, and D Uttamchandani. Miniature humidity micro-sensor based on organic conductive polymer–poly (3, 4-ethylenedioxythiophene). *Micro & Nano Letters*, 4(2):84–87, 2009.

[250] L Juhász and J Mizsei. Humidity sensor structures with thin film porous alumina for on-chip integration. *Thin Solid Films*, 517(22):6198–6201, 2009.

[251] Kazuhiro Murata. Super-fine ink-jet printing for nanotechnology. In *Proceedings International Conference on MEMS, NANO and Smart Systems*, pages 346–349. IEEE, 2003.

[252] Ana Moya, Gemma Gabriel, Rosa Villa, and F Javier del Campo. Inkjet-printed electrochemical sensors. *Current Opinion in Electrochemistry*, 3(1):29–39, 2017.

[253] Henrik Andersson, Anatoliy Manuilskiy, Tomas Unander, Cecilia Lidenmark, Sven Forsberg, and Hans-Erik Nilsson. Inkjet printed silver nanoparticle humidity sensor with memory effect on paper. *IEEE Sensors Journal*, 12(6):1901–1905, 2011.

[254] Mallika Bariya, Ziba Shahpar, Hyejin Park, Junfeng Sun, Younsu Jung, Wei Gao, Hnin Yin Yin Nyein, Tiffany Sun Liaw, Li-Chia Tai, Quynh P Ngo, et al. Roll-to-roll gravure printed electrochemical sensors for wearable and medical devices. *ACS nano*, 12(7):6978–6987, 2018.

[255] Hakyung Jeong, Youngwook Noh, and Dongjin Lee. Highly stable and sensitive resistive flexible humidity sensors by means of roll-to-roll printed electrodes and flower-like tio2 nanostructures. *Ceramics International*, 45(1):985–992, 2019.

[256] ASG Reddy, BB Narakathu, MZ Atashbar, M Rebros, E Rebrosova, and MK Joyce. Gravure printed electrochemical biosensor. *Procedia Engineering*, 25: 956–959, 2011.

[257] Shaukat Khan, Mazhar Ul-Islam, Muhammad Wajid Ullah, Yeji Kim, and Joong Kon Park. Synthesis and characterization of a novel bacterial cellulose–poly (3, 4-ethylenedioxythiophene)–poly (styrene sulfonate) composite for use in biomedical applications. *Cellulose*, 22:2141–2148, 2015.

[258] Seunghyeon Lee, Yeongbeom Hong, and Bong Sup Shim. Biodegradable pedot: Pss/clay composites for multifunctional green-electronic materials. *Advanced Sustainable Systems*, 6(2):2100056, 2022.

[259] R Pradeep Kumar and Annie Abraham. Pvp-coated naringenin nanoparticles for biomedical applications–in vivo toxicological evaluations. *Chemico-biological interactions*, 257:110–118, 2016.

[260] Adnan Haider and Inn-Kyu Kang. Preparation of silver nanoparticles and their industrial and biomedical applications: a comprehensive review. *Advances in materials science and engineering*, 2015:1–16, 2015.

[261] David Roe, Balu Karandikar, Nathan Bonn-Savage, Bruce Gibbins, and Jean-Baptiste Roullet. Antimicrobial surface functionalization of plastic catheters by silver nanoparticles. *Journal of antimicrobial chemotherapy*, 61(4):869–876, 2008.

[262] Amit Gupta, Kazuaki Matsui, Jeng-Fan Lo, and Simon Silver. Molecular basis for resistance to silver cations in salmonella. *Nature medicine*, 5(2):183–188, 1999.

[263] Jose Ruben Morones, Jose Luis Elechiguerra, Alejandra Camacho, Katherine Holt, Juan B Kouri, Jose Tapia Ramírez, and Miguel Jose Yacaman. The bactericidal effect of silver nanoparticles. *Nanotechnology*, 16(10):2346, 2005.

[264] MK Inglesby and SH Zeronian. Direct dyes as molecular sensors to characterize cellulose substrates. *Cellulose*, 9:19–29, 2002.

[265] Jin-Woo Han, Beomseok Kim, Jing Li, and M Meyyappan. Carbon nanotube based humidity sensor on cellulose paper. *The Journal of Physical Chemistry C*, 116(41):22094–22097, 2012.

[266] Zhouping Yin, Yongan Huang, Yongqing Duan, and Haitao Zhang. *Electrohydrodynamic direct-writing for flexible electronic manufacturing*. Springer, 2018.

[267] GP Alcantara and CGM Andrade. A short review of gas sensors based on interdigital electrode. In *2015 12th IEEE International Conference on Electronic Measurement & Instruments (ICEMI)*, volume 3, pages 1616–1621. IEEE, 2015.